OPTICAL CHARACTERIZATION AND DEVICE APPLICATION OF THE SEMICONDUCTORS ZNSE AND ZNS

Jiazhen Zhang

A Thesis Submitted for the Degree of PhD
at the
University of St Andrews

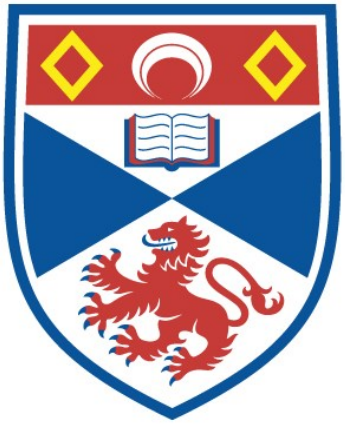

1991

Optical Characterization and Device Application of the Semiconductors ZnSe and ZnS

A thesis presented by

Jiazhen Zheng (B.Sc)

to

the University of St.Andrews

in application for the degree of Doctor of Philosophy

October, 1990

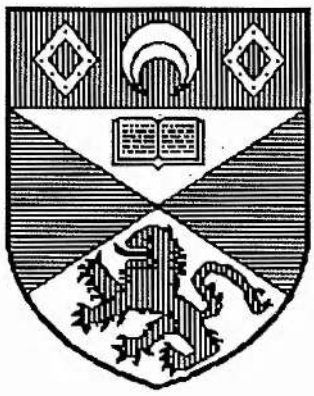

Department of Physics and Astronomy

North haugh, St. Andrews

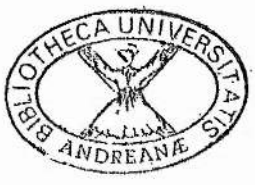

ProQuest LLC.
789 East Eisenhower Parkway
P.O. Box 1346
Ann Arbor, MI 48106 – 1346

DECLARATION

I hereby certify that this thesis has been composed by me, and is a record of work done by me, and has not previously been presented for a higher degree.

The research was carried out in the Wolfson Institute of Luminescence within the School of Physical Sciences in the University of St. Andrews under the supervision of Professor J.W. ALLEN.

Jiazhen Zheng

CERTIFICATE

I certify that Jiazhen Zheng has spent nine terms at research work in the Wolfson Institute of Luminescence within the School of Physical Sciences in the University of St. Andrews under my directions, that he has fulfilled the condition of the Resolution of the University Court, 1967, No.1, and that he is qualified to submit the accompanying thesis in application for the degree of Doctor of Philosophy.

Professor J.W. ALLEN

(Research Supervisor.)

CAREER

I first matriculated in the Physics Department of Xiamen University, P.R. China, in September 1981. I obtained the degree of Bachelor of Science in Physics and Electronics in 1985 and started a three year M.Sc course on semiconductors in the same University.

In October 1987, following the award of a Sino-British Friendship Scholarship, I ceased my M.Sc course in Xiamen University, and enrolled as a research student in the University of St.Andrews under the Resolution of the University Court, 1967, No.1, as a candidate for the degree of Doctor of Philosophy.

ACKNOWLEDGEMENTS

First of all, I would like to thank my supervisor Professor J.W. Allen for his invaluable insights, experience and guidance throughout the last three years' research work.

I would like to thank Professor J.O. William and Dr. Yates for the supply of MOCVD grown ZnSe. Dr. D.M. Finlayson very kindly lent me the magnet and cryostat which were used for the Hall effect measurements. And Bob Mitchell is very much appreciated for the time he has spent on repairing the vacuum systems.

I would like to thank all my colleagues at work, especially Nan and Jorma for their moral support.

I would also like to thank my wife for the time I could not share with her because of my research work, and for her understanding and encouragement.

Financial support for the research was provided by a joint program between the Chinese Government and the British Council (The Sino-British Friendship Scholarship Scheme).

ABSTRACT

We have presented evidence that the blue emission band, which is dominant at room temperature in ZnSe made under a wide variety of conditions, arises from a transition between a free hole and an electron bound to a donor, but not all donors contribute. There is a cutoff energy within the spread of donor levels above which there is negligible contribution to the emission. It is suggested that the cutoff corresponds to a localization edge of the same nature as the mobility edge. The line shape calculation based on a simple model agrees well with the experimental data. The origin of the blue emission seen at room temperature in the electroluminescence is examined to be the same. We have also discussed the injection mechanism of minority carriers in the ZnSe MIS diodes.

It has been shown that annealing as-grown MOCVD ZnSe in the temperature range 300-400 °C can lead to large increases in resistivity. The effect is large for annealing in air or selenium and smaller for annealing in vacuum or zinc vapour. The process involved has an activation energy of only 0.26 eV and appears to be caused by a lattice defect acting as an acceptor. The photocapacitance spectra show that the acceptor is likely to be the so-called M-centre in ZnSe. We have shown that the attribution of the M-centre to copper-red centre is by no means conclusive. The possibility is still open that the M-centre is a lattice defect.

We have made double light source steady-state photo-capacitance measurements on ZnS single crystals. The Schottky diodes were made by evaporating a metal contact onto a chemically cleaned ZnS surface. Levels were found at 0.9 eV and 2.0 eV below the conduction band and 0.8 eV above the valence band in both melt-grown and iodine-transported material. These centres might be due to lattice defects. An additional level at 1.6 eV below the conduction band occurred in the iodine-transported material.

CONTENTS

Figures

Chapter 4

Page

Chapter 5

Chapter 6

Tables

Chapter 1 Introduction

1.1 Historical perspective

The invention of the transistor in 1947[1] and its later embodiment in junction form[2] marked a new era in electronics. Not only did the vacuum tube become almost obsolete, but also many new device functions emerged, and unbelievable size reductions and enormous packing densities in very large-scale integrated circuits (VLICs) resulted. The transistor began with Ge because Ge could be made very pure at that time and its band gap is large enough for room temperature operation. Silicon has a wider band gap than Ge and its surface properties are very stable. The real emergence of Si as a transistor material came early in 1955 when diffused-impurity Si devices[3] were first constructed at Bell Laboratories. Because of the transistor, both Ge and its successor Si have been purified to such high levels and have been grown with such perfection that Si even serves as the standard for determination of Avogadro's number[4].

Although most of the electronics devices which are capable of performing functions such as signal generation, amplification, switching, etc, are made with Si, it is not a universal semiconductor and has certain limitations. The band gap of Si is indirect and is fixed at about 1.1 eV, and hence it is not useful for light emitters, not even in the infrared where they emit. The energy band structure is not suitable for transferred electron devices (Gunn oscillators)[5,6]. The development of compound

semiconductors was to extend electronic functions and to find applications which the elemental semiconductors cannot achieve.

Successful electronic devices made with III-V compounds such as GaAs are the high speed transistors and the transferred electron devices, which are widely used in microwave circuits. It was realized as early as 1958 that GaAs could have significant advantages as a high frequency, high temperature transistor material because of its higher electron mobility, higher saturated drift velocity, and wider band gap than silicon. Electron mobility in GaAs can further be increased greatly in modulation-doped GaAs-$Al_XGa_{1-X}As$ superlattices because the ionized scattering donors (n-type material) or acceptors (p-type material) are located in the $Al_XGa_{1-X}As$ layer[7]. Now the most important high frequency (> 4 GHz) transistor of any type is the GaAs field effect transistor (FET)[8]. The GaAs transistor is not used in lower frequency applications because its cost is greater than that of the Si transistor.

It was the light emission capability of the III-V compound semiconductors that finally encouraged their large-scale development. This was particularly true after the report of efficient spontaneous emission from GaAs p-n junctions[9] and the subsequent demonstration of infrared[10,11] and visible-red[12] stimulated emission from III-V compound p-n junctions. Homojunction GaAs diodes prepared by Zn diffusion or by Si doping were well developed by the early seventies[13]. Diodes with higher electrical to optical conversion efficiencies can be obtained by using double heterostructure $Al_XGa_{1-X}As$-GaAs-$Al_XGa_{1-X}As$ either by LPE or MOCVD[14,15]. In the visible region,

$GaAs_{1-X}P_X$ and GaP: Zn,O are the main LED materials. For $X > 0.4$, $GaAs_{1-X}P_X$ becomes an indirect gap material and impurities like nitrogen have to be incorporated into the alloys to increase the radiative recombination rate. Nitrogen in $GaAs_{1-X}P_X$ is a short range isoelectronic trap with a shallow binding energy. The theory of the behaviour of nitrogen in $GaAs_{1-X}P_X$ continues to be advanced, but the increase in LED brightness depends more upon improvement in crystal growth, doping, and junction quality. In application, LEDs provided a replacement for the alphanumeric displays such as nixie tubes, and by 1968 the first integrated solid-state displays were on the market. These took the form of either a 7×5 array of light emitting diodes capable of presenting all the alphanumerics, or 7 illuminated bars which could display numerals only. Such displays are now common in a wide range of digital intruments.

The semiconductor laser is probably the most spectacular of all the semiconductor devices developed since the transistor. It is small, compact, highly efficient and can operate from the far infrared to the visible. Nowadays, its greatest importance is as a source for optical fibre communications, but it is now also diversifying into fields such as satellite communication and optical disc reading. Homojunction laser diodes were the first to be constructed in GaAs[10,11] and $GaAs_{1-X}P_X$[12], nowadays essentially all studies and further developments of semiconductor lasers are concentrated on double heterostructure diodes[16] and quantum well structures[17]. In a conventional double heterostructure laser the active layer (0.1 ~ 0.3 μm) is surrounded by a material with a wider band gap to contain the

carriers and with a lower refractive index to guide the light. A quantum well laser has a number of advantages over the conventional double heterostructure laser. The active region is narrowed to one or more wells of 10 nm wide or less. Population inversion can be achieved at lower carrier densities with a potentially lower ratio of spontaneous emission to stimulated emission and with a longer lifetime of Auger recombination for the minority carriers. Also, the squeezing of the bound states in quantum wells increases the kinetic energy of carrier confinement and can therefore vary the wavelength of the emission light. Apart from the most common GaAs - $Al_XGa_{1-X}As$ lasers[18,19], single and multiple quantum well lasers have been fabricated in a host of other material systems such as $In_{1-X}Ga_XAs$-InP[20], $In_{1-X}Ga_XAs_{1-Y}P_Y$ - InP[21], $In_{1-X}Ga_XAs$ - $In_{1-X}Al_XAs$[22], and $In_{1-X}Ga_XAs$ - GaAs[23]. One of the important features of the $In_{1-X}Ga_XAs_{1-Y}P_Y$ - InP devices is that the band gap of the centre active region can be tuned in composition to the wavelengths (~ 1.55 μm) at which optical fibres exhibit optimum transmission characteristics[24].

The usual III-V compounds and their binary and quaternary systems have proven to be of use in semiconductor devices, and they have applications which silicon is unable to fulfil. But they also possess certain limitations. Their band gaps can be wider than silicon, but are not wide enough for some luminescent devices. Because semiconductors strongly absorb radiation which has a photon energy greater than their band gap, the LEDs which are made from the usual III-V compound semiconductors can only give colour emissions up to green. The shortest wavelength III-V

compound LED currently available is the green GaP: N one. As the direct gap material is essential for laser diodes, the shortest wavelength III-V compound semiconductor laser currently available is in the red to yellow region. There is ample evidence showing that the light emission process in a direct gap crystal is much stronger than in an indirect gap material. For example, when the pressure on $Al_XGa_{1-X}P$ [25] or $In_{1-X}Ga_XAs_{1-Y}P_Y$ [26] (direct gap) laser diodes is increased, the X indirect band minima and the Γ direct minimum shift and approach one another; as $E_\Gamma \rightarrow E_X$, electrons transfer from Γ to X and the laser operation is quenched.

Another limiting application of the III-V compound semiconductor devices is the material cost. The raw materials themselves are extremely expensive, especially the Ga based semiconductors. For example, the IR lenses made with GaAs are much more expensive than those made with ZnSe. At present the largest economical device size for III-V compounds is about 1 cm across, and it is unlikely for them to find applications in large area display or illumination.

Large-area electroluminescent devices were first discovered by Destriau in 1936[27]. He suspended particles of ZnS powder in oil which was then poured between two parallel-plate electrodes. When an a.c voltage was applied to the plates the ZnS: Cu phosphor emitted blue-green light. But it was only after the device structure proposed by Inoguchi et al[28] that more stable, longer lifetime thin film devices of ZnS: Mn resulted. Because ZnS is comparatively cheap, so large area displays are economically feasible. Now both the ZnS: Mn and the ZnS: Cu devices are in

commercial production. The high field electroluminescence in these devices involves electron generation and acceleration, excitation of the emitting centre and photon emission, sometimes with energy transfer between centres[29]. ZnS, with a large direct band gap of 3.7 eV at room temperature, is a commercially important phosphor. In principle, devices can be constructed which emit light throughout the visible range.

An attraction of the II-VI compound semiconductors such as ZnSe and ZnS is their large band gaps which correspond to short wavelengths. Optical devices and electro-optic circuit elements operating in the blue or near ultraviolet regions are not currently readily available but are needed for optical data processing and storage because of the higher packing density and smaller diffraction losses in coupling. These are probably the primary motives for the current investigation of blue emission[30-33] and optical bistability[34,35] in ZnSe and ZnS. It is clear that there are other applications in ZnSe and ZnS like optical windows and optical lenses, which are already in commercial production.

It is hoped that this historical perspective, which cannot possibly cover every landmark, could provide a brief outline of some of the developments in semiconductor technology, and indicates the potential importance of wide band gap II-VI compounds in the future.

1.2 Outline of this work

The development of semiconducting materials for blue and ultra-violet optical devices is generally complicated by either

the crystal growth conditions (SiC) or the difficulties in achieving good p-type conductivity (ZnSe, ZnS, and GaN). Although there have been small quantities of SiC blue LEDs by Siemens, which are very difficult to make reproducibly and the cost is very high. It seems that the most promising material for the blue emitter could be ZnSe.

For device application, the luminescent properties showing a bright blue luminescence at room temperature as well as the electrical controllability are very important. To improve the quality of growth material and the device fabrication, it is clearly essential to do all sorts of characterization and to reveal the physics behind the device application. This is what we have done recently on the semiconductors ZnSe and ZnS.

Photoluminescence measurement is a powerful optical technique for characterization of semiconductors. Merz et al[36], Dean et al[37] and Isshiki et al[38] have made extensive studies of the donor bound-exciton in ZnSe through the photoluminescence spectra of the donor bound exciton transitions and the associated two electron transitions. They were essentially concerned with the identification of the impurities or defects at low temperatures. Donors and acceptors in ZnSe can also be identified by photoluminescent excitation spectra and the discrete pair lines in the donor-acceptor-pair spectra. Room temperature blue luminescence in ZnSe has been studied by a number of authors[39-41], and the attributions have been made to the free exciton recombination[39], to the free-to-bound recombination[40], and to the band-to-band recombination[41], etc. It is clearly important to identify the mechanism for producing the room temperature blue

luminescence. Therefore, in chapter 2, we discuss the origin of the blue luminescence in ZnSe at room temperature. We have made extensive measurements on the blue photoluminescence in strongly n-type MOCVD grown ZnSe. From the detailed analysis of the line shape and peak position as a function of temperature and carrier concentration, we are able to conclude that the blue emission is due to a transition between a free hole and an electron bound to a donor. However, not all donors contribute. There is a cut-off energy within the spread of donor levels above which there is negligible contribution to the blue emission. It is suggested that the cutoff corresponds to a localization edge of the same nature as the mobility edge[42].

In chapter 3, we discuss the blue electroluminescence from forward biased ZnSe MIS structures, with the insulating layer either being an oxide layer produced by chemical etching or by oxidation, or being an insulating ZnS layer produced by sublimation. This can be an alternative structure for a blue LED if the ZnSe p-n junction[32,33], which normally shows higher electrical-to-optical conversion efficiency than the MIS structure in III-V compounds, cannot be grown reproducibly or cannot work adequately. One aim of this work is to see whether the room temperature blue emission seen in electroluminescence is of the same origin as the blue emission seen in photoluminescence, and to understand the mechanisms in operation. Although there are a few attributions of the room temperature blue electroluminescence in ZnSe in the literature[39,43-45], we have demonstrated that the blue emission seen in electroluminescence is the same as the one seen in

photoluminescence, i.e., due to the recombination of a free hole with an electron bound at a localized donor. Other emissions could exist under certain conditions, but their contributions to the room temperature blue luminescence are insignificant. We have also discussed the possible hole injection mechanisms for the blue emission in the ZnSe MIS diodes.

It is known that ZnSe can be a highly compensated material. Bulk ZnSe grown at high temperatures always shows high resistivity, and has to be heat-treated in molten zinc to make it conducting. This was attributed by Woodbury and Aven[46] to the removal of deep acceptors, particularly those associated with Cu and Ag. There have been long standing disputes on whether the compensation is due to foreign impurities or due to departure from stoichiometry. Now, n-type ZnSe can be grown in a controllable manner by MBE and MOCVD. Even so the origin of the donor responsible for the n-type conductivity in MOCVD material which is not deliberately doped is still a subject of controversy[47,48]. In contrast to excellent control of n-type conductivity, good p-type ZnSe can now be grown by techniques such as MBE[32] or MOCVD[31], but with poor reproducibility. The source of compensation in p-type conductivity is still a controversial issue, i.e., by lattice defects, or foreign impurities which could be amphoteric[49]. With the aim of understanding the thermodynamic effects on the low temperature grown MOCVD ZnSe, we have made a series of annealing experiments in the temperature range of 300 °C to 450 °C in different ambients. The results are discussed in chapter 4. It was seen that the resistivity of n-type MOCVD ZnSe with an as-grown carrier

concentration of 10^{18} cm^{-3} can be changed by three orders of magnitude by such low temperature annealing. The process involved has an activation energy of only 0.26 eV, and appears to be caused by a lattice defect acting as an acceptor[50].

It is seen from chapter 4 that with comparable concentrations of shallow and compensating levels, a small fractional change of the deep levels can decrease the net carrier concentration by several orders of magnitude. It is therefore necessary to characterize various deep levels in ZnSe in order to understand the mechanisms of impurity or defect related compensation. Deep electron levels in n-type ZnSe have been studied using deep level transient spectroscopy (DLTS) by other authors[51-53]. Four electron traps with activation energies of 0.17, 0.3, 0.64, and 1.4 eV below the conduction band have been observed in LPE layers of ZnSe[52]. For deep levels in the lower half of the ZnSe band gap, the DLTS method is unsuitable because one has to go to very high temperature to do so, hence the photocapacitance techniques are normally used in such case. In particular, there is a predominant deep level in many crystals of ZnSe at ~ 0.7 eV above the valence band, with a characteristic photoionization spectrum[54-57], which is called the M-centre. The M-centre was first attributed to manganese[54,55] and then to copper[56,57]. It is now known that the assignment of the M-centre to manganese is wrong but the evidence for the Cu-red centre is by no means conclusive. In chapter 5, we discuss the origin of the M-centre in ZnSe by re-examining the evidence for and against the assignment of the M-centre to the Cu-red centre, and present our new photocapacitance data on MOCVD grown epitaxial ZnSe[58].

In chapter 6, we present the results of a photocapacitance study of deep levels in ZnS. Zinc sulphide is a good phosphor material, and has been used in the past mainly for television screen and thin film electroluminescent panels. As attention is focussed more and more on the properties of ZnS as a semiconductor, it is obvious that the deep level characterization of ZnS is important. Grimmeiss et al[59] made DLTS and photocapacitance measurements on crystals in the ZnS_xSe_{1-x} series, using Schottky contacts on cleaved crystal surfaces, but could only go to x = 0.95 and could not make measurements on ZnS itself. Fornell et al[60] made dual light source steady-state (DLSS) photocapacitance measurements on ZnS and ZnS: Mn crystals, again using Schottky contacts on cleaved surfaces. They restricted themselves to a single pump photon energy and presented hole photoionization spectra in the range between 0.75 eV and 1.55 eV. Instead of using Schottky contacts made on cleaved surfaces, we use Schottky contacts made on chemically etched surfaces. This is a common characterization technique which can, for example, also be applied to epitaxial layers of ZnS. Diodes made in this way are of poorer electrical characteristics than those made on cleaved surfaces, but this was not a problem in our photocapacitance measurements because we used a true resistance-capacitance bridge. Levels with energy of about 0.9 eV and 2.0 eV below the conduction band and about 0.8 eV above the valence band have been observed in both iodine-transported and melt-grown ZnS, while an additional level at about 1.6 eV below the conduction band was observed in the iodine-transported material[61].

In chapter 7, we present some conclusions of this thesis and emphasize the implications behind them. We also outline some problems which need further attention now and in the future. It is known that our current knowledge about II- VI compounds is much less than III-V compounds. It is hoped that this thesis will add some knowledge to our understanding of the semiconductors ZnSe and ZnS, and ultimately lead to better crystal growth and better device fabrication.

Chapter 2 The origin of the blue luminescence in ZnSe at room temperature

2.1 Introduction

It has been known for many years that zinc selenide can show blue luminescence at room temperature. An early example was the demonstration of blue electroluminescence by Ryall and Allen[39] using a forward-biased Schottky diode with an oxide layer beneath the metal contact. In such a structure, holes are injected through the oxide layer into the n-type semiconductor to recombine with electrons, although the exact injection mechanism is not quite known. A more recent example is a similar demonstration of blue electroluminescence by Yasuda et al[32] using a p-n junction. In spite of the lack of reproducibility and stability in these demonstrations, these and other observations have led to the hope that one might eventually realize efficient blue light-emitting diodes, blue semiconductor lasers, and other optoelectronic devices in ZnSe. The material has the advantage of having a direct band gap of 2.7 eV at room temperature. It has the disadvantage of being susceptible to self-compensation. The advent of molecular-beam epitaxy (MBE) and metalorganic chemical vapour deposition (MOCVD) growth methods and their variants, by means of which epitaxial layers can be grown under closely controlled conditions at low substrate temperature, has led to increased hope that the disadvantage can be overcome.

For progress, it is clearly important to identify the mechanism for producing the room temperature blue luminescence. There are many reports on the blue near-band-edge emission in ZnSe at room temperature[39-41,62], but the attribution of this blue emission is not consistent in the literature. In this chapter, we provided photoluminescence data from measurements on strongly n-type MOCVD grown ZnSe, together with information from the published literature, and discuss the assignment of the blue emission in detail. Our attention is focused on the blue emission band seen at room temperature under moderate excitation intensity (electrical or optical) in n-type ZnSe as this is of potential practical importance. There are many other blue emissions in ZnSe, especially at low temperatures, which are only marginal to the title of this chapter.

2.2 Experimental set-up and materials

Photoluminescence is radiation which is spontaneously emitted by a semiconductor when the material is optically excited. The wavelengths of the photoluminescence are independent of the wavelength of the excitation, when the excitation energy is bigger than the band gap. The experimental set-up which was used in this work to detect and spectrally resolve the photoluminescence is shown in Fig.2.1.

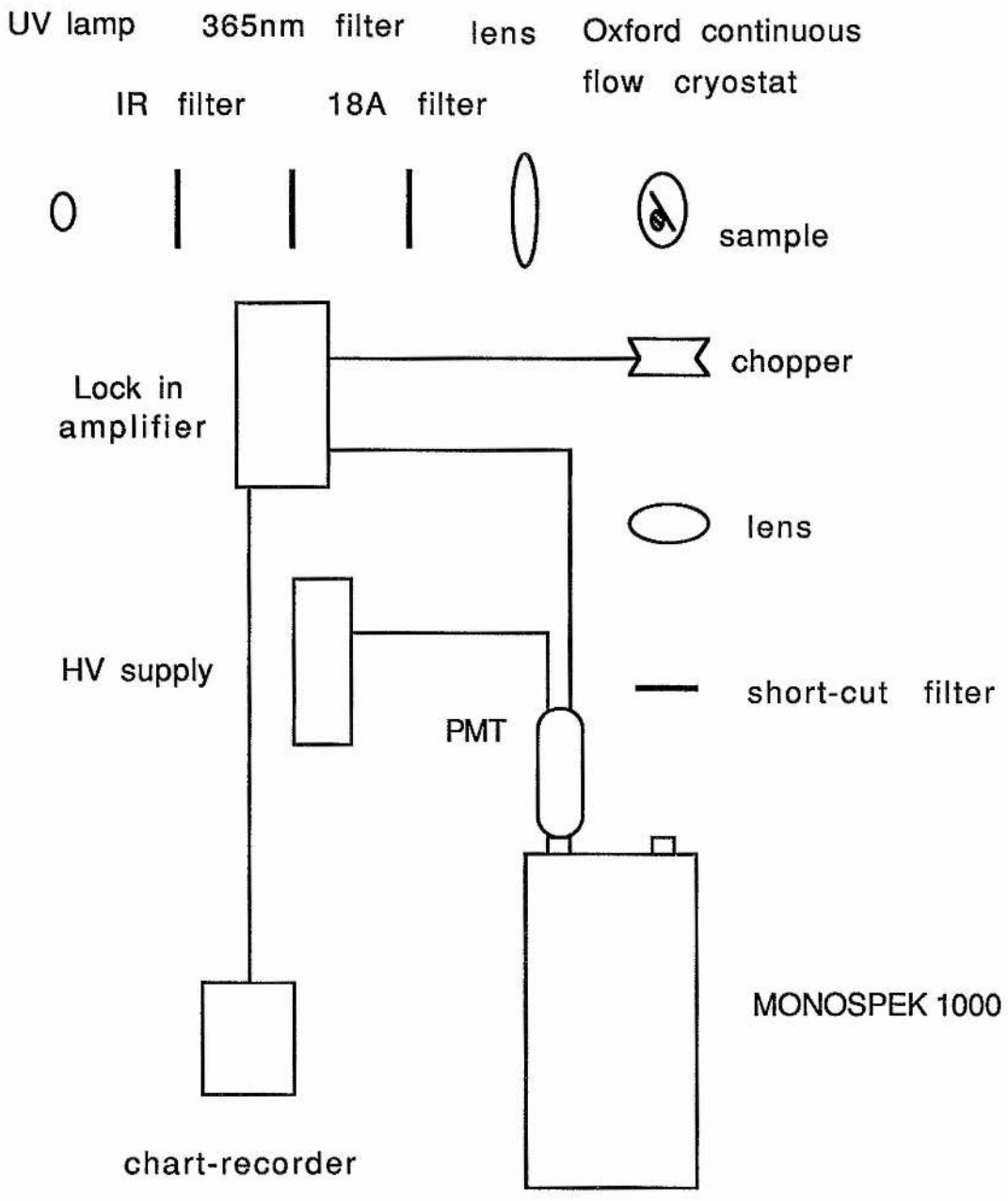

Fig.2.1 Schematic diagram of the experimental set-up for the photoluminescence measurements.

The light from a high pressure mercury lamp is passed through three filters: an infrared filter, a mercury 365 nm pass filter and a Kodak Wratten 18A filter, and is then focused onto a spot (about 1 to 2 mm in diameter) incident on the sample which is mounted on a metal block inside an Oxford continuous flow cryostat. Photoluminescence as well as the reflected 365 nm excitation light is chopped, passed through a 400 nm short-cut filter which passes the photoluminescence but blocks the excitation light, and is finally focused onto the entrance slit of a Monospek 1000 scanning monochromator with a dispersion of 8.2 Å/mm. Light output from the exit slit of the monochromator is detected by an S-20 photomultiplier tube (PMT). The chopped signal from the PMT is amplified and restored to a dc signal by a Brookdeal type 401 lock-in amplifier and displayed on a chart recorder as photoluminescence intensity versus emission wavelength. The signal from the PMT can also be detected by a microcomputer-controlled photon counting system when the chopper is removed.

In practice, it is difficult to optimise the optical path. The experimental arrangement described above solves this problem by reflecting the excitation light along the same line as the photoluminescence signal. With the short-cut filter removed, the optics can easily be aligned so that the strong excitation light is detected. When the short-cut filter is inserted, the system is aligned to detect photoluminescence by small adjustment of the focus lens.

The resolution of the monochromator is of importance to the accurate measurements of the luminescence line shape. Since the photoluminescence signal was usually weak, a reasonable compromise between signal strength and resolution was necessary. For the low temperature photoluminescence measurements, a slit width of 0.05 mm to 0.4 mm was normally used, corresponding to an energy resolution of 0.26 meV to 2.1 meV at the band gap energy of ZnSe, which is about 2.82 eV at liquid helium temperature. For the room temperature photoluminescence measurements, a slit width of 0.2 mm to 0.75 mm was used.

The wavelength calibration of the monochromator was carried out carefully by using standard mercury lines emitted from a low pressure mercury lamp. Line profiles of the blue emission were not corrected for the system response because the spectral range of the band is less than 0.2 eV with the peak near 2.7 eV. Neither the spectrometer dispersion nor the photomultiplier response varies greatly in this range.

Epitaxial layers of ZnSe were grown on GaAs substrates by MOCVD in the Solid State Chemistry Group of the University of Manchester Institute of Science and Technology (UMIST). The growth was at atmospheric pressure using dimethylzinc and hydrogen selenide, with a substrate temperature of 280 °C. The epilayer thickness was between 3 μm to 5 μm, sufficient for mismatch strain to be relaxed.

Carrier concentrations of the MOCVD ZnSe used in this study obtained from capacitance-voltage characteristics of a Schottky diode, Hall and resistivity measurements were in good agreement. One of the more thoroughly investigated materials has an electron concentration of 1.1×10^{18} cm^{-3} at room temperature with iodine as dopants. This is well to the metallic side of the metal-insulator transition and also well above the concentration at which the shallow donor ionization energy goes to zero[46], which is about 3×10^{17} cm^{-3} in ZnSe. Figure 2.2, a plot of carrier concentration of an as-grown MOCVD ZnSe from Hall measurements as a function of temperature, illustrates this, as no carrier freezeout is seen.

2.3 Properties of the blue emission band

Our measurements extended photoluminescence data to material with high carrier concentration (~ 10^{18} cm^{-3}). Figure 2.3 shows the typical luminescence spectra of our MOCVD materials measured at 5.2 K, 100 K, and 292 K. This is the emission band which we are going to discuss in detail. The characteristic features are that the band is in the blue, just below the band gap energy of ZnSe; it is much wider even at low temperatures than features such as bound excitons which produce narrow emission lines[37], and although the emission intensity decreases with increasing temperature, it is still appreciable at room

temperature. In this section some properties of the emission are listed.

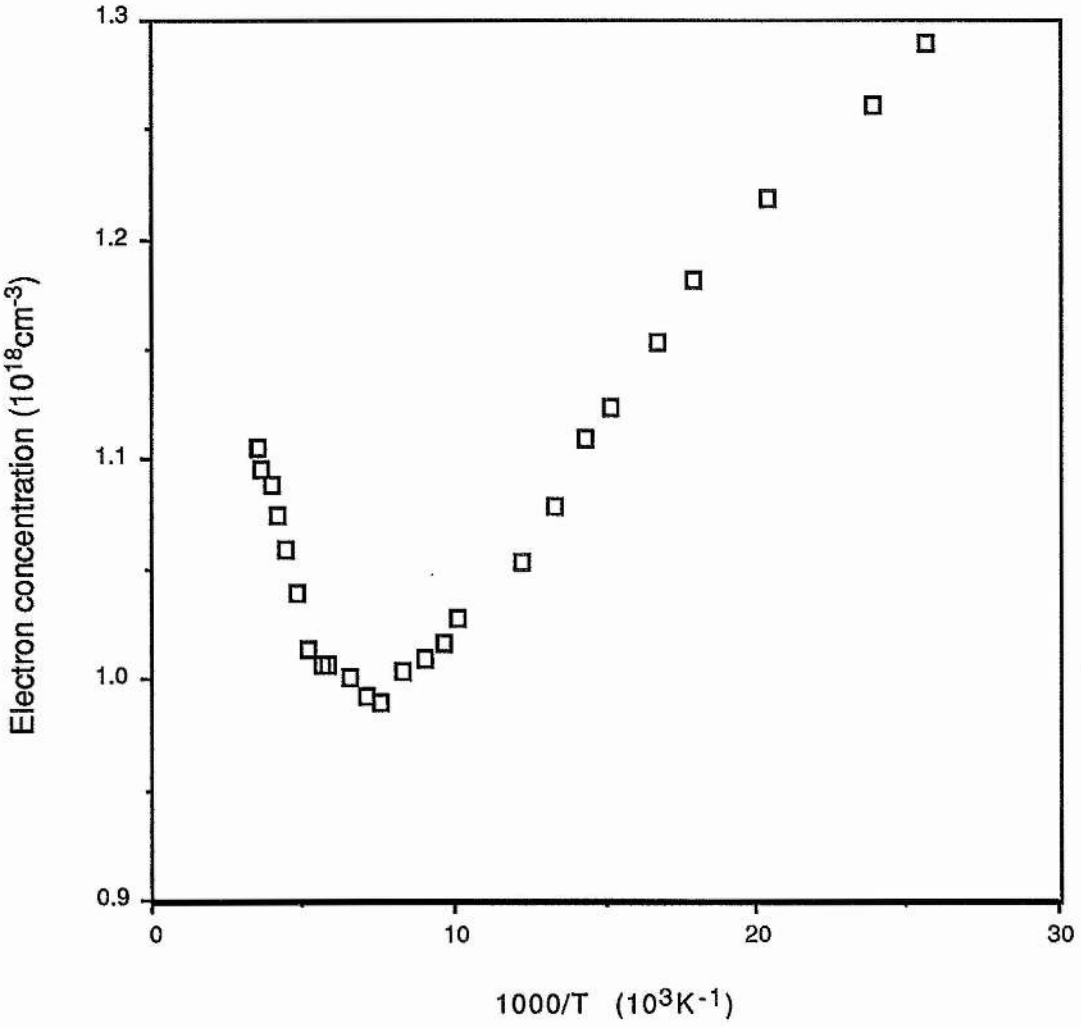

Fig.2.2 Temperature variation of the free electron concentration determined from the Hall effect measurements for an as-grown MOCVD ZnSe epilayer, showing the absence of a donor ionization energy at such high donor concentration.

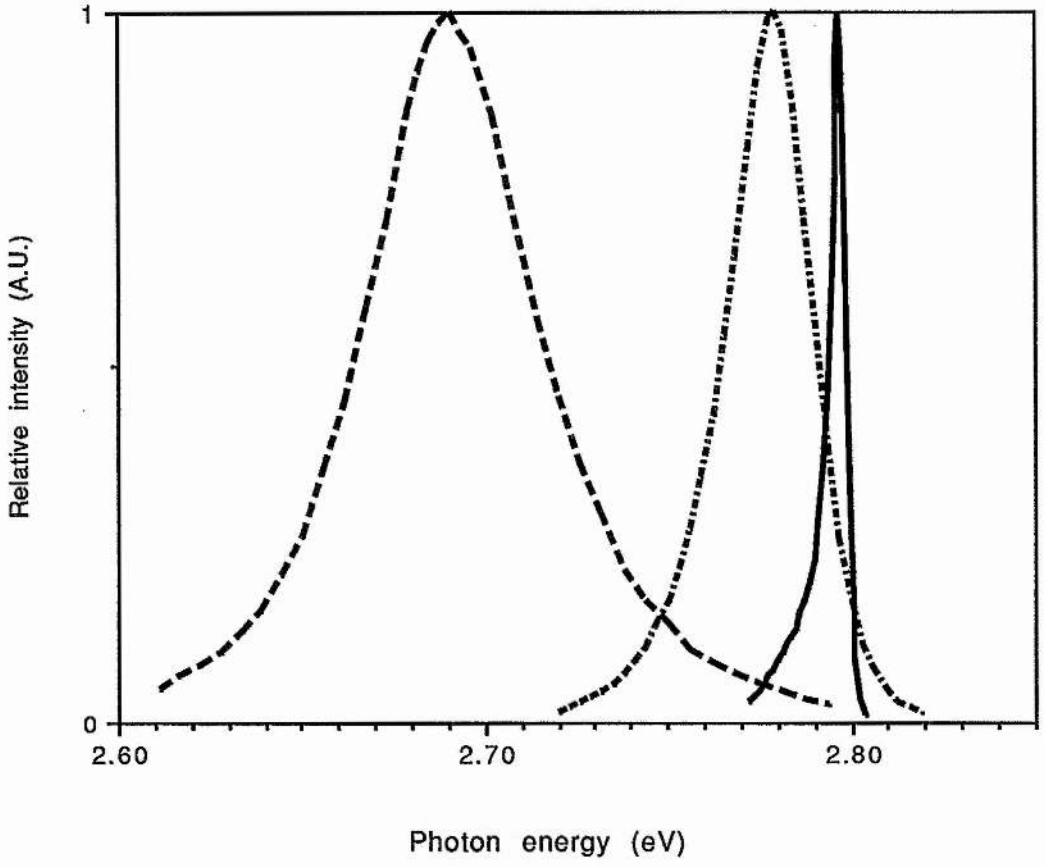

Fig.2.3 Photoluminescence spectra at 5.2 K, 100 K, and 292 K of an as-grown MOCVD ZnSe epilayer with electron concentration of 1.1×10^{18} cm^{-3}. The three spectra are normalized to the same peak intensity. (-) 5.2 K, (-.-.)100 K, and (---) 292 K.

2.3.1 Intensity

The intensity of the blue band increases with electron concentration up to about 10^{18} cm^{-3}, after which it decreases again. Figure 2.4 shows data taken from Yoshikawa et al[30] for iodine-doped ZnSe grown by MOCVD and from Ohkawa and co-workers[31] for chlorine-doped ZnSe grown by MBE. Considering the difference in growth methods, the similarity in the two sets

of data is striking. Both groups plotted peak intensity rather than total emission intensity. Since the bandwidth increases with increasing donor concentration, a plot using total intensity would be steeper than the plot using peak intensity, i.e., the variation of total intensity with electron concentration is more linear than appears from Fig.2.4. At room temperature in these materials most of the shallow donors are ionized, so Fig.2.4 shows that the intensity of the blue emission increases with donor concentration up to about 10^{18} cm^{-3}.

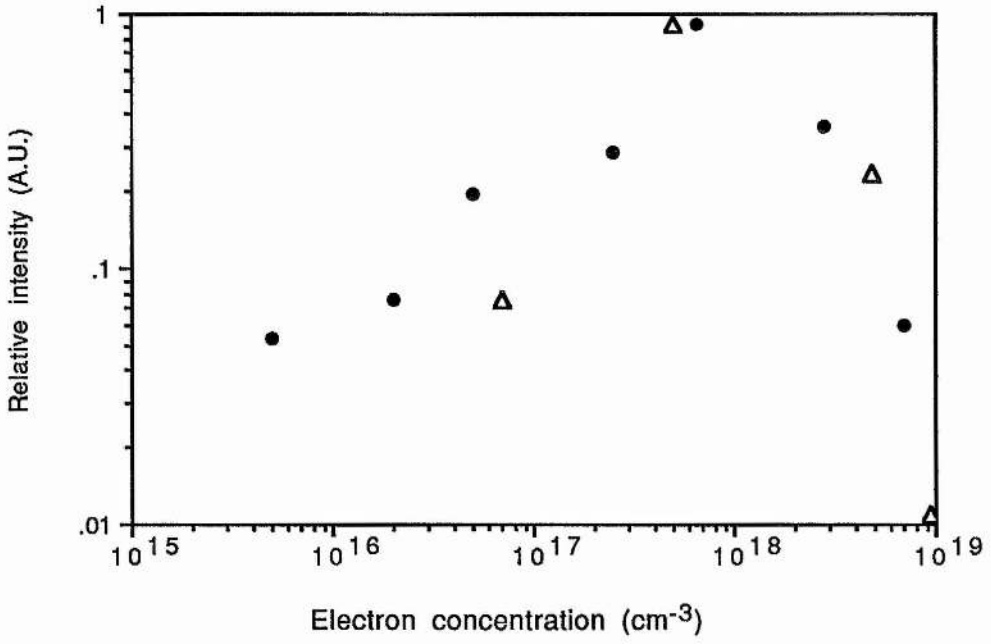

Fig.2.4 The peak intensity of the blue band at room temperature as a function of electron concentration. (•) MOCVD grown iodine doped epilayers after Yoshikawa et al[30], (Δ) MBE grown chlorine doped epilayers after Ohkawa et al[31]. The two sets of data have been normalized at the maximum intensity.

At carrier concentration larger than 10^{18} cm^{-3} , the fall of the intensity is believed to be due to other effects, such as Auger quenching of luminescence, or due to some other recombination mechanisms.

The intensity of the blue band decreases with increasing temperature. At low temperatures the situation is confused by the existence of other blue emissions in the same photon energy range. Above about 100 K these are in effect completely thermally quenched, so between room temperature and 100 K one sees the blue band only. Shirakawa and Kukimoto[40] found that in this temperature range the intensity decreased as exp(-E/kT) with E = 27 meV, although it is not clear whether this value was obtained from peak or total intensity. Their ZnSe was grown from an indium solution and had high resistivity which decreased to 1-10 Ω cm after treatment in molten zinc. The donor concentration was probably not greatly changed by this treatment, being about 10^{17} cm^{-3}, while the free-electron concentration changed by about five orders of magnitude. It is interesting that Shirakawa and Kukimoto[40] found the same thermal quenching activation energy, 27 meV, for as-grown and zinc treated materials. For our material with a donor concentration of 10^{18} cm^{-3} we find an activation energy of approximately 18 meV, the integrated intensity being used. As may be seen from Fig.2.3, in our material the blue band is dominant even at liquid helium temperature and sharp lines due to, e.g., bound excitons, are not observed.

2.3.2 Position

Ryall and Allen[39] plotted the peak photon energy of the blue electroluminescence as a function of temperature and found that, within the accuracy of the measurements, it corresponded with the free-exciton energy determined by Hite et al[63] from reflectivity measurements. Fujita et al[41] produced similar data for photoluminescence of ZnSe grown from a Zn-Ga solution.

Shirakawa and Kukimoto[40] made detailed measurements on the variation of the peak position of the blue band with temperature. For as-grown material with low electron concentration but with donor concentration probably $\sim 10^{17}$ cm^{-3}, they found that in a temperature range of 40 to 193 K, the peak position of the blue band was 9 meV below the free-exciton position which was determined by excitation spectra. At lower temperature the situation was complicated by other emissions and at high temperatures the emission was quenched in this material. They were able to determine the free-exciton absorption energy in the same material as the luminescence by observing a sharp dip in the excitation spectrum of the photoluminescence from deep centres. This dip was seen up to 220 K: for high temperatures an extrapolation formula could be used. This ability to determine the blue peak position and the exciton energy in the same material was an advance over previous attempts at comparison. In zinc-treated material, in which the donor concentration was probably unchanged but the electron concentration was $\sim 10^{17}$ cm^{-3}, they could follow the blue

emission to room temperature. In the temperature range of 100 to 200 K, where measurements on as-grown and zinc-treated materials could be compared without too much interference from other emissions, the spectra are almost identical in both position and shape. The peak position at room temperature is again 9 meV below the extrapolated free-exciton energy.

The peak photon energy of our emission band as a function of temperature are shown in Fig.2.5 together with the free exciton energies obtained by Hite et al[63] from reflectivity measurements and by Shirakawa and Kukimoto[40] from the excitation spectra. One readily sees that there is some difference in the two sets of free exciton energy, although we cannot tell at present which set of free exciton energy is more accurate. Our observed emission peak is about 2 to 4 meV below the free exciton energy obtained by Hite et al[63], and is 6 to 9 meV below the free exciton energy obtained by Shirakawa and Kukimoto[40] in a more lightly doped material.

This near constancy of the blue peak position, independent of the methods of growth and electron or donor concentration, is striking. The peak position at room temperature lies between 2.690 eV and 2.695 eV for ZnSe grown by MBE with chlorine doping[31], by liquid phase epitaxy (LPE) from Zn-Ga solution[41], or from In solution[40] and by MOCVD with iodine doping (present work). Yoshikawa et al[30] gave photoluminescence spectra for iodine-doped MOCVD grown ZnSe. At both 18 K and room temperature the peak position is independent of carrier

concentration in the range of 2.8×10^{16} cm^{-3} to 6.0×10^{17} cm^{-3} but shifts to higher energies for concentrations of 4.3×10^{18} cm^{-3} and 7.4×10^{18} cm^{-3} .

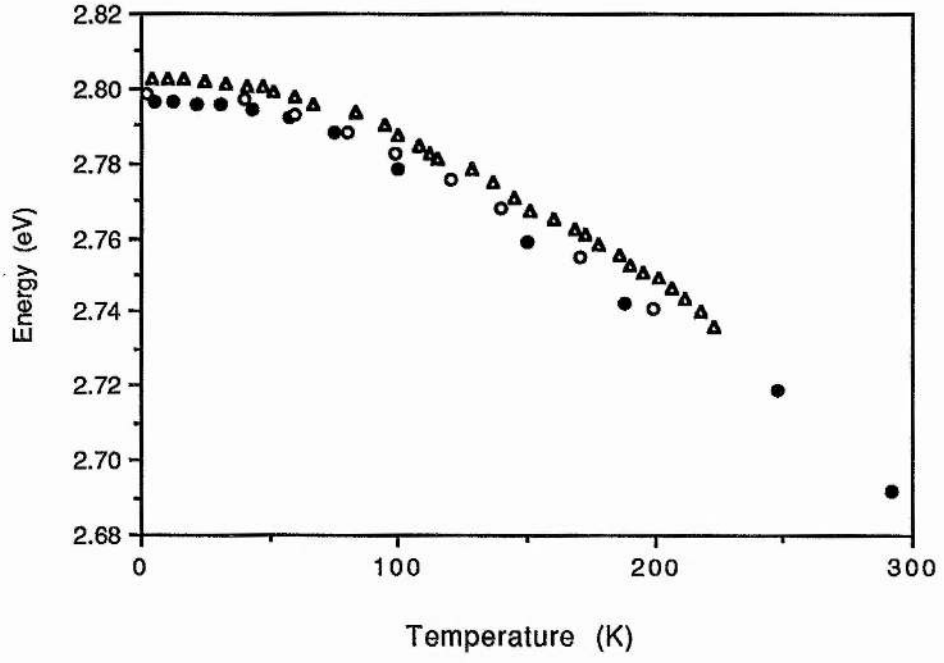

Fig.2.5 The observed peak energy (•) of the blue band as a function of temperature together with the free exciton energy from Hite et al[63] (o) and from Shirakawa et al[40] (Δ).

2.3.3 Shape

At low temperatures the blue emission band is narrow. As the temperature increases the band broadens on the high-energy side, as can be seen from Fig.2.6.

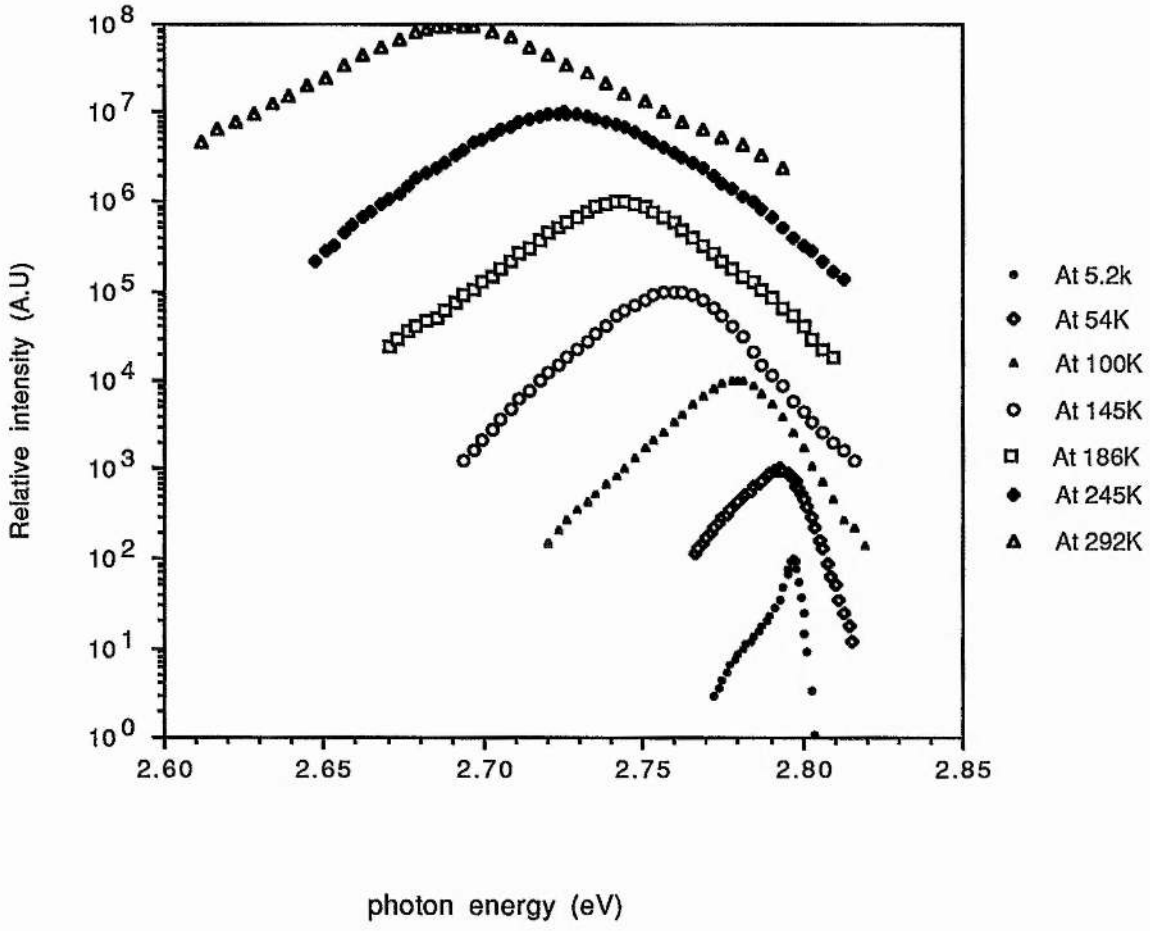

Fig.2.6 The logarithmic intensity of the blue emission band at several temperatures, showing the variation as exp(-hν/kT) on the high-energy side. Only the shapes are concerned here and the intensities have been shifted for convenience.

Above about 20 K the shape of the high-energy side is described by exp(-hν/kT), indicating that a free particle with thermal energy is involved in the transition. Figure 2.7 shows the temperature dependence of the half-width of the emission band taken on the high energy side, i.e., taken with respect to the peak position. As expected from a Maxwell-Boltzmann shape, the dependence is linear although there is a small offset of about

1.5 meV at low temperature. Shirakawa and Kukimoto[40] gave a similar plot and, although they did not say so, the best straight-line fit to their experimental points also give a small offset at low temperature. We have also found that in our material with high donor concentration the width on the low-energy side increases weakly with increasing temperature, as can be seen from Fig.2.6.

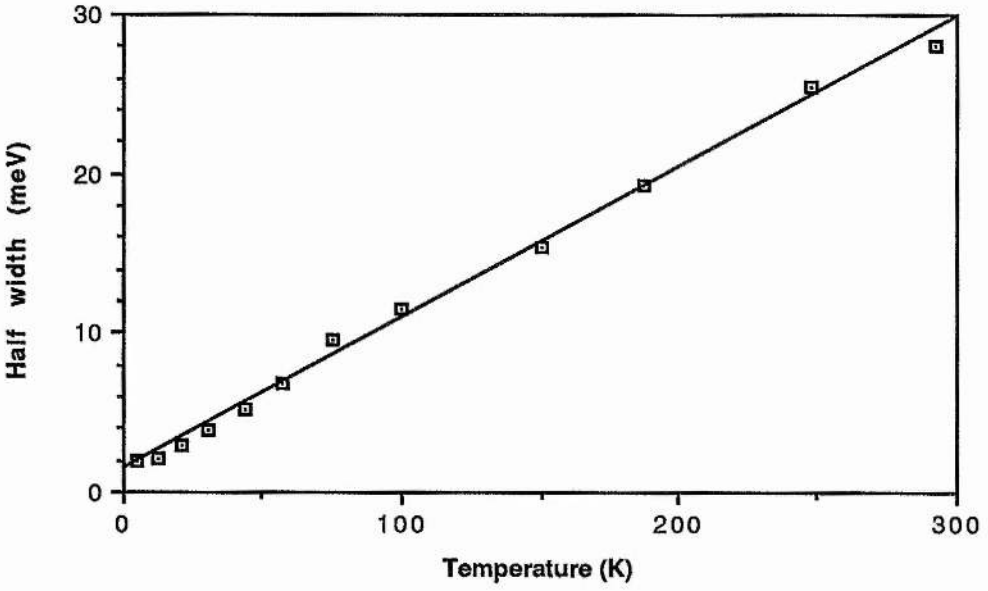

Fig.2.7 Temperature dependence of the half-width of the emission band on the high-energy side for a MOCVD ZnSe epilayer with carrier concentration of 1.1×10^{18} cm^{-3}.

As the electron concentration increases the blue emission band broadens on the low-energy side. Figure 2.8 shows the blue emission spectra measured at liquid helium temperature for carrier concentrations of 8×10^{16} cm^{-3} and 1.1×10^{18} cm^{-3}, which are the room temperature values determined from Hall and

resistivity measurements. Because the thermal energy does not affect the spectra greatly at liquid helium temperature, one can see the broadening on the low-energy side of the emission band. As both the materials were grown at the same substrate temperature, and as most of the donors in ZnSe are ionized at room temperature, the results show that the increased broadening on the low-energy side of the blue emission band is probably due to the increasing of the donor concentration. Yoshikawa et al[30] gave luminescence line shapes of the blue band which showed an increased broadening on the low-energy side as the carrier concentration increased from 2.8×10^{16} cm^{-3} to 6.0×10^{17} cm^{-3}, although they did not point this out.

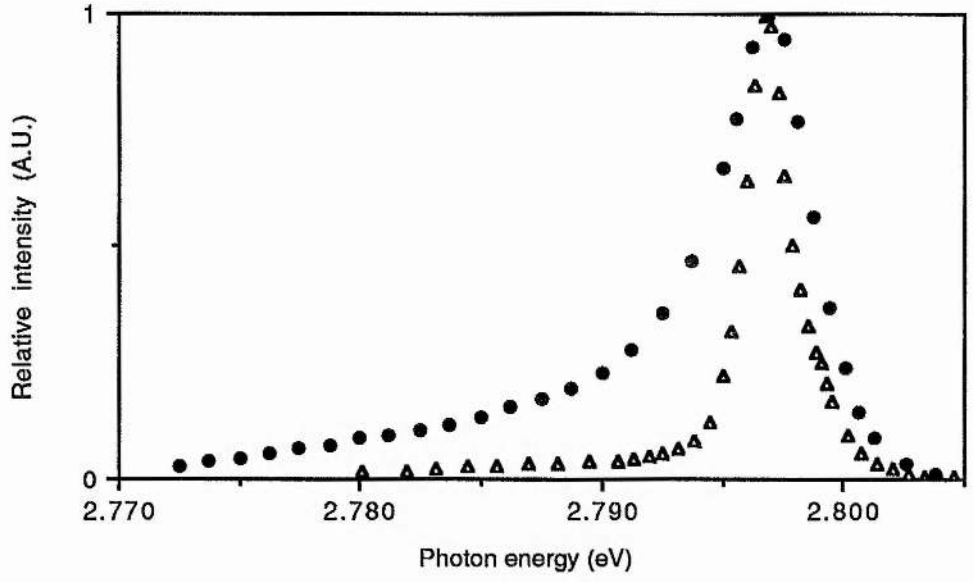

Fig.2.8 Photoluminescence spectra at liquid helium temperature of two MOCVD ZnSe epilayers with room temperature electron concentration of 1.1×10^{18} cm^{-3} (•) and 8.0×10^{16} cm^{-3} (Δ). The spectra have been normalized to the same peak intensity.

2.4 Possible assignments

A crystal can change its total energy through such mechanisms as transitions of the electrons (and holes), and creation and annihilation of phonons, plasmons, and polarons. Photo-luminescence involves transitions of the free or bound electrons and holes, and phonons are usually involved.

In this section we discuss some possible assignments of the blue emission by going through all the possible near-band-edge transitions. We re-emphasize that it is a particular emission band, with properties described in the last section, that is under discussion and not the many other blue emissions seen in appropriate conditions in ZnSe.

2.4.1 Band to band

A band-to-band transition in which a free electron in the conduction band recombines with a free hole in the valence band involves carriers with thermal energies, so the emission line shape on the high-energy side matches to that of the blue band under discussion. This led Fujita et al[41] to attribute the blue emission band at room temperature in their LPE grown ZnSe to band to band transitions. However, a free exciton in ZnSe has a binding energy of approximately 18-20 meV[36,63] and the peak position of the blue emission under discussion is 6 to 9 meV lower than the free exciton energy (the exciton energy obtained by Shirakawa and Kukimoto[40] is used here for comparison), hence the emission peak is substantially lower than the band gap energy

(the band gap shrinkage is not significant at carrier concentrations of 10^{16} cm^{-3} to 10^{18} cm^{-3}). This assignment can therefore be ruled out.

2.4.2 Free exciton

The energy of the photon emitted when a free exciton annihilates is the band gap energy minus the exciton binding energy (E_{ex}). Emission from recombination of free excitons has a shape, assuming constant matrix element, varying as

$$I(h\nu) \propto (h\nu-E)^{1/2}\exp(-(h\nu-E)/kT), \qquad (2.1)$$

where E ($E = E_g - E_{ex}$) is measured from the threshold at which the exciton kinetic energy is zero, k is the Boltzmann constant, and T is the absolute temperature.

The shape on the high-energy side of the emission band therefore matches to an adequate approximation that of the blue band, although on the low-energy side it does not. Also the peak position of the blue band is within a few meV of the free exciton position, see Fig 2.5. These facts led Ryall and Allen[39] to attribute the blue emission band to the free exciton recombination. The thermal activation energy for luminescence quenching, 27 meV from Shirakawa and Kukimoto [40] and approximately 18 meV from our present work, is not too far from the exciton binding energy, so dissociation of the free exciton could possibly account for the thermal quenching. However, closer investigation reveals problems. The free exciton energy determined from absorption or electro-reflectance is effectively

that for zero exciton kinetic energy, i.e., $E_g - E_{ex}$. The emission peak, using the shape function given in equation(2.1), is $\frac{1}{2}kT$ higher. Since the blue emission peak is a few meV lower than the free exciton energy, and this energy separation is independent of temperature, this assignment is impossible. Further evidence against this assignment is given by our observation of the blue emission in material with an electron concentration of ~ 10^{18} cm^{-3}. Since at this electron concentration the electron-hole Coulomb attraction in an exciton should be strongly screened, so the free exciton emission should be shifted slightly to higher energy and the intensity will be substantially reduced.

2.4.3 Bound excitons

Excitons which are bound to impurities or defects radiate at lower energies than the free excitons by an amount equal to the energy binding the excitons to impurities or defects. The binding energy of exciton to shallow donors in ZnSe is about 6 meV[36-38], so this gives the emissions in the required energy range (the peak is 6 to 9 meV below the free exciton energy obtained by Shirakawa and Kukimoto[40]) . However, the binding energy is only a few meV so virtually all the excitons are thermally detached from these centres at liquid nitrogen and higher temperatures, i.e., bound exciton emissions are strongly quenched thermally. Also, because no carrier with thermal kinetic energy is involved, the bound exciton emissions consist of sharp lines and have a different shape from that of the observed emission. This assignment can therefore be ruled out.

2.4.4 Donor-acceptor pairs

Donor-to-acceptor transitions are the radiative recombination of an electron bound to a donor and a hole bound to an acceptor. The energy of the emitted photon is given by

$$h\nu = E_g - (E_a + E_d) + \frac{e^2}{\varepsilon r} \qquad (2.2)$$

for a large donor acceptor separation. Here E_d and E_a are the donor and acceptor binding energies, $\frac{e^2}{\varepsilon r}$ is the Coulomb interaction energy between a donor-acceptor-pair separated by r. Donor-acceptor-pair emissions are at lower energy than the blue band under discussion and are more strongly quenched thermally, and because no free carrier is involved, there is no variation as $\exp(-h\nu/kT)$ on the high-energy side of the emission. This assignment can also be ruled out.

2.4.5 Free electron to acceptor

For a radiative recombination of a free electron with a hole at a hydrogenic acceptor, the energy of the emitted photon is given by

$$h\nu = E_g - E_a + E_k \qquad (2.3)$$

where E_a is the acceptor binding energy, E_k is the kinetic energy of the free electron. The line shape of the free electron to bound hole transitions is given by the same form as equation(2.1) except that in this case $E = E_g - E_a$.

Therefore, recombination of a free electron with a hole bound on an acceptor should have the required shape on the high-energy side of the emission, the intensity should increase with free-carrier density, as observed, if the acceptor concentration does not decrease equally rapidly. However, the effective-mass binding energy of shallow acceptors in ZnSe is more than 100 meV and experimentally observed values are not less than this[64]. Hence, the peak position of free electron to acceptor recombination in ZnSe would be at least 75 meV lower in energy than the blue emission under discussion. So we rule out this assignment.

2.4.6 Free hole to donor

The free hole to bound electron transitions have the same characteristics as the free electron to bound hole transitions. The energy of the emitted photon is given by

$$h\nu = E_g - E_d + E_k \qquad (2.4)$$

where E_d is the donor binding energy, typically about 27 meV in ZnSe[64,38], and E_k is the kinetic energy of the free hole in the valence band. The line shape of the transition between a free hole to an electron bound at an isolated donor takes the form of equation(2.1), but now $E = E_g - E_d$. One can readily find out that the peak energy of this emission is

$$E_p = E_g - E_d + \frac{1}{2}kT \qquad (2.5)$$

Therefore, recombination of a free hole with a electron bound on a donor would have the required shape on the high-energy side

of the emission band and gives a peak position in the required energy range. This possibility is discussed in greater detail in the next section.

2.5 Recombination of a free hole with an electron on donor

The free hole to donor recombination is attractive as a mechanism for the blue emission, as emphasized by Shirakawa and Kukimoto[40]. A free carrier is involved, as required by the thermal broadening of the high-energy side of the emission band. An increase of the free electron concentration is accompanied by an increase of the concentration of electrons on donors so the corresponding increase in intensity shown in Fig.2.4 is explained at least qualitatively. The energy of the emission peak is about 27 meV below the band gap and this is where most shallow donors in ZnSe have their energy[38]. The thermal quenching can then be attributed to thermal ionization of the donors.

Closer investigation reveals problems with this assignment. Firstly, the shape of the emission band should follow equation(2.1) with $E = E_g - E_d$ being the energy above the threshold energy. The emission peak should be $\frac{1}{2}kT$ above the threshold energy, as can be seen from equation(2.5). This is inconsistent with the observation that the separation between the emission peak and the free exciton position does not change with temperature. Secondly, the donor binding energy decreases with

increasing donor concentration[46], and goes to zero at $N_d^+ \sim 3 \times 10^{17}$ cm^{-3}. It is then surprising that the observed peak position is almost independent of carrier concentration, even in our material with metallic conductivity and zero ionization energy. Although the band gap decreases with increasing carrier concentration this is a comparatively small effect, insufficient to balance the decrease in the donor binding energy. Finally, the shape of the emission band should have a steep rise in the low-energy side, as implied in equation(2.1). This is inconsistent with the observed shape in the low-energy side, which broadens with increasing donor concentration.

There is a possible resolution of the difficulties. As the donor concentration increases the donor wave functions overlap and the donor level broadens into a band. Because of the random distribution of donor atoms on the lattice sites there is an additional spread of the donor levels through donor-donor Coulomb interaction. The situation is shown schematically in Fig.2.9. At low donor concentrations the density of states approaches a δ-function. At intermediate concentrations the increased broadening and the shift of the peak towards the conduction band eventually leads to the donor levels merging with the conduction band. There is an approximately exponentially decreasing tail in the donor density of states at low energy. In this tail there are levels from donors which, by chance, have a greater separation from other donors than average. At first sight one expects the donor-free-hole recombination to show the donor banding, with the tail of states giving a broadening of the

luminescence on the lower-energy side. Figure 2.3 shows that at temperature of 5.2 K, where the thermal broadening due to the kinetic energy of the hole does not obscure the effects, there is indeed a low-energy tail but there is an unexpected cutoff on the high-energy side. It looks therefore as if the emission comes predominantly from the more isolated donors and the strongly interacting donors do not contribute substantially.

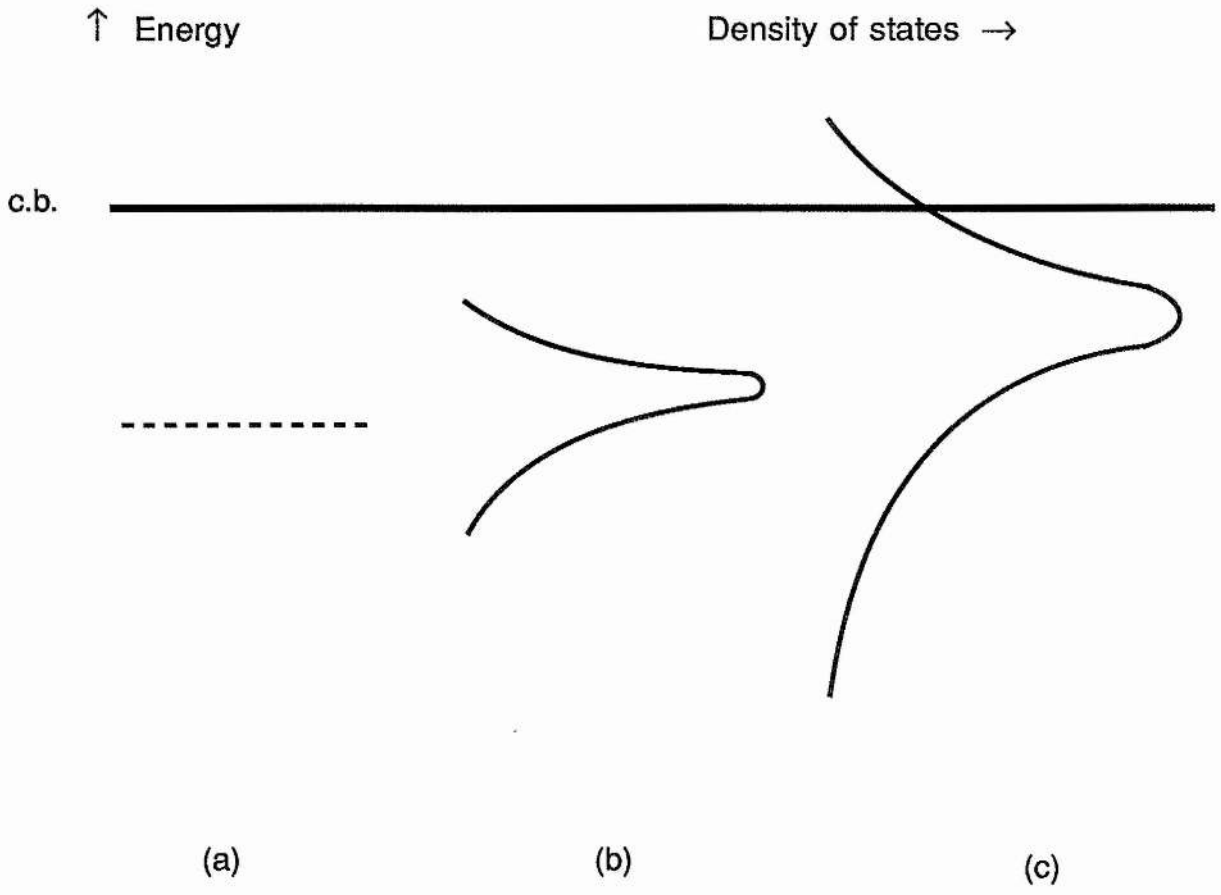

Fig.2.9 Schematic diagram of the density of states in the donor band at (a) low, (b) intermediate and (c) high donor concentrations, showing the broadening and the shift towards the conduction band.

The cause of the cutoff in the donor density of states is not immediately clear. It cannot arise from occupancy, i.e., a Fermi level cutoff, because in the materials we have discussed, the Fermi level varies by several tens of meV but the peak position does not. Also, Shirakawa and Kukimoto[40] found the same blue emission spectrum in an as-grown material with low electron concentration and in a zinc-treated material with high electron concentration. If there were a quasi-equilibrium distribution of electrons over the donor levels the level occupation would be quite different in the two cases. However, if capture into donors is faster than other processes, then in the as-grown material the density of occupied states in the energy tail will be proportional to the density of states. In the zinc-treated material all states in the tail are occupied. Hence if the cutoff is at an energy well below the Fermi energy in the zinc-treated material the shape of the emission band will be the same in the as-grown and zinc-treated material, as observed. It is possible that the cutoff is related to a localization edge in the donor energy distribution which may be the same as the mobility edge[65]. The donor wave functions are to a good approximation a linear combination of Bloch functions $u(\mathbf{k},\mathbf{r})e^{i\mathbf{k}\cdot\mathbf{r}}$ taken from near the bottom of the conduction band. The $u(\mathbf{k},\mathbf{r})$ are mainly *s* type for the conduction band and are mainly *p* type for the valence band so their contribution to the matrix element is allowed. Because the crystal momentum of the photon is small, efficient radiative recombination requires that the donor wave functions must have sufficient spread in **k** space (and hence must have sufficient

localization in **r** space) to cover the thermal spread of holes in **k** space. Hence recombination through the localized states in the donor tail below the localization edge is more probable than through delocalized states above it. This effect is enhanced by transport processes. When an electron in an energy level in the donor tail below the mobility edge recombines with a hole, the level can only be replenished by an electron moving to its spatial position, i.e., by an electron from above the mobility edge. The localization edge corresponds with donors with a certain spacing within the distribution of donor spacings and hence to a certain donor energy. This explains why the peak position of the blue emission, which is determined mainly by the cutoff energy, does not depend on donor concentration.

2.6 Line shape calculation based on a simple model

As we have pointed out in the last section, if the donor density of states is a δ – function (low donor concentration) then the emission shape is largely governed by the hole distribution function and the emission peak position is at $\frac{1}{2}kT$ above the threshold energy. If, instead, the donor is broadened into a band then the emission shape is given by a convolution of the donor density of states, the transition probability as a function of energy, and the hole distribution function. The peak position is determined by the localization edge. As the temperature dependence of the localization edge is the same as the temperature dependence of the free exciton position, this

explains why the separation between the emission peak and the free exciton position does not change obviously with temperature.

A numerical calculation can be carried out based on the following assumptions.

(1) The donor density of states has an exponential tail at low energy.

(2) There is an energy cut-off in the donor density of states. Only those donors with energies below the cut-off energy contribute to the donor-free-hole recombination. The contribution of donors with energy higher than cut-off energy is negligible.

(3) Constant matrix element for those donors which contribute to the recombination.

With the above assumptions, we have the convolution formula for the intensity I(hν) of the donor-hole recombination as follows

$$I(h\nu) = \int_{-\infty}^{h\nu} f(E)(h\nu - E)^{1/2} \exp\left(-\frac{h\nu - E}{kT}\right) dE. \qquad (2.6)$$

For f(E) we used the function,

$$f(E) = A\exp(E/E_o), \qquad E < E_{co},$$

$$f(E) = 0, \qquad E > E_{co},$$

where A is a scale factor, E_o is a constant for the exponential tail of the donor density of states in the donor band, and E_{co} is the

cutoff energy, which could be related to a localization edge in the donor energy distribution.

We have calculated the convoluted intensity of donor-hole recombination at 30 K and 290 K by using equation (2.6). These two spectra are shown in Fig.2.10 and Fig.2.11 together with the experimental luminescence line shapes of material with electron concentration of 1.1 $\times 10^{18}$ cm^{-3}, which is obtained by Hall and resistivity measurements at room temperature. It can be seen that this simple model, with two parameters E_{co} and E_o adjustable, fits the observed spectra reasonably well. E_{co} normally takes the emission peak value, which changes with temperature the same way as the band gap does. E_o changes slightly with temperature, this is because of the thermal effect. Actually, one could improve the simple model, for instance, including a phonon broadening in the convolution to take into account the fact that the value of E_o required to give the best fit varies with temperature. However, one would have too many disposable parameters for the fit to be convincing.

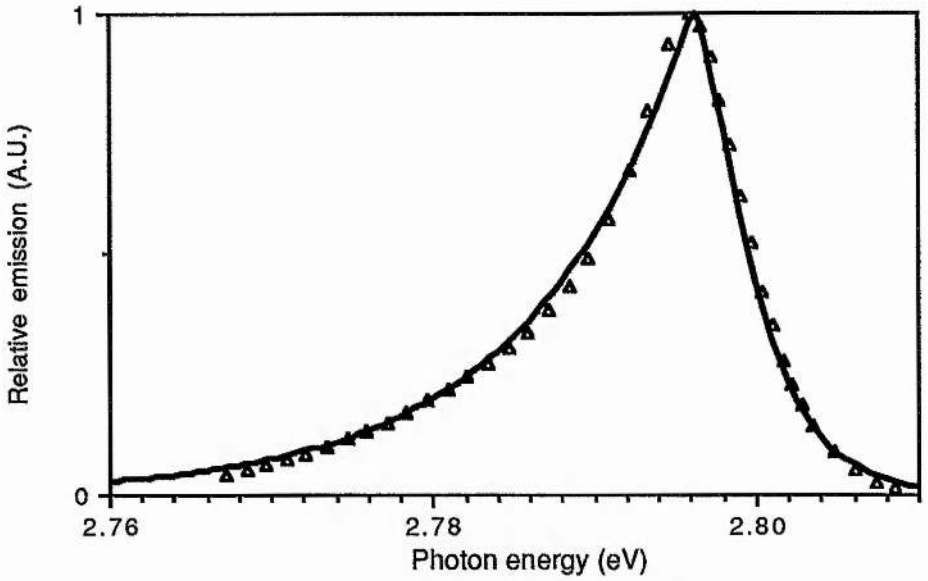

Fig.2.10 The measured luminescence line shape at 30 K (Δ) for a MOCVD ZnSe with carrier concentration of 1.1×10^{18} cm^{-3} and the convoluted intensity (solid line) calculated by equation (2.6) with E_o=10 meV and E_{co}=2.796 eV at the same temperature.

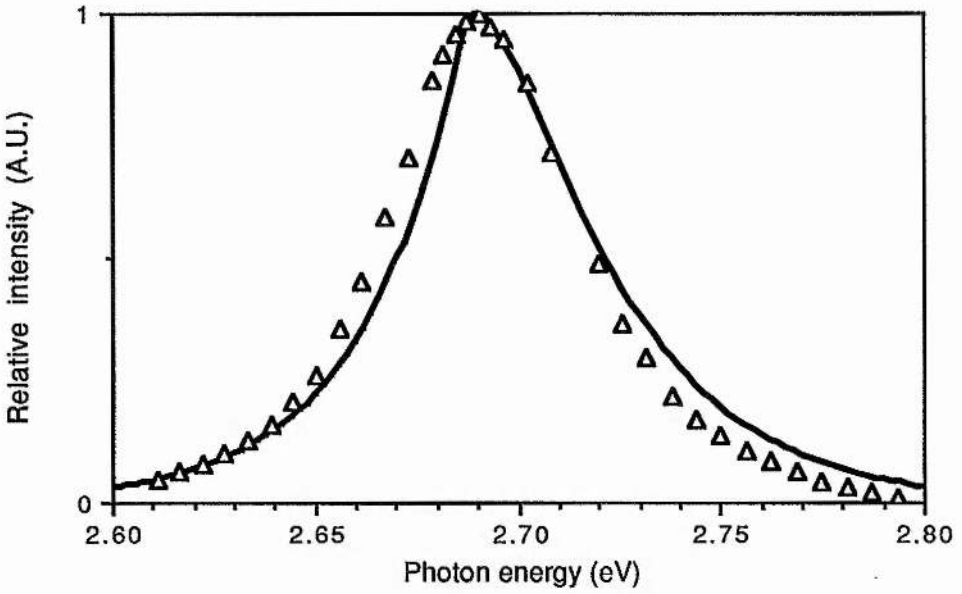

Fig.2.11 The measured luminescence line shape at 292 K (Δ) for a MOCVD ZnSe with carrier concentration of 1.1×10^{18} cm^{-3} and the convoluted intensity (solid line) calculated by equation (2.6) with E_o=20 meV and E_{co}=2.690 eV at the same temperature.

2.7 Discussion and conclusions

The blue emission band under discussion, which is dominant at room temperature in zinc selenide crystals made under a wide variety of conditions, appears to arise from a transition between an electron bound to a donor and a free hole as pointed out by Shirakawa and Kokimoto[40]. However, this simple transition cannot explain the observed line shape and temperature dependence of the emission peak position. In the material for which we produce new data the donor concentration is so high that a metallic band merged with the conduction band has formed, but the emission is still seen with the same peak energy as in low donor concentration material. We have discussed in the last two sections that not all donors contribute to the transition when the donor concentration is high enough for an appreciable spread of donor energies to occur. There is an upper energy cutoff in the donor density of states, which may be the same as mobility edge[65]. Only those donors with energies below the cutoff energy contribute to the recombination. We have presented evidence that this may be associated with the fact that, within the spread of donor energies, the deeper donors are more localized than the shallow donors and have greater recombination probability with free holes. Therefore we suggest that the emission comes predominantly from donors that by statistical fluctuation are more separated from other donors than average.

Under other conditions other emissions are possible at room temperature, although the intensity may not be strong enough to

have practical use. The spectra of Yoshikawa et al[30] for electron concentrations greater than 1.0×10^{18} cm^{-3} show a much broader band with a shift on the high-energy side which would be consistent with a band-to-band transition shifted by the Moss-Burstein effect of band filling. At such high carrier concentration, the three-carrier Auger quenching, in which the energy of the emitted photon is given to a third carrier, is the main reason for decrease of the radiative recombination efficiency. The fall of the intensity at electron concentrations higher than 1.0^{18} cm^{-3}, which is shown in Fig.2.3, indicates that one cannot have a stronger blue emission in ZnSe by very high doping.

Because the particular emission which we are discussing decreases in intensity as the donor concentration decreases, we expect that in material with sufficiently low donor concentration (which is not synonymous with low electron concentration) the free exciton emission will be dominant even at room temperature. This emission could be too weak at room temperature to be useful for blue LEDs, but as a possible recombination mechanism, accurate spectrum measurements in material with very low donor concentration will be necessary to establish this.

A motive for investigating the origin of the room temperature blue emission is the possibility of making blue light emitting diodes, as already demonstrated[32,39]. Further, it might be possible to make blue semiconductor injection lasers. In pursuit of this latter aim there have been many investigations of quantum

well structures based on zinc selenide and the mixed crystals of zinc selenide and zinc sulphide. In analogy with III-V compounds it is expected that the confined exciton will have a sufficiently enhanced radiative recombination probability that good emission can be obtained at room temperature. It is interesting to note that in ZnSe and $ZnSe_xS_{1-x}$ quantum wells emissions from confined excitons and from donor to free hole transitions could be in competition at room temperature.

Room temperature lasing in ZnSe with electron-beam excitation has been reported by Colak et al[66]. These authors were unable to identify the transition involved. Their spectra taken below the lasing threshold are similar to the ones discussed here except that the peak position is at slightly lower energy, e.g., 2.63 eV, when the specimen is nominally at 300 K. The shift could be due to self-absorption on the high-energy side because the emission was observed on the opposite side to the excitation for 10-30 μm thick samples, or due to the band gap shrinkage at high density of electron-hole pairs in the electron-beam excitation. More careful experiments should reveal whether in these lasers the transition is also between a free hole and an electron bound to a donor.

Chapter 3 Blue electroluminescence in ZnSe

3.1 Introduction

A semiconductor can generate light when electron-hole pairs are created in the material, or when carriers are excited into higher impurity levels from which they fall to their equilibrium states. These non-equilibrium carriers can be created by optical excitation, electron bombardment and injection of carriers across a p-n junction. If the material is excited electrically through contacts, the resulting luminescence is called electro-luminescence. Commercially, the most important electro-luminescent device is the light-emitting diode (LED), in which some of the minority carriers that are injected across a forward-biased p-n junction recombine radiatively.

For the usual III-V compound p-n junction LEDs, there is a fairly good understanding of what goes on. However, the conversion efficiency of electrical to optical power is still very low (no more than 5% for a good commercial $Al_xGa_{1-x}As$ red LED, though as high as 25% for a recent experimental result)[67]. As a semiconductor strongly absorbs photons with higher energy than the band gap of the material, the LEDs made from the usual III-V compounds can emit light only up to green. When one goes to wider band gap materials like GaN, SiC, ZnSe or ZnS to extend the emission to shorter wavelength, a number of problems occur. Firstly, the development of wider band gap materials for blue or ultraviolet electroluminescent devices is generally complicated by either the crystal growth conditions (SiC) or the difficulty in achieving good p-type conductivity (ZnSe, ZnS, GaN) because of

the compensation which is partly due to thermodynamic effect. Secondly, the chance of getting deep levels (impurities or lattice defects: these centres can be radiative or non-radiative) within the band gap increases greatly in the wider band gap materials, as a result these materials are good deep-level phosphors, which is undesirable for devices making use of the near-band-edge emission. Thirdly, the technology for making contacts to these materials has not yet been well developed.

ZnSe has long been considered as a candidate for producing blue light. Despite over 20 years of development, the blue ZnSe LEDs have not shown up in the market. Recent progress in low temperature growth techniques such as MOCVD and MBE has demonstrated that n-type conductivity in ZnSe can be achieved in a controllable manner[30,31]. Now problems mainly lie on the difficulties in obtaining controllable good p-type conductivity and good minority carrier injection. Good p-type ZnSe can also be grown by using growth techniques such as MBE or MOCVD which avoid high temperatures so the grown material is not in thermodynamic equilibrium. There are a great number of works on growing p-type ZnSe with dopants such as nitrogen, sodium, lithium and lithium nitride, and making ZnSe p-n junctions[32,33,68,69], however, reproducibility of p-type growth has not yet been achieved. Moreover, the degradation of devices made from a ZnSe p-n junction could be a problem because of the non-equilibrium growth. This remains to be seen.

In this chapter we discuss the blue electroluminescence in ZnSe by using the metal-insulator-semiconductor (MIS) structure. (The insulator, insulating layer, semi-insulating layer and zinc

oxide layer are used with the same meaning throughout this chapter.) This could be an alternative structure for producing blue LEDs if the p-n junction blue ZnSe LEDs turn out not to work adequately. There are a few reports on the blue electroluminescence from the forward bias ZnSe MIS diodes at room temperature[39,43,44,45], but there is no general agreement on the assignment of the blue emission at room temperature and on the hole injection mechanism. We report here the blue electroluminescence spectra from MIS structures of both bulk and epitaxial ZnSe, and the photoluminescence spectra from the same devices. Our discussions are focussed on the following problems:

(1) What is the origin of the blue electroluminescence in ZnSe at room temperature? Is it the same as the one observed in photoluminescence?

(2) What is the most probable minority carrier injection mechanism for the blue electroluminescnece? How can we improve the injection efficiency?

3.2 Materials and sample preparation

Both bulk and epitaxial n-type ZnSe crystals were used in this study. The bulk ZnSe was grown by a sublimation method at 1025 °C in our laboratory and had been heat-treated in molten zinc/aluminium at 960 °C to make it conducting. The carrier concentration at room temperature was ~ 10^{16} cm^{-3}, which was determined from capacitance-voltage measurements. Epitaxial layers of ZnSe were grown on GaAs substrates by MOCVD with

iodine as the dopant in the Solid State Chemistry Group at UMIST. The growth was at atmospheric pressure using dimethylzinc and hydrogen selenide, with a substrate temperature of 280 °C. The epilayer thickness was between 3 to 5 μm. Carrier concentrations at room temperature obtained from capacitance-voltage characteristics and from Hall and resistivity measurements are in the range of 10^{17} to 10^{18} cm^{-3}, which depends on the flux ratio of dimethylzinc to hydrogen selenide during the crystal growth.

Dice with dimensions of $2 \times 2 \times 1$ mm^3 were cut from the bulk single crystal. After polishing and etching, ohmic contacts were made by alloying indium dots. A Schottky contact was made by evaporating a thin aluminium dot with ~ 1 mm diameter. Prior to the evaporation of the aluminium contact the material was etched in a solution of 5% bromine in methanol. This chemical etching leaves a layer of zinc oxide and selenium on the surface. The selenium readily dissolves in carbon disulphide and the remaining zinc oxide constituted the insulating layer[70]. Similar chemical etching procedure for the production of the insulating layer did not work well for the epitaxial layers because the ZnSe film is only a few micrometers thick. Instead, the insulating layer was prepared in one of the following two ways: by oxidising the epitaxial ZnSe film in acetone at about 80 °C to produce an insulating or semi-insulating zinc oxide layer on the ZnSe surface or by evaporating a thin ZnS film onto ZnSe using a Nanotech evaporator with a thickness monitor. The thickness of the ZnS layer is between 500 Å to 700 Å. In order to avoid the effect of the interface between ZnSe and GaAs, both the ohmic contacts and Schottky contact are made on the ZnSe surface. Figure 3.1 shows

the structures of the MIS diodes on both the bulk and epilayer ZnSe. Most of the ZnSe diodes prepared in these ways with an insulating or semi-insulating layer beneath the metal Schottky contact show spotty electroluminescence under forward biases.

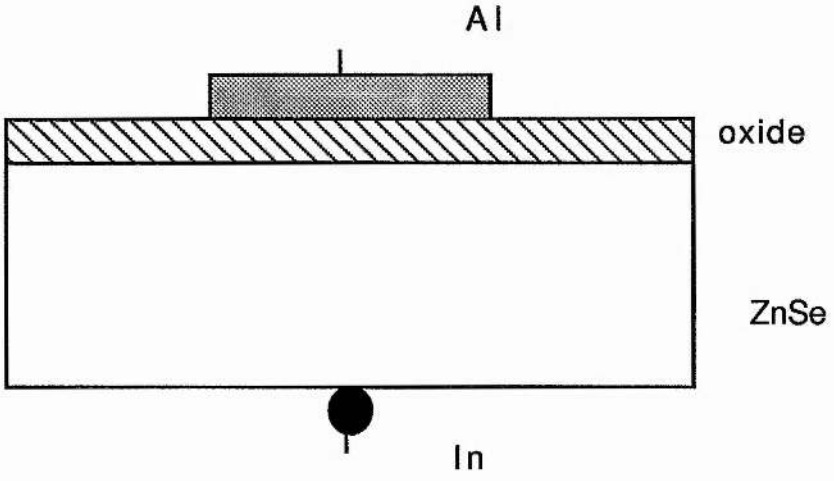

(a)

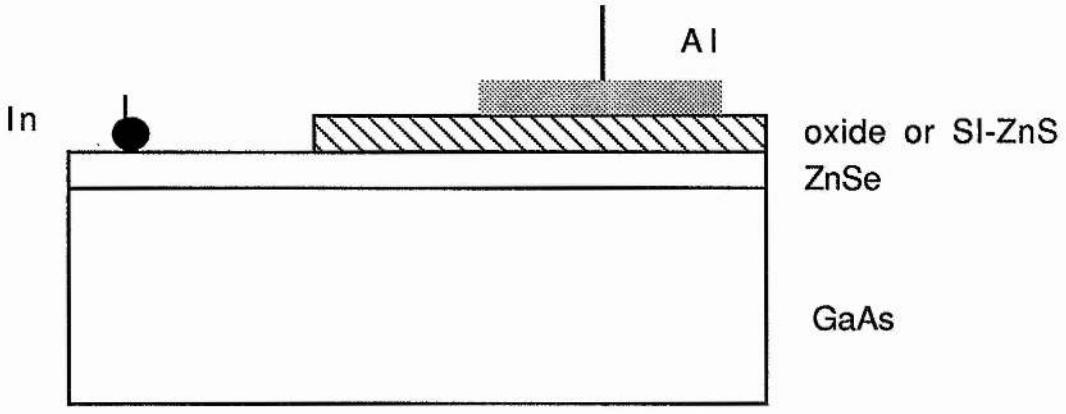

(b)

Fig.3.1 Schematical diagrams of the structures of MIS diodes on both bulk (a) and epilayer (b) ZnSe.

The sample is mounted with a small indium dot under spring pressure on a cold finger of a gas-flow cryostat. The sample temperature can be continuously varied between liquid helium and room temperature. A grating monochromator with a dispersion of 8.2 Å/mm was used to spectrally resolve the luminescence. The detector was a photomultiplier type 9558B with S-20 response. The spectral distribution of the electroluminescence was measured by a photon counting system which can be controlled by a microcomputer or by a Boxcar averager depending on whether the excitation is by DC bias or pulsed bias. The photoluminescence spectra were measured by the lock-in technique with the 365 nm line from an intense mercury lamp as the excitation source. The spectra shown in this chapter have not been corrected for system response, as the blue spectra reported here only cover an energy range of 0.2 eV.

3.3 Experimental results

3.3.1 Characterization of MIS ZnSe diodes

The presence of the insulating layer in our MIS structure ZnSe diodes can easily be seen from reverse bias capacitance-voltage measurements at a frequency of 1MHz. At lower frequencies the measurements are affected by the interface states. In general a plot of C^{-2} vs V is linear, the slope giving the carrier concentration of the material and the voltage intercept indicating the thickness of the insulating layer. Figure 3.2 shows the capacitance-voltage plots on MOCVD ZnSe diodes with and

without a deliberately produced insulating layer. From the slope a carrier concentration of $\sim 5 \times 10^{17}$ cm^{-3} is obtained. From the intercept with the voltage axis, and using Cowley's theory[71], we estimate the thickness of the insulating layer (zinc oxide or ZnS) in all our MIS diodes to be more than 200 Å.

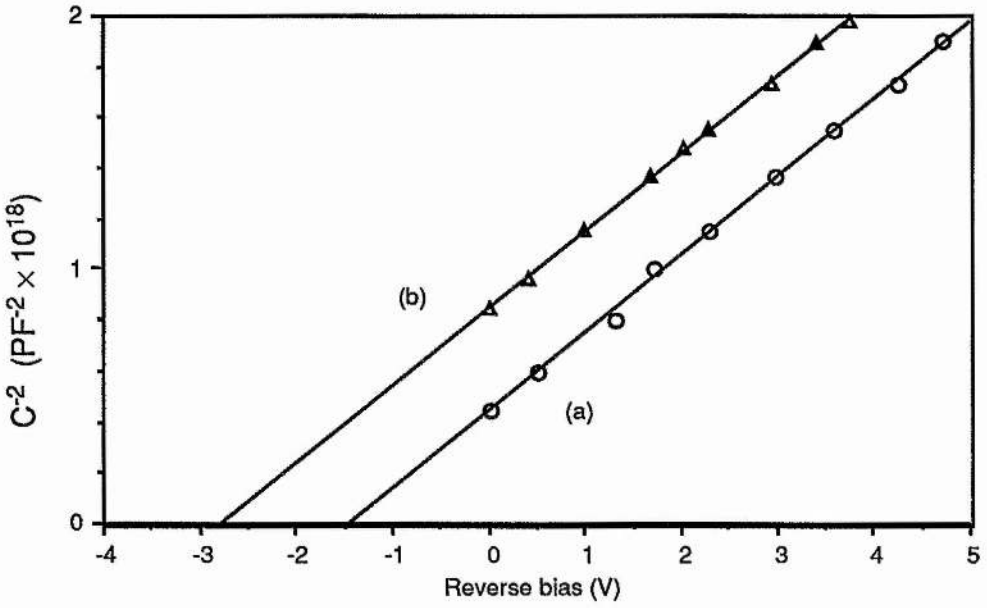

Fig.3.2 The reverse bias capacitance-voltage characteristics of a typical MOCVD ZnSe diode with (b) and without (a) a deliberately added insulating layer.

Figure 3.3 shows the room temperature forward bias and reverse bias current-voltage relationships of a typical MOCVD ZnSe MIS diode. In forward bias, the current increases approximately exponentially with applied voltage until the voltage drop on the series resistance becomes big. The forward bias current decreases with increasing insulating layer thickness at the same applied voltage. The diode shows good rectification

under reverse bias. There is no obvious dependence on the shape of the current-voltage curves with temperature.

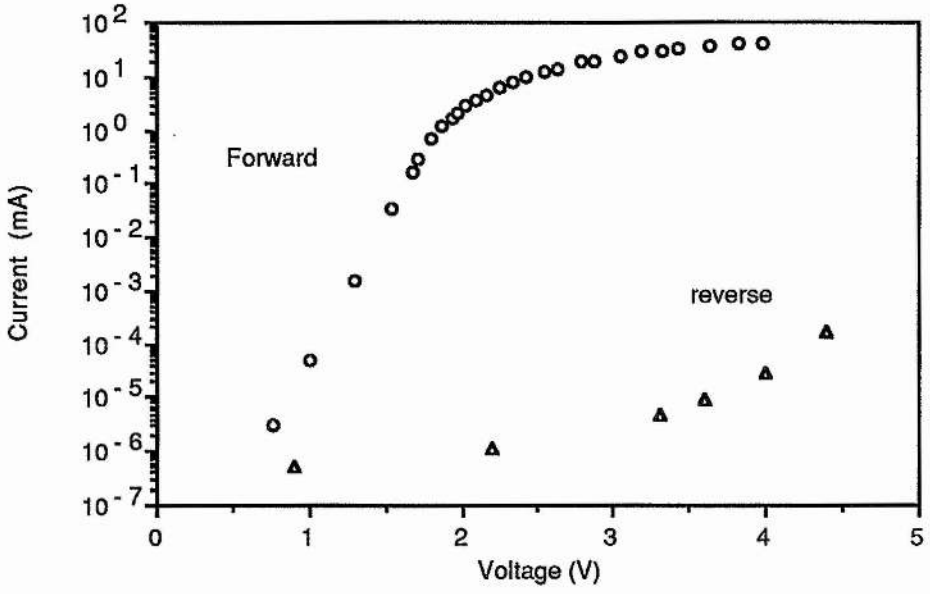

Fig.3.3 The forward and reverse bias current-voltage relationships of an epilayer ZnSe MIS diode at room temperature.

3.3.2 Electroluminescence spectra

At 77K most of the MIS diodes emitted blue light when a forward bias was applied. The emission appeared fairly uniform in the bulk grown ZnSe diodes while it appeared to be localized in several spots in the epilayer ZnSe diodes. The minimum threshold voltage for electroluminescence was found to be 1.3V and 1.6V in the MIS diodes with zinc oxide and insulating ZnS as the insulator respectively. Only the epilayer ZnSe diodes showed appreciable blue electroluminescence at room temperature.

The edge electroluminescence spectra at liquid nitrogen temperature from a bulk grown ZnSe MIS diode are shown in Fig.3.4. The spectra consist of two bands, which are named as E1 band and E2 band respectively. The E1 band has a peak energy of 2.787 eV and the E2 band consists of a zero-phonon line at 2.692 eV and three LO-phonon replicas with phonon energy of 31 ± 1 meV. Other than these edge emissions, a weak self-activated (SA) emission has also been observed in the electroluminescence with peak energy at 2.06 eV (at a wavelength of 6020 Å) at liquid nitrogen temperature. When the temperature increased, both the E1 and E2 band were quenched thermally. Figure 3.5 shows the temperature dependence of the peak intensity of the E1 band and zero-phonon line of the E2 band. These peak intensities were measured at the same forward bias current of 10 mA. The E2 band could not be detected at temperatures higher than 140 K by our measuring system and the E1 band could not be detected at temperatures higher than 250 K. Figure 3.6 shows the E1 emission band taken at 200K, which was measured by a photon counter with a forward bias current of 20 mA passing through the diode.

Figure 3.7 shows the blue electroluminescence spectra at liquid nitrogen temperature and room temperature from a MOCVD grown epitaxial ZnSe MIS diode. The emission was from several spots and looked blue to the human eye. Only a single emission band was observed in the electroluminescence at both temperatures. The peak energy is 2.788 eV at liquid nitrogen temperature and 2.69 eV at room temperature. The total half-width of the blue emission is about 17 meV at liquid nitrogen

temperature and 50 meV at room temperature. The spectrum at 77 K is measured by a Boxcar averager at a forward bias pulsed current of 50 mA, and the spectrum at room temperature is measured by a photon counter at a forward bias current of 20 mA.

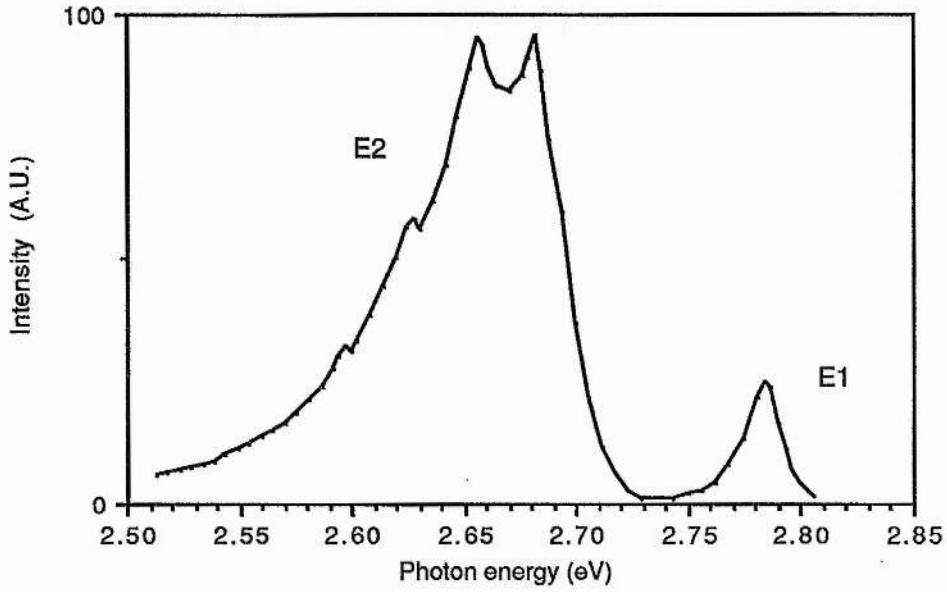

Fig.3.4 The forward bias electroluminescence spectrum from a bulk grown ZnSe MIS diode at liquid nitrogen temperature.

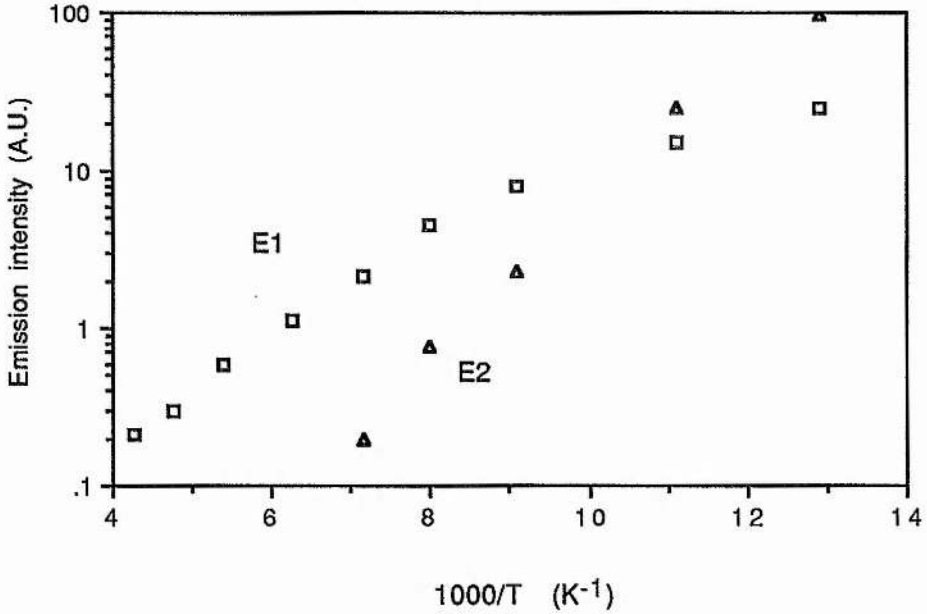

Fig.3.5 The temperature dependence of the peak intensity of the E1 and E2 emission bands shown in Fig.3.4, the intensity was measured at the same forward bias current of 10 mA.

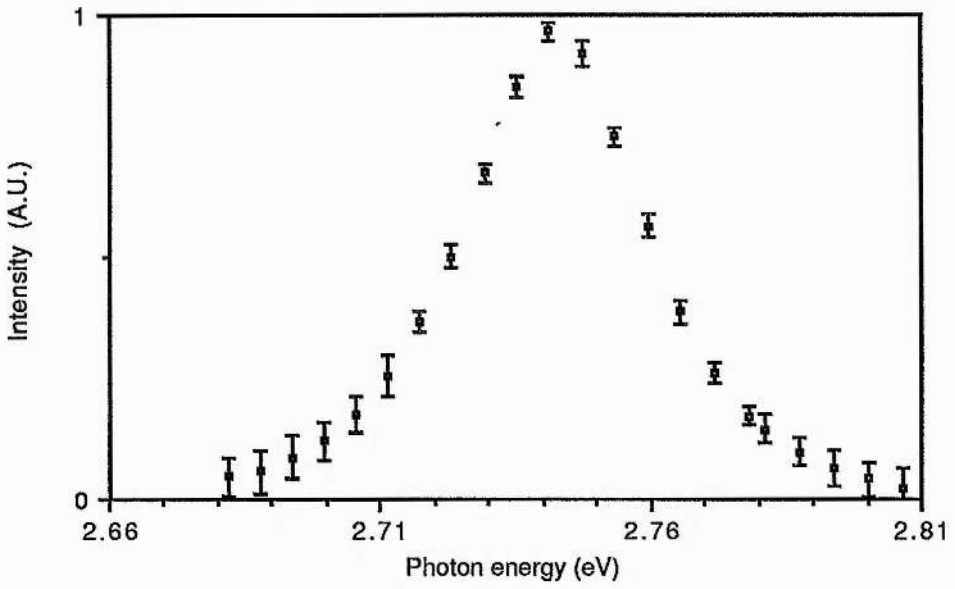

Fig.3.6 The forward bias electroluminescence spectrum from a bulk grown ZnSe MIS diode at 200 K. The spectrum was measured by a photon counting system.

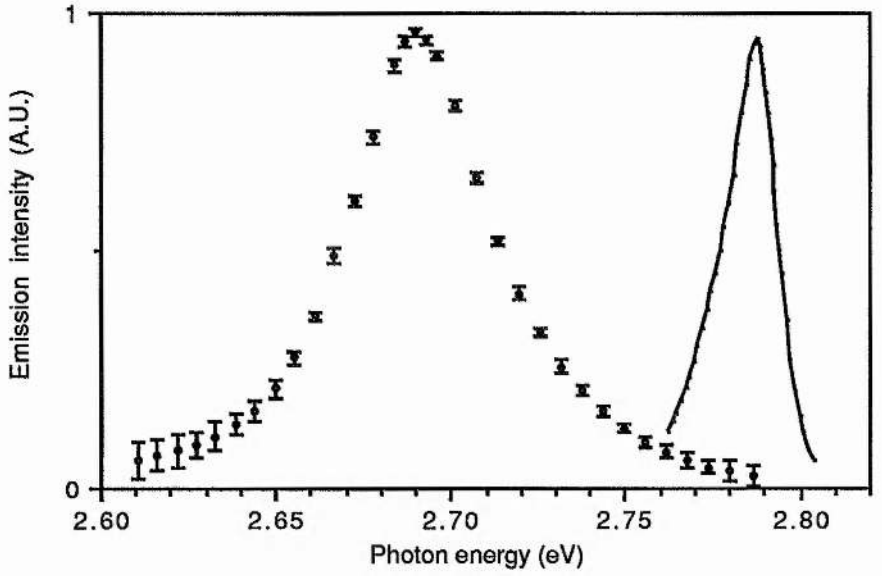

Fig.3.7 The forward bias electroluminescence from a MOCVD grown ZnSe MIS diode at liquid nitrogen temperature (solid line) and room temperature (dots with error bars). The peak intensities have been normalized to the same height.

3.3.3 Photoluminescence spectra

In order to compare the electroluminescence with photoluminescence directly, we have made photoluminescence measurements on MIS ZnSe diodes. The results are presented in this section.

The photoluminescence spectra of the bulk ZnSe at liquid nitrogen temperature have the same emission shape and energy position as the electroluminescence spectra, but the relative intensities of the emission bands are different. The ratio of the peak intensity of the E1 band to the peak intensity of the E2 band is 0.25 in electroluminescence and 0.03 in photoluminescence, while the intensity ratio of the E1 band to the SA band is 3.0 in electroluminescence and 0.3 in photoluminescence. All these values were taken at 77 K.

Figure 3.8 shows the room temperature photoluminescence spectrum of the MOCVD grown ZnSe with the insulating layer and the metal contact on the the ZnSe surface. The blue emission shows higher peak intensity than the SA emission in the photoluminescence spectrum at room temperature, but the integrated intensity of the SA emission is stronger. In order to compare the electroluminescence with photoluminescence, the edge photoluminescence is shown in Fig.3.9 together with the electroluminescence, both spectra have been normalized at the peak intensity. One readily sees that they have a similar line shape and the same energy position. The increased width of the emission in the electroluminescence is probably due to the poorer resolution being used in the electroluminescence measurements.

The SA emission is seen in the photoluminescence with a peak intensity ratio of 0.3 to the blue emission, but it is not seen in the electroluminescence probably because it is below the detection limit.

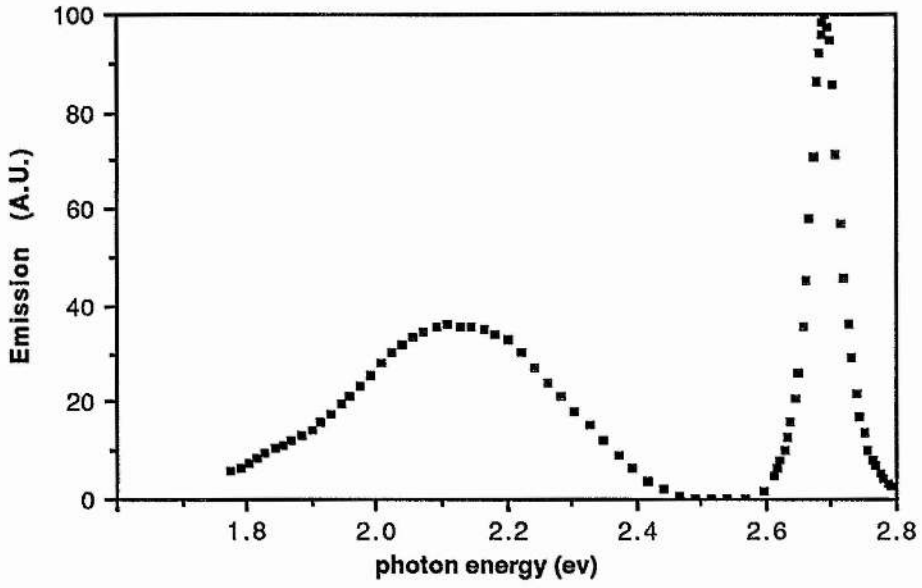

Fig.3.8 The near-band-edge and deep level emissions of a MOCVD grown ZnSe at room temperature.

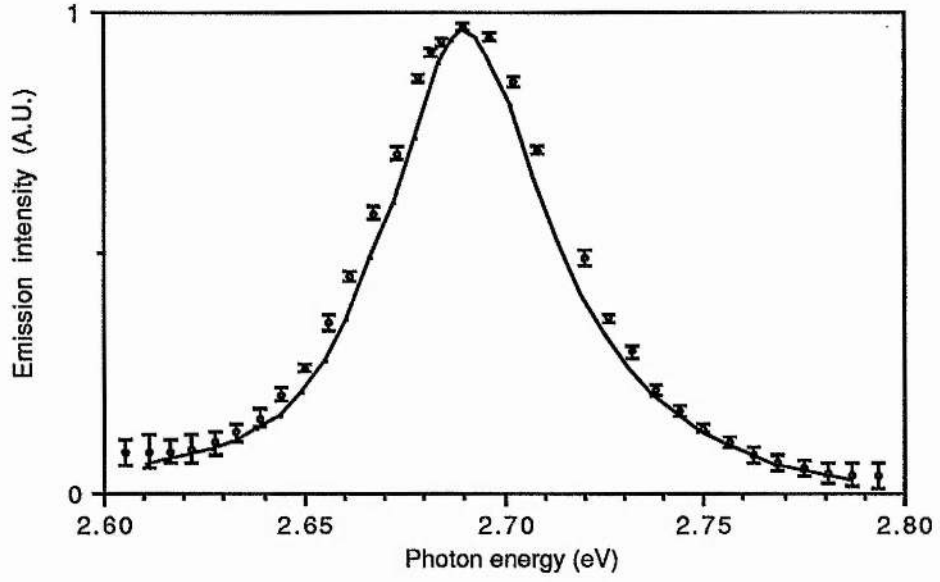

Fig.3.9 The comparison of room temperature blue photo-luminescence (solid line) with froward bias electroluminescence (dots with error bars) from a MOCVD grown MIS ZnSe.

3.4 Discussion

3.4.1 The origin of the blue electroluminescence in ZnSe at room temperature

There has been a considerable amount of work on minority carrier injection with MIS structures in ZnSe in order to produce blue light. But most of the work on blue electroluminescence reported is at low temperatures, only some at room temperature. We discuss here the attributions of the room temperature blue emission which have been made in the literature.

Ryall and Allen[39] saw blue electroluminescence from 95 K to room temperature in MIS ZnSe diodes with zinc oxide as the insulating layer. The authors attributed the blue emission to the recombination of free excitons because the emission peak energy agrees well with the exciton energy obtained by Hite et al[63]. Figure 3.10 shows the peak energy of the blue emission as a function of temperature by Ryall and Allen[39], the free exciton energy obtained by Hite et al[63] from reflectance measurements, and the free exciton energy obtained by Shirakawa and Kukimoto[40] from the excitation spectra. One sees that the peak position in the electroluminescence is close to the free exciton energy and also agrees approximately with the blue emission peak in our photoluminescence (see chapter 2). However, if the blue electroluminescence is due to the free exciton recombination, the peak position should be $\frac{1}{2}$ kT higher than the free exciton energy, as was discussed in chapter 2. Therefore, the assignment of the blue emission to free exciton recombination is unlikely.

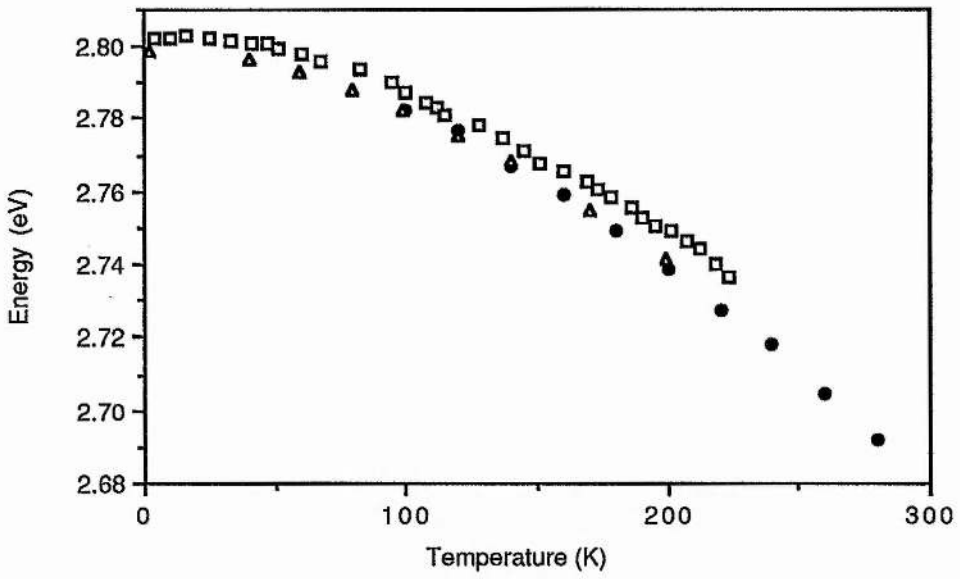

Fig.3.10 The peak energy (•) of the blue electroluminescence band obtained by Ryall and Allen[39] as a function of temperature together with the free exciton energy from Hike et al[63] (Δ) and the free exciton energy from Shirakawa and Kukimoto[40] (□).

Yamaguchi et al[43] measured blue electroluminescence from forward bias ZnSe MIS diodes with either zinc oxide or ion implanted layer as the insulating layer in the temperature range of 80 K to 300 K. The peak position of the blue emission was 2.655 eV at room temperature. The authors attributed the blue emission to the exciton bound to neutral donor (i.e., I_2 line) without giving any sound justification. As the binding energy of bound excitons to donors in ZnSe is only a few meV[36-38], they will all be thermally detached from donors at room temperature (thermal energy of 25 meV). Also the peak position of the emission band is at least 40 meV below the free exciton energy. Therefore the assignment is incorrect.

Fan and Woods[44] saw two emission bands in the electroluminescence at 4655Å (2.660 eV) and 4770Å (2.596 eV) at room temperature, while at low temperatures they observed many exciton lines, donor-acceptor-pair emission bands, etc. The authors followed the change of emission lines with temperature and attributed the two blue emission bands seen at room temperature to free exciton emission and 2LO-phonon assisted free exciton emission. At 20 K, they attributed the small peak at 2.804 eV in the spectrum to free exciton recombination. This peak energy agrees with the free exciton energy obtained by Shirakawa and Kukimoto[40] within experimental error, but it is about 5 meV higher than the free exciton energy obtained by Hite et al[63]. While at 290 K, the peak position of the emission which they attributed to free exciton recombination lies between 2.638 eV to 2.660 eV depending on the sample. This peak position is at least 35 meV lower than the free exciton energy obtained by either Hite et al[63] or Shirakawa and Kukimoto[40] following an extrapolation to room temperature (see Fig.3.10). Furthermore, the peak energy should be $\frac{1}{2}$ kT higher than the free exciton energy if the emission is due to free exciton recombination, as explained in chapter 2. Therefore, the assignment is improbable, but the origin of the two peaks seen at room temperature is still not clear.

Hua et al[45] observed a broad emission band (from 3500 Å to 7000 Å) centred at 2.48 eV with a shoulder at 2.695 eV (4600 Å) at room temperature in the electroluminescence of a MOCVD grown ZnSe MIS diode with a Langmuir-Blodgett film as the insulating layer. They attributed the 2.695 eV emission to band-

to-band recombination without giving any justification. The peak position of this emission is at the same energy as the one seen in our photoluminescence (see chapter 2) and is a few meV lower than the free exciton energy. As a free exciton in ZnSe has a binding energy of approximately 18-20 meV[36,63], the 2.695 eV emission band is substantially lower than the band gap energy of ZnSe. Therefore, it is not due to band-to-band recombination but could be due to a free hole to a bound electron transition, as discussed in chapter 2. The very broad band peaked at 2.48 eV was seen by Hua et al[45] in electroluminescence but not in photoluminescence. This is not a common feature that one usually sees. It is likely that this broad band is due to the transitions of hot electrons between valleys within the conduction band[72], which is sometimes observed in reverse biased Schottky diodes. But one could see the transitions even in the forward bias if the ohmic contact was poor and had rectification.

We have seen two edge emission bands in the electroluminescence of bulk grown ZnSe at liquid nitrogen temperature, see Fig.3.4. The E2 band with zero-phonon line at 2.692 eV and several phonon replicas has been attributed to the donor-acceptor pair recombination by Lozykowski et al[73] with evidence from the time-resolved measurements of the emission spectra and the band shape calculation. Assuming the band gap energy of ZnSe is 2.812 eV at liquid nitrogen temperature, the E1 band is about 25 meV below the band gap. The origin of the E1 band is not clear at this particular temperature, because the donor-bound exciton emission and the free hole to bound electron recombination would have similar emission peak position at low

temperatures. Both the E1 and E2 emission bands were quenched rapidly with increasing temperature and were not appreciable at room temperature.

We have also measured the blue electroluminescence spectra at 77 K and at room temperature in the MOCVD grown ZnSe MIS diode under forward bias. The room temperature electroluminescence spectrum is the same as the one observed in photoluminescence (see Fig.3.9). As we have studied this blue emission with a peak at 2.695 eV seen at room temperature in photoluminescence in great detail and have provided evidence that it is due to the free hole to bound electron recombination (see chapter 2), it is concluded that the blue electroluminescence seen at room temperature is also due to recombination of a free hole with a bound electron at a donor. Only those donors below the cut-off energy (see chapter 2) contributed to the recombination. Other emissions can be seen in the electroluminescence at low temperature, but they are thermally quenched and are not significant at room temperature.

For the different intensity ratio of the deep level emission to the blue emission observed in electroluminescence and photo-luminescence, there is a possible explanation. In the photoluminescence measurements, there is not only band-to-band excitation for the production of electron-hole pairs but also deep impurity-to-band excitation, therefore a considerable number of deep impurities are in the non-equilibrium states. This leads to a strong deep level emission in the photoluminescence at a moderate excitation level. While in the electroluminescence, only minority carriers are injected into the depletion region of the

semiconductor, and there is competition between different recombination channels. The resulting emission intensity depends on the individual recombination rate and the concentration of recombination centres.

3.4.2 Hole injection mechanisms in the ZnSe MIS diodes

Minority carriers can be generated electrically by injection across a p-n junction, from another semiconductor and from an electrode. We will confine ourselves to applications of the metal-insulator-semiconductor (MIS) structures. When a MIS diode is biased with metal Schottky contact positively, minority carriers are injected from the metal contact or from the insulating layer somehow into the semiconductor, and light emission from the semiconductor can be observed, but the efficiency has been very low.

There are several proposed models for the minority injection mechanisms in MIS diodes, which we now discuss. As the lowest threshold voltage for electroluminescence was found to be about the same in both types of our MIS diodes with either zinc oxide or ZnS as the insulating layer, we are not going to distinguish them in the following discussion, although the exact injection mechanism in the two types of MIS diodes can be different.

The tunneling injection model was proposed by Fischer and Moss[74] and subsequently elaborated upon by Card and Rhoderick[75]. The principles involved in this model can be explained by reference to the energy-band diagram of Fig.3.11.

When a voltage is applied to a MIS diode with the Schottky contact positively, a potential drop across the insulator is developed, and the metal Fermi level is able to descend on the band diagram towards the valence band of the semiconductor. This causes a reduction in the barrier height for minority carriers. If sufficient bias is applied, the voltage drop across the insulator raises the semiconductor valence band edge until it is level with unfilled electron levels (i.e., hole levels) in the metal, then minority carriers can tunnel from the metal into the valence band of the semiconductor. The quantum efficiency on diodes of this type (green emission from GaP MIS diodes)[76] showed a maximum for film about 40 Å thick and decreased rapidly with films thicker than 40 Å. As the insulating layer thickness of our MIS diodes is larger than 200 Å, it is too thick for this model to be applicable.

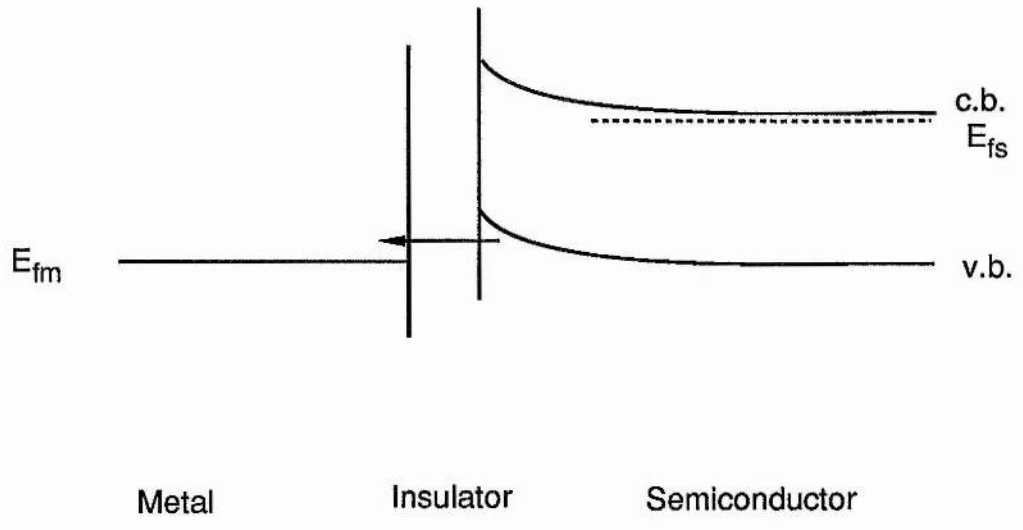

Fig.3.11 Holes are created in the valence band of ZnSe when electrons tunnel directly from the valence band of the semiconductor through the insulating layer into the metal.

Livingstone et al[70] produced Au/ZnO/ZnSe devices, which are similar to part of our devices discussed here, and obtained an enhanced quantum efficiency for yellow emission at oxide layer thickness in excess of 500 Å, which is much in excess of those allowing significant direct tunneling between the metal and semiconductor valence band. However, for these thick zinc oxide layers, which are semi-insulating and contain many defects, electron transport through the oxide can occur by hopping between defects, i.e., electrons travel from the valence band of the semiconductor through the oxide defects to the metal[77], which is the same as injection of holes into the semiconductor (see Fig.3.12). Livingstone et al[70] also measured the quantum efficiency at a current of 20 mA as a function of the applied bias necessary to maintain that current, and showed that the quantum efficiency has a threshold voltage of 1.3 V, which is approximately equal to the voltage necessary to lower the metal Fermi level down to the valence band of ZnSe, assuming the barrier height is 1.4 V.

An Auger excitation at the metal electrode was proposed by Fischer[78]. In this model electrons move from the n-type semiconductor into the metal, release certain amount of energy before they thermalized with the metal lattice, see Fig.3.13. It is assumed that this energy can be transferred to electrons in metal much below the metal Fermi level, lifting electrons up above the metal Fermi level and thus creating energetic holes, which then can be injected into the valence band of the semiconductor. However, the Auger excitation on the metal electrode cannot be efficient for hole injection because of the following reasons.

Firstly, the energy transfer can be inefficient because there are several scattering mechanisms for the incoming electrons from the semiconductor, therefore the probability of a hole being created by an electron through Auger excitation can be small. secondly, the hole lifetime in a metal is about 10^{-15} s, in order for there to be significant injection, the free hole would have to move out of the metal into the semiconductor very quickly. Finally, taking the maximum hole velocity as 10^8cm/s, then only holes produced in less than 10 Å from the metal-insulator interface could travel to the interface before they recombine with electrons.

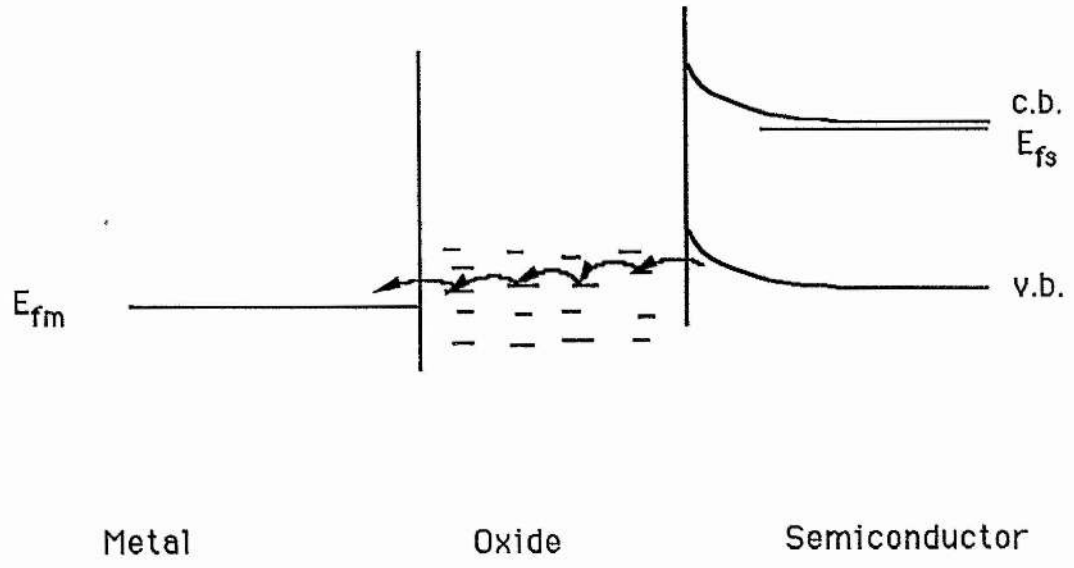

Fig.3.12 Holes are created in the valence band of ZnSe when electrons hop from the valence band of the semiconductor through defects in the insulator to the metal.

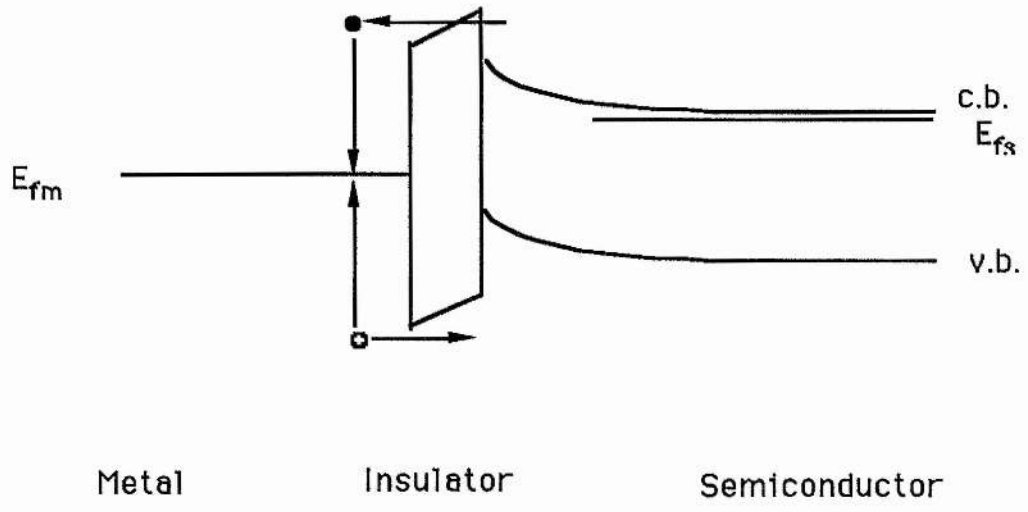

Fig.3.13 Schematic diagram showing hole creation in the metal by Auger excitation and hole injection into the semiconductor.

An impact ionization model was also proposed by Fischer[78]. In this model an electron injected from the n-type semiconductor is accelerated under the high field in the insulating layer until it gains enough energy to impact a lattice electron, the hole produced in this way in the insulator can then inject into the semiconductor (see Fig.3.14). The band gap of zinc oxide is about 3 eV and the band gap of ZnS is 3.7 eV at room temperature, the electron needs at least 3 eV (or 3.7 eV) energy before it can produce a band-to-band impact ionization in the zinc oxide (or ZnS) layer. Assuming that the potential barrier between the metal Fermi level and the conduction band of the insulator is 1.0 eV, one expects light emission from the MIS diodes only when the applied bias is larger than 4.0 V (or 4.4 V) for the zinc oxide (or ZnS) layer if the impact ionization is to account for the hole injection. Because the light emission is seen when the applied

voltage is as low as 1.3 V, and 1.6 V for both types of our MIS diodes. it is improbable that the injection is due to the impact ionization.

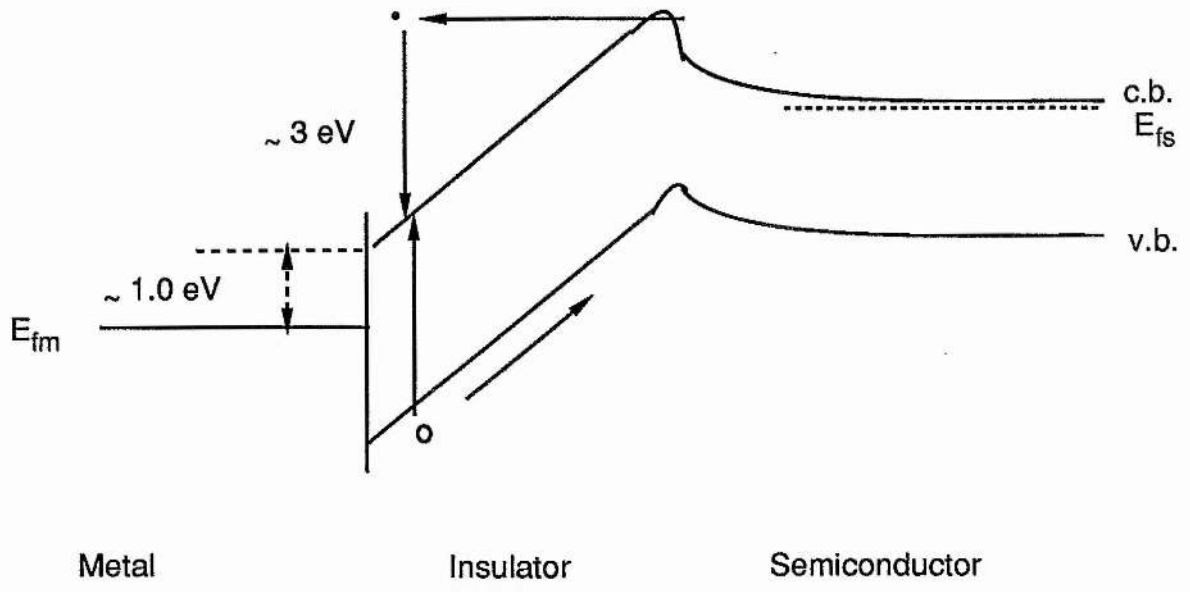

Fig.3.14 Schematic diagram of hole creation by an impact ionization of a lattice electron at the insulating layer and hole injection into the valence band of the semiconductor.

Thompson and Allen[79] proposed a two-step impact ionization model for the production of holes, see Fig.3.15. In this model an electron, accelerated under the high field in the insulating layer, impact ionizes an electron from an impurity centre to the conduction band and a second energetic electron impacts an electron from the valence band to fill the impurity centre, so producing a hole in the valence band of the insulating layer which can be injected into the semiconductor. This model is also not

applicable in our present case because the threshold voltage for the light emission would be at least 2.5 V or 2.9 V for both types of our MIS diodes.

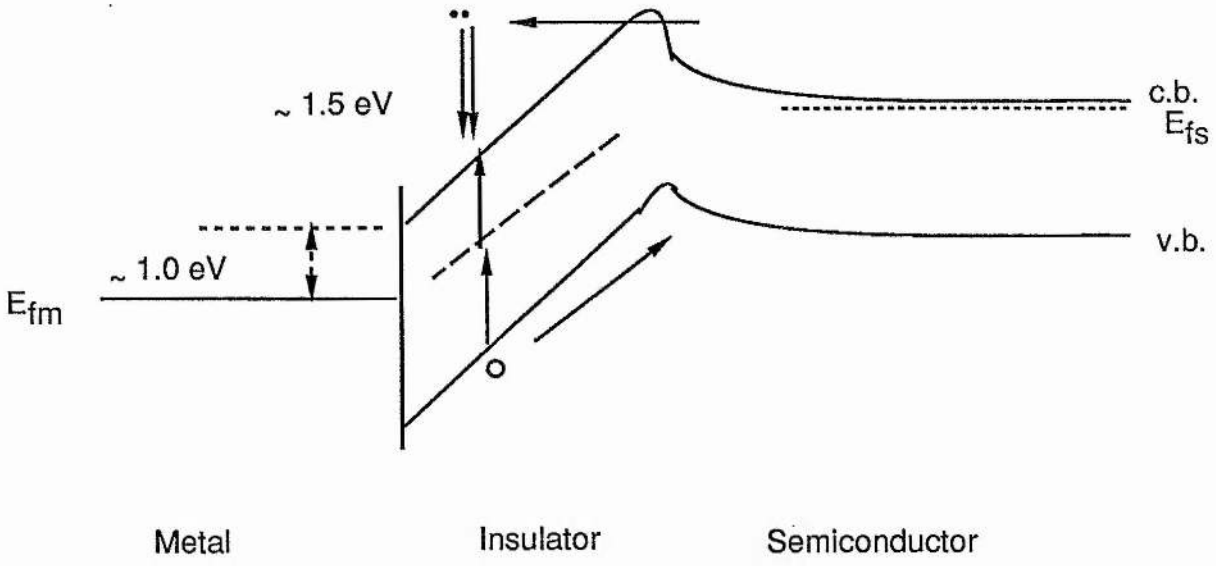

Fig.3.15 Schematic diagram of hole creation by a two-step impact ionization at the insulating layer and hole injection into the valence band of the semiconductor.

As most of the current is carried by electrons from the conduction band of the semiconductor, the absence of a pronounced temperature dependence in the current-voltage characteristics of our diodes suggests that the electron transport is of tunneling type but not of thermal emission type. However, the transport is not by direct tunneling between metal and semiconductor because the insulating layer is more than 200 Å thick, but is possibly by electron tunneling between defects in the insulating layer. Only a small component of the current is carried by holes.

From the above analysis, the most probable mechanism for the injection of holes is by the electron hopping through defects or impurities in the insulator[77]. If the insulator sustains enough voltage drop to enable the metal Fermi level to be lower than the valence band of the semiconductor, electrons can tunnel from the valence band of the semiconductor to the metal by hopping between different charge states in the insulator under the electric field. If there is a much higher concentration of defects with energy levels in the lower part of the insulator gap than in the upper part, then it is easier for electrons to travel from the valence band through the defects to the metal, i.e., to have hole injection into the semiconductor, than it is for electrons to travel from the conduction band to metal. Therefore, one could improve the injection efficiency by choosing proper insulating layer which has high concentration of defects or impurities in the lower half of the band gap. This remains to be seen.

The main problems in the blue ZnSe MIS diodes are the low efficiency and short operating life time. The blue ZnSe MIS diodes are usually not stable and are easily broken down at high applied voltage or after prolonged operation. In this section we have discussed some factors affecting the efficiency but the stability is still an unsolved problem.

3.5 Conclusions

We have made MIS diodes on both bulk and epilayer ZnSe with either zinc oxide or insulating ZnS as the insulating layer. Blue

electroluminescence has been observed in both types of material with either type of the insulating layer, i.e., zinc oxide or insulating ZnS, but only the epilayer ZnSe MIS diodes show appreciable blue electroluminescence at room temperature. The higher efficiency of the blue emission from MOCVD grown ZnSe is expected as the MOCVD ZnSe has better quality and higher carrier concentration than the sublimation grown ZnSe (referring to chapter 2). The origin of the blue electroluminescence at room temperature is the same as the one observed in photoluminescence, i.e., the recombination of free holes with bound electrons at donors, as discussed in chapter 2.

The majority carrier transport is of tunneling type, but the tunneling is not direct between semiconductor and metal. It is proposed that the electron hopping between defects in the insulating layer is the main transport mechanism. The minority carrier injection mechanism is not clear, but we have provided evidence that the hole injection by direct tunneling, by Auger excitation, by band-to-band impact ionization and by two-step impact ionization is not significant in our diodes. Electrons tunneling from the valence band of ZnSe to the metal by hopping through defect or impurity centres in the insulator could account for the hole injection.

Chapter 4 The effect of annealing on MOCVD grown ZnSe

4.1 Introduction

The potential applications of ZnSe for blue light emitters have been discussed in Chapter 2 and chapter 3. The preparation of conductive n-type and p-type ZnSe crystals with controlled carrier concentration and with high near-band-edge radiative recombination efficiency is of key importance for realizing p-n junction blue light emitting diodes. Much progress has been made in the crystal growth of both n-type[30,31] and p-type[32,33] ZnSe with the low temperature growth techniques such as MBE and MOCVD.

The electrical and optical properties of ZnSe are largely governed by the defect structure due to deviation from stoichiometry and by dissolved impurities, including accidental ones. There have been long-standing disputes as to which factor is dominant in any particular situation. In the classical view[80], the electrical conductivity was thought to be governed by native defects. A few years ago Bhargava[81] pointed out that all the shallow donors and acceptors responsible for the electrical conductivity at 300 K are impurity point defects. Recently Morimoto[47] measured the dependence of carrier concentration on the flux ratio of (growth parameter) hydrogen selenide to dimethylzinc, and claimed that the dominant donor in the MOCVD grown ZnSe which were not deliberately doped is a selenium vacancy, with carrier concentrations up to 3×10^{17} cm^{-3}. Therefore this is still a controversial issue.

From the device point of view, the electrical and optical stability of ZnSe is essential for the production of blue LEDs. It has been noticed in this laboratory that the blue light emitted from MIS structure ZnSe Schottky diodes under forward bias was not stable and the life time of the blue emission was short (i.e., the blue emission disappeared and the orange-red emission appeared in some diodes after prolonged operation). This is an unsolved problem of chapter 3. The cause is not clear but could be associated with the insulating layer beneath the metal Schottky contact or with the production of deep centres in ZnSe due to thermodynamic effect under forward bias.

Annealing crystals in certain ambients can provide evidence about the electrical and optical properties of lattice defects. Previous annealing experiments such as those of Smith[82] provided evidence for electrical activity of non-stoichiometric defects but this was at 650 °C and higher. Recently Kishida et al[83] reported deep level emission induced by annealing bulk grown ZnSe in selenium and zinc vapour. With low temperature growth techniques such as MBE and MOCVD, which avoid thermodynamic effect. The effect of the self-compensation during crystal growth could be suppressed to some extent, and therefore annealing at lower temperature becomes important.

In this chapter we present the effect of annealing between 300 °C and 450 °C on the electrical and optical properties of strongly n-type MOCVD grown ZnSe. It was found that a large change in carrier concentration can be produced by annealing at such low temperatures. The process involved has an activation

energy of only 0.26 eV and appears to be caused by a lattice defect acting as an acceptor.

4.2 Material and experiment

The ZnSe was grown epitaxially on GaAs substrates by MOCVD at UMIST. The growth was at atmospheric pressure using dimethylzinc and hydrogen selenide, with a substrate temperature of 280 °C. The layers were about 1 cm^2 in size, 3μm to 5μm thick and had electron concentration of about $(1.0 \pm 0.3) \times 10^{18}$ cm^{-3}. Strips with width about 1 mm were cut from an epitaxial layer using a Unipress wire saw, followed by cleaning with several organic solvents (i.e., toluene, acetone, and propanol), and dilute hydrochloric acid, and then were heat-treated in different atmospheres. To minimize the contamination of copper and other impurities during heating the strips were placed in containers made from high-purity germanium which were then placed in Spectrosil silica tubes. For heating in air the silica tube was open, for heating in vacuum the silica tube was connected to a rotary vacuum pump and continuously pumped during heating, and for heating in zinc or selenium vapour the silica tube was evacuated and closed after appropriate amounts of zinc or selenium had been added. All samples were cleaned with 50% NaOH solution at 50 °C for at least 10 minutes after annealing.

In order to measure the resistivity of the ZnSe epilayer, ZnSe films grown on semi-insulating GaAs substrates were used. Ohmic contacts were made to the ZnSe surface with indium dots by heating at about 310 °C in 90% N_2 / 10% H_2 Forming gas

atmosphere for 30 seconds. A current-voltage plot shows a straight line, which indicates good ohmic contacts (no rectification). The resistivity of the ZnSe epilayer is calculated from the slope of the current-voltage curve, and the carrier concentration is estimated from the resistivity by taking the electron mobility as 200 $cm^2v^{-1}s^{-1}$ at room temperature, which was obtained from a Hall effect measurement on an as-grown MOCVD ZnSe epilayer.

The photoluminescence measurements were made on the heat-treated ZnSe samples with the 365 nm line from a high intensity mercury lamp as the excitation source, the sample being in a gas-flow cryostat so that the temperature could be varied between liquid helium and room temperature. The resolution of the monochromator used to spectrally resolve the photoluminescence is 8.2 A°/mm. The luminescence spectra presented in this chapter have not been corrected for the system response, as we only want to distinguish between the self-activated emission and the Cu-red emission.

Photocapacitance measurements were made at liquid nitrogen temperature on samples with and without heat treatments. Both transient capacitance and the Double Light Source Steady-state (DLSS) techniques were used. The details of the set-up for photocapacitance measurements and the junction capacitance techniques are described in section 6.2 and section 6.3 of chapter 6. In order to avoid the effect of the interface between the ZnSe epilayer and the GaAs substrate, ZnSe grown on semi-insulating GaAs was used. Both the indium ohmic contact and the

aluminium Schottky contact (by evaporation) were made on the ZnSe side.

4.3 Experimental results

4.3.1 Conductivity measurements

Six strips cut from one epitaxial layer were annealed in air for 30 minutes at temperatures between 300 °C and 400 °C. The room temperature resistivity changed by nearly three orders of magnitude, which indicates a large decrease in the carrier concentration of the ZnSe epilayer. A plot of $\ln(\rho_o-\rho)$ against T^{-1} gave a straight line with an activation energy of 0.26 eV, as shown in Fig.4.1. Here ρ_o and ρ are the resistivities of ZnSe without and with thermal annealing. The reason for this form of plotting the data is given in the discussion section. A second series cut from another epitaxial layer were annealed under the same conditions but for 20 hours. A similar plot for this series gave an activation energy of 0.25 eV. The plot is also shown in Fig.4.1.

Strips cut from one epitaxial layer were annealed in vacuum of ~ 10^{-3} torr for 30 minutes in the temperature range 300 °C to 450 °C. The results also showed the increase of resistivity in the annealed samples, but the change was only one order of magnitude up to 400 °C, which was much smaller than the change of resistivity for annealing in air. There was less reproducibility from run to run, possibly because the vacuum pressure was not accurately controlled.

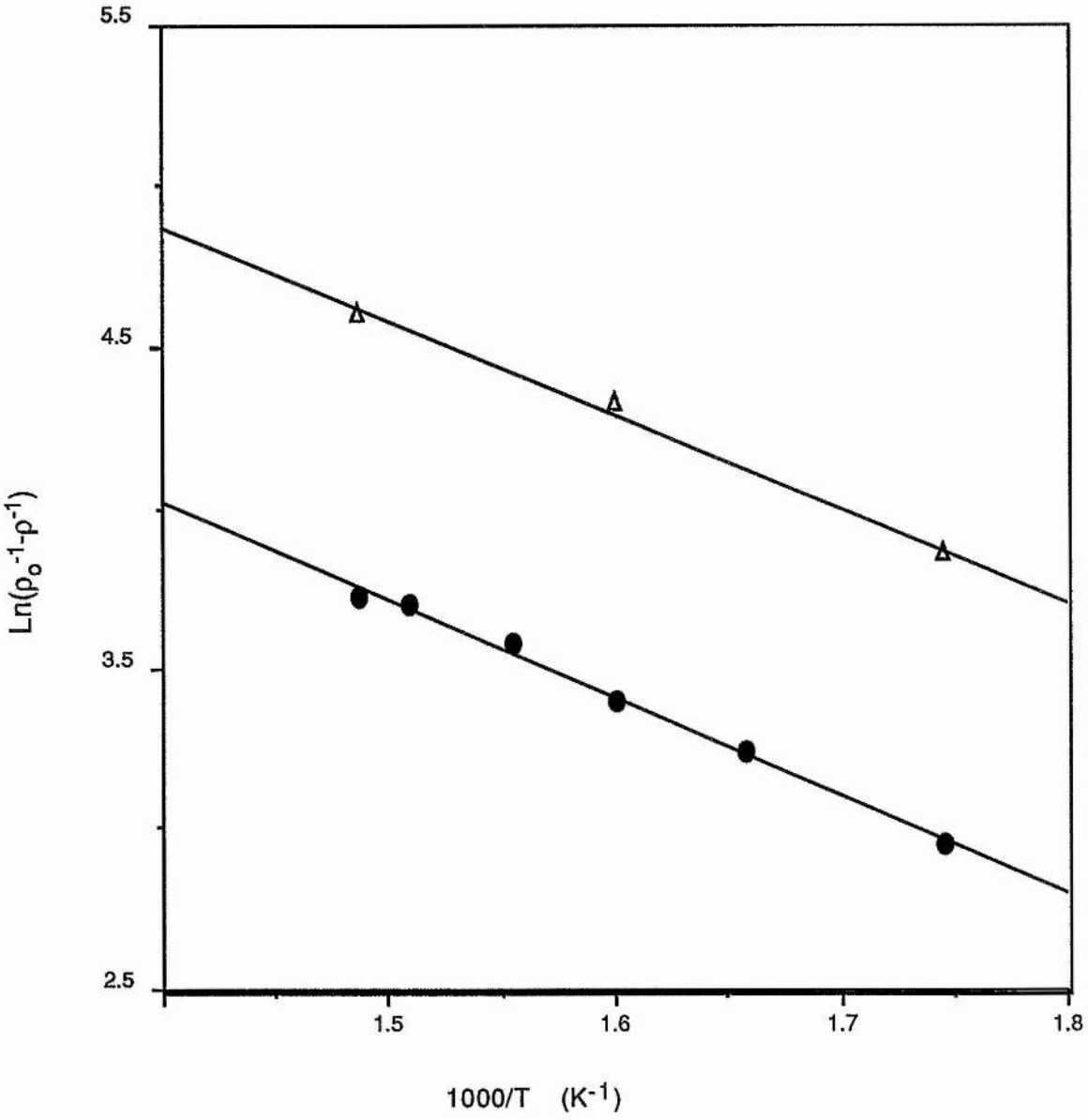

Fig.4.1 The change of resistivity of MOCVD grown n-type ZnSe after annealing, plotting according to equation (4.7). (•) 30 minutes, (Δ) 20 hours.

Strips from another epitaxial layer were annealed at 380 °C for 30 minutes in different ambients (i.e., air, vacuum, zinc vapour and selenium vapour). The resistivity of as-grown material was 0.026 Ωcm. The resistivity after annealing in air

was 0.96 Ωcm, in vacuum was 0.085 Ωcm, in saturated zinc vapour was 0.060 Ωcm, and in saturated selenium vapour was 1.42 Ωcm. It is clear that annealing in air or selenium vapour produces similar results while annealing in vacuum is similar to annealing in zinc vapour. It can be seen that the annealing in saturated zinc vapour (the zinc vapour pressure was very low at this temperature compared to the vacuum pressure being used) at such low temperature does not reduce the resistivity, this differs from the behaviour observed in bulk grown ZnSe which was usually made conducting by heating in molten zinc at high temperatures.

In order to check the copper contamination a set of strips were soaked in $CuSO_4$ solution for a few minutes and then annealed in air in conditions without minimizing copper contamination (i.e., samples were put inside another silica tube directly) for 30 minutes. The observed resistivity changes were much bigger and much more rapidly varying with temperature than for strips annealed in conditions minimizing copper contamination. For example an air annealed sample without copper changed from 0.024 Ωcm to 0.085 Ωcm after 30 minutes at 350 °C while with copper another sample changed from 0.014 Ωcm to 15.6 Ωcm.

4.3.2 Photoluminescence measurements

The photoluminescence spectra of the as-grown ZnSe epilayer show a near-band-edge emission which is attributed to recombination of a free hole with an electron bound on a donor, as discussed in Chapter 2, together with a deep level emission. Because several emission bands in the red-orange region have

been reported in ZnSe in the literature, we have made detailed measurements on the temperature dependence of the deep level emission spectra. Figure 4.2 shows the deep level emission spectra at several temperatures.

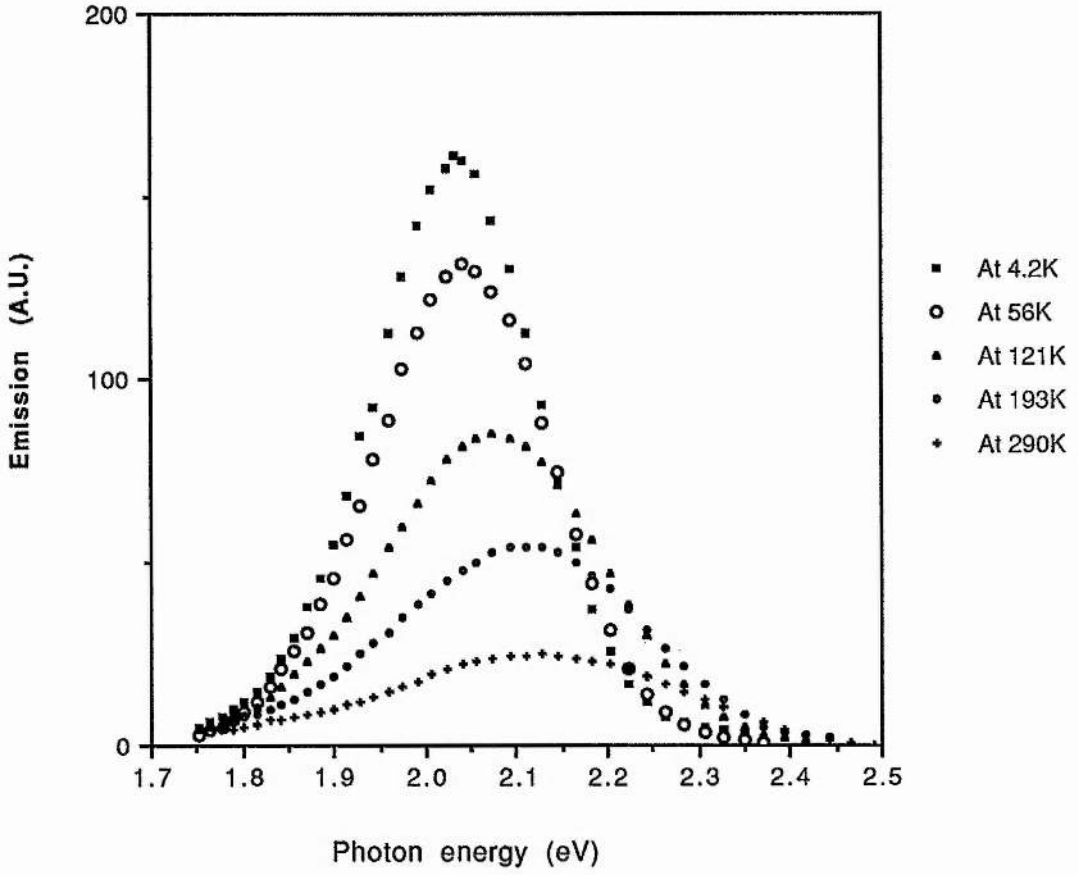

Fig.4.2 Temperature dependence of the deep level emission in an as-grown MOCVD ZnSe, showing the shift of the emission peak position to higher energy with increasing temperature.

The temperature dependence of the emission peak energy and half width are shown in Fig.4.3 and Fig.4.4 respectively. The

emission peak shifts to higher energy with increasing temperature (2.03 eV at liquid helium temperature and 2.125 eV at room temperature), this is typical behaviour of the self-activated emission but not of the copper-red emission in ZnSe[84,85]. The half-width and the temperature quenching feature of the emission band are also those of the self-activated emission but not of the copper-red emission.

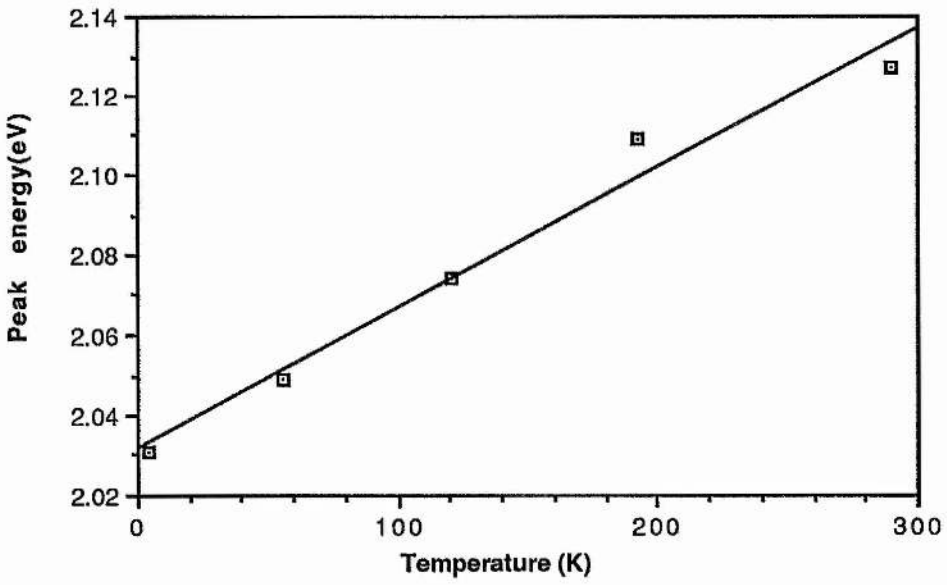

Fig.4.3 Temperature dependence of the deep level emission peak energy in an as-grown MOCVD ZnSe.

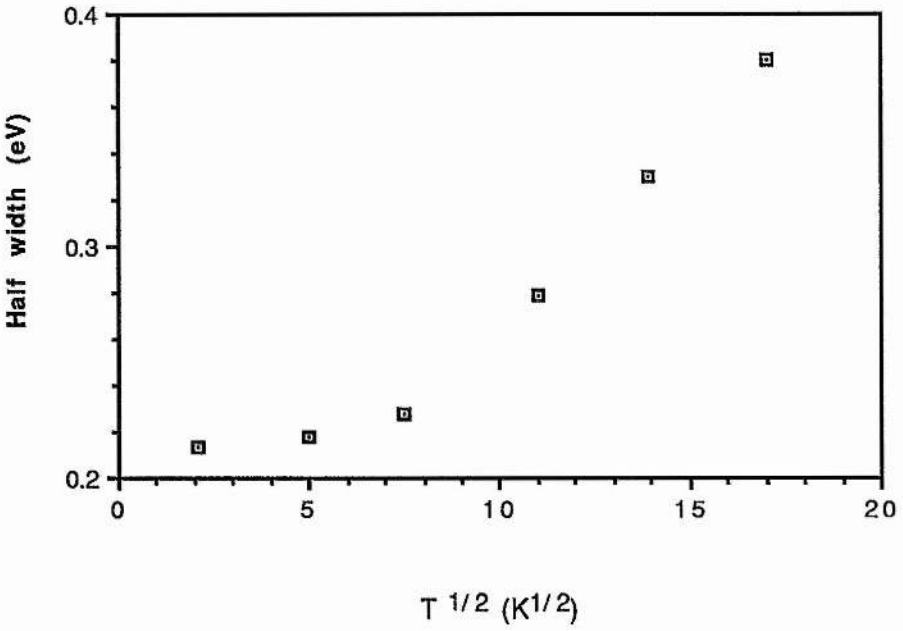

Fig.4.4 Variation of the half width of the SA emission in an MOCVD ZnSe as a function of $T^{1/2}$, showing the expression $W = B + A[\coth(h\nu/2kT)]^{1/2}$ is applicable.

The deep level emission in ZnSe, which were annealed in different atmospheres in conditions with minimizing copper contamination, shows similar spectra to the self-activated emission. However, the intensity of the self-activated emission increases after annealing while the intensity of near-band-edge emission decreases. The ratios of the self-activated emission intensity to the near-band-edge emission intensity at room temperature of ZnSe samples, which were annealed in different ambients at 380 °C for 30 minutes, are listed in Table 4.1. The near-band-edge emission at liquid helium temperature of a sample annealed in air at 400 °C for 20 hours is shown in Fig.4.5 together with the edge emission of an as-grown MOCVD ZnSe. One can see that instead of the single blue peak in the as-grown material, the liquid helium temperature spectrum of the annealed

sample shows three more peaks at 2.783, 2.752 and 2.720 eV. The origin of these peaks is not clear but it has been suggested that they are associated with an exciton bound at a neutral acceptor, either at a zinc vacancy or its complex[38,86], or at a copper atom on a zinc site[87], together with phonon replicas of spacing 31 meV. As the copper-red or copper-green emissions were not observed, the copper bound exciton emission could be ruled out in this case.

Table 4.1 The effect of annealing in different ambients at 380 °C for 0.5 hour on the resistivity and room temperature photoluminescence of MOCVD ZnSe

Sample No.	H6-00	H6-01	H6-02	H6-03	H6-04
Ambients	as-grown	air	vacuum	Zn vapour	Se vapour
ρ (Ωcm)	0.026	0.96	0.085	0.060	1.42
I_{deep}/I_{edge}	0.4	16.6	2.2	1.6	60.0

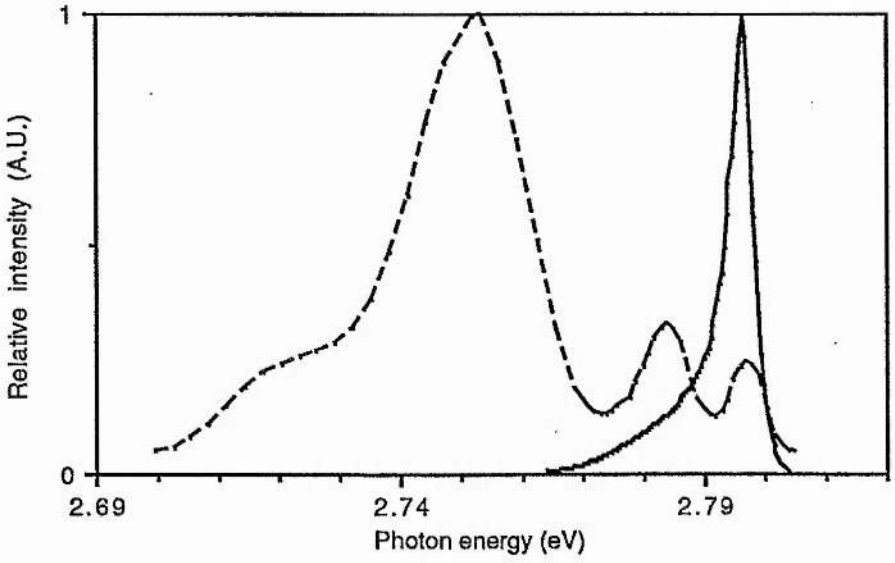

Fig.4.5 The near-band-edge emissions of two MOCVD ZnSe at liquid helium temperature. (solid line) as grown, (broken line) after annealing in air at 400 °C for 20 hours.

In contrast, samples heated after treatment in $CuSO_4$ solution showed the usual copper features of a red emission band at room temperature, narrower and at a lower energy than the SA emission, and a red and a green emission band at low temperatures as shown in Fig.4.6. The peak position shifts to lower energy as the band gap does with increasing temperature, this differs from the self-activated emission.

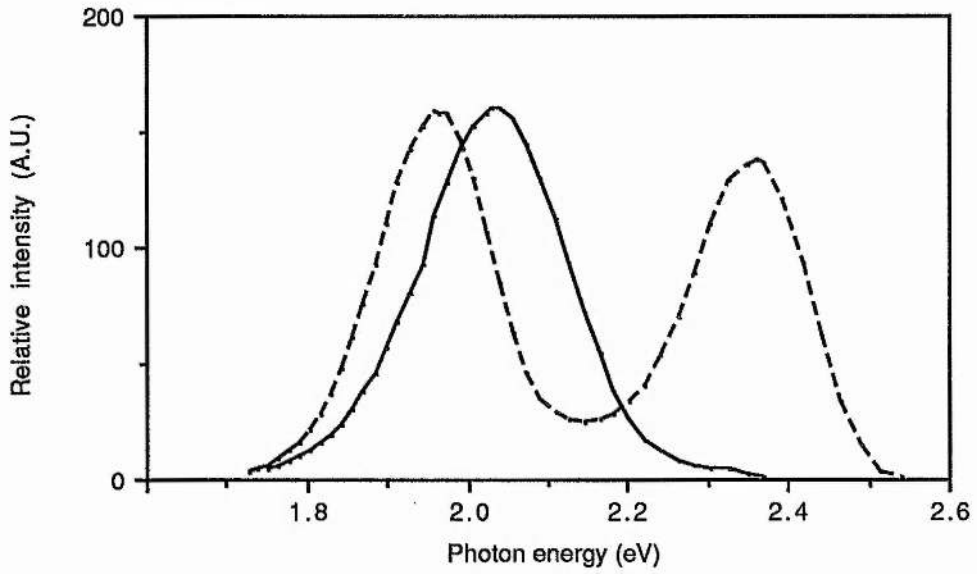

Fig.4.6 Deep level emissions of two MOCVD ZnSe samples at liquid helium temperature. (solid line) as grown, (broken line) annealed in the prescence of copper. The spectra are normalised to the same height.

4.3.3 Photocapacitance measurements

In order to obtain information on the deep level parameters in ZnSe and to obtain any change in the deep level concentration due

to annealing, junction capacitance measurements were made on samples with and without annealing. The only deep centre found in large concentration in the as-grown and annealed samples has a hole photoionization spectrum similar to that of the M-centre[55], with a threshold energy for hole photoionization at 0.63 ± 0.02 eV. The photoionization spectrum of the M-centre is presented in the next chapter and will be discussed further there. Here we outline a method for the determination of deep level concentrations.

The deep level concentration N_T can be determined from the change in junction capacitance induced by an external illumination with the following formula

$$N_T = \frac{e_p^o + e_n^o + cn(x)}{e_n^o} \frac{C^2 - C_d^2}{C_d^2} n , \qquad (4.1)$$

provided that the measurement is performed at low temperature and the thermal emissions can be neglected. Here e_n^o and e_p^o are the electron and hole emission rate of the centre, c is the capture constant for electrons in the conduction band, C_d and C are the junction capacitance before and after shining the light, n is the free carrier concentration in the bulk and n(x) is the electron concentration as a function of position in the depletion region. Because the M-centre is in the lower-half of the band gap, absolute values of N_T cannot be obtained without knowing the values of e_n^o, e_p^o , c and n(x). For simplicity we make the abrupt approximation (see chapter 6 for detail), i.e., we neglect the electron capture from the conduction band, and assume $e_n^o = e_p^o$ for a particular excitation photon energy (this photon energy was

found to be 2.48 eV for the M-centre in ZnSe by Grimmeiss et al[55]). then

$$N_T = 2 \frac{C^2 - C_d^2}{C_d^2} n . \qquad (4.2)$$

This will give a lower limit value of the deep level concentration.

Experimentally, a 1.5 volts forward bias was first applied to the diode, this will fill all the deep centres. After the applied bias was removed, light of photon energy 1.6 eV was shone onto the diode to empty traps present in the upper half of the band gap, the change of the junction capacitance by this was very small. This indicated that the concentrations of deep centres present in the upper half of the band gap are small. Finally, light of photon energy 2.48 eV was shone on to the diode, and the change of junction capacitance was measured.

For an as-grown ZnSe epilayer with free carrier concentration of 7.5×10^{17} cm^{-3}, the M-centre concentration was estimated by equation(4.2) to be about 1.2×10^{17} cm^{-3} from the change of the junction capacitance; while for an annealed sample with carrier concentration of 9.2×10^{16} cm^{-3}, the M-centre concentration was determined to be 1.5×10^{17} cm^{-3} by equation (4.2). It is striking that the M-centre concentration can be nearly the same order of magnitude as that of the shallow donors, which is about 10^{18} cm^{-3}. Also the M-centre concentration appeared to increase slightly after annealing, although only lower limit values of the M-centre concentration were obtained.

4.4 Discussion

The decrease in electron concentration on annealing could be due to a decrease of donor concentrations or an increase of compensating acceptors.

Annealing as-grown MOCVD ZnSe in air produced a large change in carrier concentration. Inevitably one suspects copper contamination when annealing compound semiconductors. This can be ruled out in our experiments, where great care was taken to minimize the effect of copper contamination, since the photoluminescence spectra of the annealed samples did not show the characteristic ZnSe: Cu spectrum[84,85] and the change of the resistivity with annealing temperature was quite different from that in samples deliberately contaminated with copper. It is true that the M-centre concentration seems to increase slightly on annealing and that this centre has been attributed to copper[56], but the attribution is by no means conclusive since in some of the experiments described by Grimmeiss et al[56] the correlation of the M-centre with copper concentration was actually negative. (The origin of the M centre in ZnSe is discussed in chapter 5). In addition, the change in carrier concentration is much larger due to air annealing than vacuum annealing. It seems that the oxygen plays an important role during the annealing.

One possibility is that some donor centres are grown in at non-equilibrium conditions at low growth temperature and that annealing allows the centres to go to an electrically inactive site. In a simple model one expects the process to be thermally activated, i.e.,

$$\frac{dN_D}{dt} = - c N_D \exp(-E/kT) , \qquad (4.3)$$

where N_D is the donor concentration, c is a constant, E is the activation energy for the disappearance of donor centres (the meta-stable donor states), kT is the thermal energy, and t is the annealing time. By integrating equation (4.3), one has

$$N_D = (N_D)_o \exp(-t/\tau), \qquad (4.4)$$

where $1/\tau = c \exp(-E/kT)$. In the approximation that all the donors are ionized at room temperature and the electron mobility is constant this leads to

$$\ln\rho - \ln\rho_o = t\, c \exp(-E/kT), \qquad (4.5)$$

where ρ_o and ρ are the resistivities of ZnSe before and after annealing. Therefore, a plot of $\ln(\ln(\rho/\rho_o))$ against 1/kT will give a straight line with a slope equal to the activation energy. However, neither the time nor the temperature dependence of the resistivity change fits this model.

Alternatively, one might hypothise that annealing introduces acceptors of some sort. The fact that similar results are obtained after annealing for 30 minutes and 20 hours indicates that the acceptors have reached a saturation condition, i.e., it might be a solubility limit. If this solubility has an Arrhenius form

$$N_A = N_o \exp(-E/kT) \qquad (4.6)$$

over the temperature range involved, where N_A is the acceptor concentration, N_o is a constant, E is the activation energy, and kT is the thermal energy, then assuming that the donor concentration

is unaffected by the annealing, that the donors are all ionized at room temperature and that the electron mobility μ is approximately constant one has

$$\frac{1}{\rho_o} - \frac{1}{\rho} = e\mu N_o \exp(-E/kT), \qquad (4.7)$$

where again ρ_o and ρ are the resistivities of ZnSe before and after annealing. Thus a plot of $\ln(\frac{1}{\rho_o} - \frac{1}{\rho})$ against $\frac{1}{kT}$ will give a straight line with a slope E. This is the plot which is used in Fig.4.1 and gives a good fit to the experimental data. Therefore the increase in resistivity after annealing is probably due to the increase of compensating acceptors.

The acceptors involved are likely to be non-stoichiometric lattice defects since there is no obvious source of acceptor impurities at such high concentrations and with so low an activation energy for solubility. Annealing in air or in selenium vapour produces a large change in resistivity. Annealing in air causes oxidation of the surfaces to zinc oxide and the release of selenium, so both these treatments produce a selenium-rich environment. Annealing in zinc or in vacuum produces much smaller changes of resistivity. Selenium is more volatile than zinc so annealing in vacuum, where there is surface dissociation, results in a condition of excess zinc. Hence heating in zinc or in vacuum have qualitatively similar results. From these considerations we deduce that the acceptor is likely to be a native defect associated with a zinc-deficient, i.e., selenium-rich, condition.

The intensity of the SA emission is increased while the intensity of near-band-edge emission is decreased after annealing. But one cannot deduce that the concentration of the SA centre is increased because many factors can affect the intensity of photoluminescence. For example, the SA emission involves a hole at the zinc vacancy-donor complex and an electron on a donor. The emission intensity is not only determined by the concentrations of the un-compensated donor and zinc vacancy-donor complex, but also by the availability of holes for the acceptors. Also, although the estimated M-centre concentration appeared to increase slightly after annealing, this is small compared to the decrease in the free carrier concentration. For example, the change of the estimated M-centre concentration is about 3×10^{16} cm^{-3} for a sample annealed at 380 °C, while the change in the free carrier concentration is about 6.5×10^{17} cm^{-3} after the annealing. Therefore we cannot positively identify the native acceptor produced in the thermal annealing from the present photoluminescence and photocapacitance measurement, although a zinc vacancy or its complex could be a candidate. In order to establish this, one needs more accurate measurements of the deep level concentration.

4.5 Conclusions

Large changes in carrier concentration can be produced by annealing as-grown MOCVD ZnSe in air. It is found that this is due

to the increase of compensating acceptors with an activation energy of 0.26 eV. The compensating acceptor is thought to be a native defect associated with a zinc-deficient condition. This observation may help to explain some features of MOCVD growth. For example it is generally observed that the electron concentration of MBE and MOCVD grown n-type ZnSe decreases as the growth temperature increases[88,89], and ZnSe epilayers grown at substrate temperature T_s > 375 °C show high resistivity. A factor may be that the same native acceptor is compensating more effectively at the higher temperatures.

As the compensation acceptor is present at ~ 10^{17} cm^{-3}, which is thought to be a native defect associated with a zinc-deficient condition, it is then difficult to believe that a selenium-deficient condition can also exist simultaneously. Then a question is raised about the results reported by Morimoto[47] that the origin of donor in their MOCVD grown ZnSe was selenium vacancy, with concentrations up to 3 × 10^{17} cm^{-3}. It is thought that the donor species in our MOCVD ZnSe are extrinsic impurities, but not the selenium vacancies.

A small activation energy of only 0.26 eV was found in the annealing for the production of compensating acceptors. The same effect could be detrimental for some devices operating at elevated temperature or even at room temperature. This could be a factor why the lifetime of blue MIS ZnSe diodes is very short, but it remains to be justified.

The technique of controlling the resistivity by post-growth annealing is proving to be useful in a number of experimental

situations in which a series of samples is required which differ only in the degree of compensation. An example is the measurement of avalanche multiplication in reverse-biased junctions. Another example is the measurement of Auger quenching of luminescence.

Chapter 5 The origin of the M-centre in ZnSe

5.1 Introduction

The investigation of deep centres (deep impurities, lattice defects, and impurity-defect complexes) in semiconductors is still very important for a number of reasons. On the academic side, there is no general formalism describing the physical properties of deep centres, even the best theoretical calculations such as the local density theory and the empirical tight-binding approximation still cannot accurately predict the energy levels of deep centres[90]. On the technological side, deep centres have both useful and detrimental features. As an example, deep centres control the lifetime of charge carriers, they are undesirable in devices where carriers must have long lifetimes, e.g., solar cells; while they are useful in fast switching devices, e.g., Au in Si. As another example, deep centres can produce radiative recombination which could give emissions from infrared through visible to ultraviolet in large band gap materials such as ZnS, while they can also induce nonradiative recombination which is undesirable for the electroluminescence devices. Therefore, a better understanding and accurate control of the various types of defects and impurities are essential in order to manipulate the properties of semiconductors.

Junction capacitance and current techniques are widely used in investigating the electrical and optical properties of the electrons and holes bound to deep centres. Because of the use of the depleted region of a p-n junction or a Schottky barrier, where

the electron and hole concentrations are zero, the rate equations become linear. This enables one to determine the concentrations, the electronic energy levels, and ionization and capture cross-sections of deep centres. However, the chemical nature of a deep centre cannot be simply identified from junction measurements. This is the reason why the nature of the DX centre and the EL2 centre in GaAs have been discussed in the literature for so many years. In this chapter we re-examine the origin of a particular centre in ZnSe called the M-centre.

Deep levels in ZnSe are of importance because of their effect not only on carrier concentrations but also on recombination process. Several deep levels in the upper half of the band gap have been found by DLTS measurements by other authors[52,53]. In the lower half of the band gap, three deep levels have been reported which are about 2 eV below the conduction band of ZnSe, i.e., in the range 0.5 to 0.9 eV above the valence band. Photoionization cross-sections have been determined mainly by photocapacitance measurements because of the unsuitability of DLTS measurements for these levels. Fig.5.1 shows the spectra of hole photoionization cross-section of the three deep centres in ZnSe seen by other authors in photocapacitance measurements[55,56]. The centre which gives rise to a peak at 0.85 eV and another peak at higher energy in the photoionization spectrum was named as the M-centre[55]. For convenience we name the other two centres shown in Fig.5.1 as L1 centre and L2 centre.

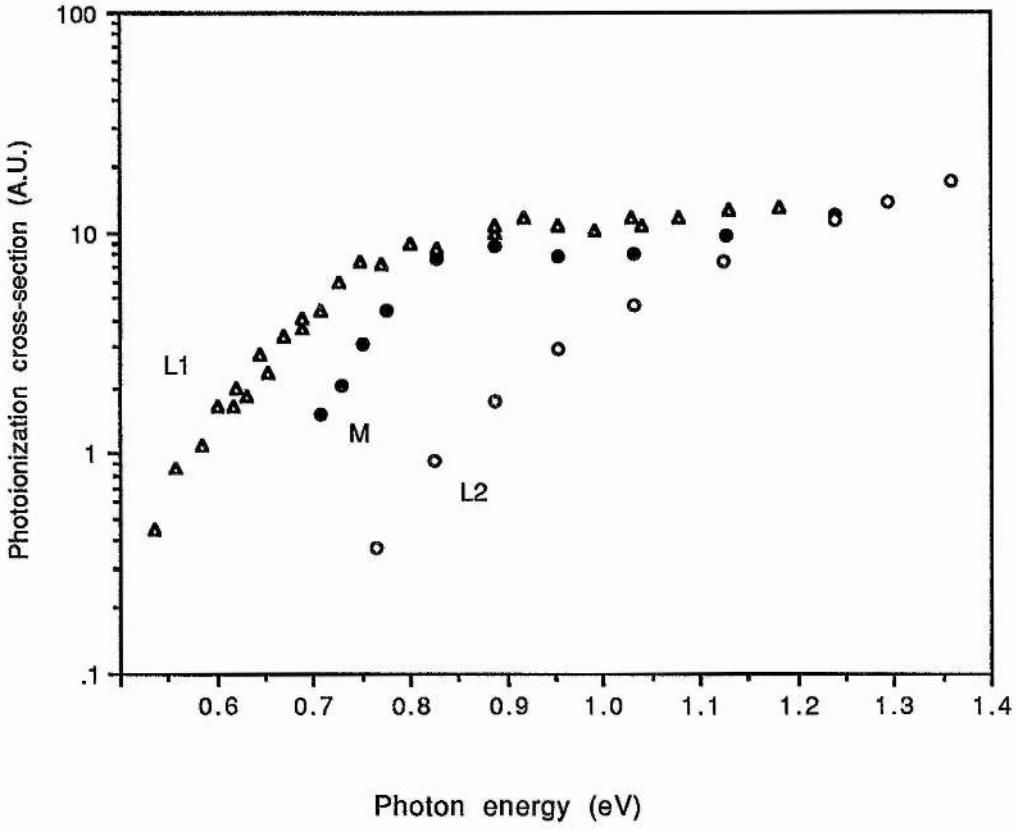

Fig.5.1 The spectra of hole photoionization cross-section of three deep centres in ZnSe measured by photocapacitance measurements. (•) for ZnSe: Mn and (o) for undoped ZnSe after Grimmeiss et al[55], and (Δ) for undoped ZnSe after Grimmeiss et al[56].

The M-centre was first found in Mn-doped ZnSe by Braun, Grimmeiss and Allen[54] using photocapacitance measurements. The energy level of the M-centre is 2.0 eV below the conduction band and 0.65 eV above the valence band at room temperature. Grimmeiss, Ovrén and Allen[55] made more detailed measurements of the photoionization spectra of the M-centre in ZnSe: Mn at several temperatures. They found that the threshold energy of the hole ionization is independent of temperature and that the threshold energy of electron ionization varies with temperature

at the same rate as the band gap energy. Fig.5.2 and Fig.5.3 show the photoionization spectra of the M-centre for holes and for electrons at several temperatures obtained by Grimmeiss, Ovrén and Allen[55] .

The problems which we are going to discuss in this chapter are focused on

(a) the origin of the M-centre, and

(b) the connection, if any, between the two peaks in the M-centre spectrum.

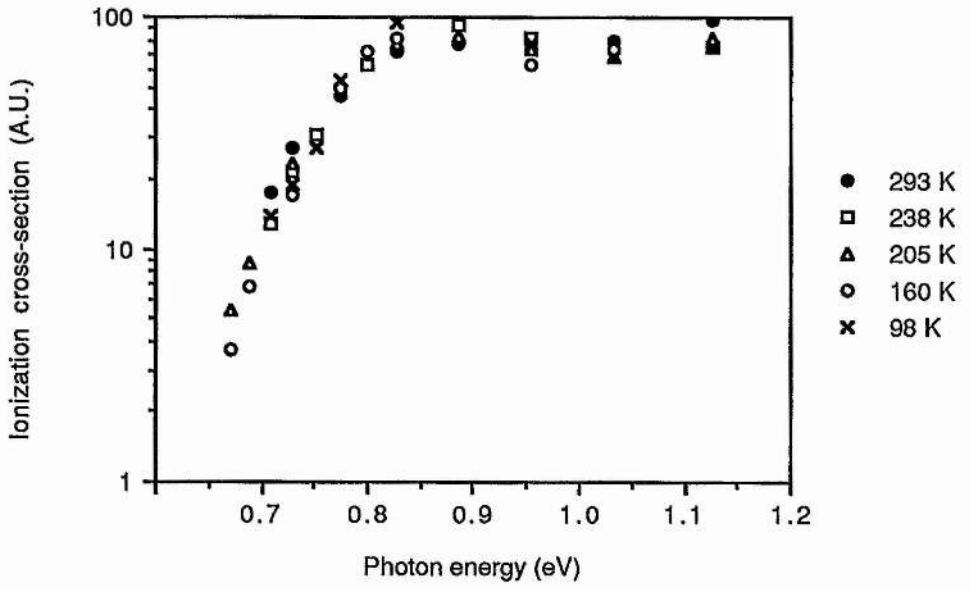

Fig.5.2 The hole photoionization spectra of the M-centre in ZnSe at different temperatures after Grimmeiss et al[55].

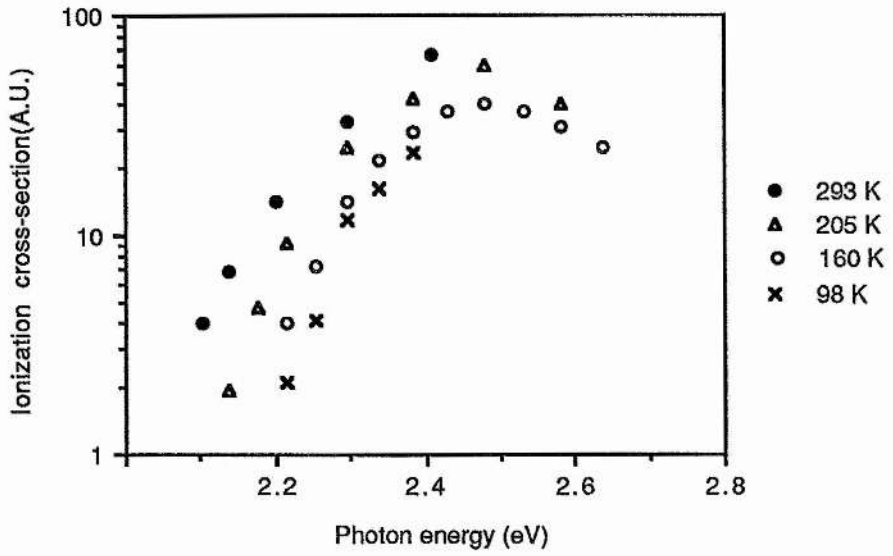

Fig.5.3 The electron photoionization spectra of the M-centre in ZnSe at different temperatures after Grimmeiss et al[55].

5.2 Previous attributions

Initially it was suggested by Braun, Grimmeiss and Allen[54] that the M-centre is possibly associated with manganese because ZnSe prepared in a similar manner but not containing manganese gave a weaker photocapacitance signal from the M-centre. Grimmeiss, Ovrén and Allen[55] obtained different hole ionization spectra of ZnSe with and without manganese, which we have called the M-centre and the L2 centre (see Fig.5.1). This together with the evidence of the small Franck-Condon shift and the agreement of E_p^t with the thermal quenching activation energy led them to attribute the M-centre to manganese, while still leaving the possibility that the M-centre could be a self-activated centre. It is now known that the assignment of the M-centre to

manganese is wrong because the M-centre is frequently seen in ZnSe which does not contain manganese in the required concentration.

Grimmeiss et al[56] made photocapacitance measurements on undoped, Mn-doped and Cu-doped ZnSe samples. They found that intentionally Cu-doped samples contained a higher concentration of the M-centres than not intentionally doped samples. In the undoped ZnSe sample, they saw another centre with a lower threshold energy for hole ionization than the M-centre, which we have called the L1 centre (see Fig.5.1). Also they measured the quenching spectrum of the Cu-red photoluminescence and found it to be the same as the hole photoionization spectrum of the M-centre. On these grounds they identified the M-centre with the Cu-red centre.

Later, Grimmeiss et al[59] made photocapacitance measurements on iodine vapour transported ZnS_xSe_{1-x} crystals (which have been treated in molten zinc) with $0 < X < 0.95$. The hole photoionization spectra of all the samples studied consist of a main peak at higher energies and a smaller peak or bump at lower energies. For ZnSe (i.e. $X = 0$) sample, the hole photoionization spectrum (see Fig.6 of ref(59)) is similar to that of the M-centre. Although similar hole ionization spectra were obtained in the undoped and Cu-doped $ZnS_{0.9}Se_{0.1}$ samples (see Fig.14 of ref(59)), and residual copper concentrations have been detected in some of the investigated samples, they attributed their spectra to the self-activated (SA) centre based on the arguments that (a) the copper concentrations in the unintentionally Cu-doped samples are too small to affect the

spectra, (b) the spectrum for x ~ 1 is similar to that for quenching of the SA photoluminescence in ZnS[91], and (c) the SA centre and a copper related centre may have similar energy positions in ZnSe as known from optical detected magnetic resonance (ODMR) measurements[92].

Therefore, the evidence presented in these papers is a little confusing. The issue is further complicated as there are several centres associated with Cu present in ZnSe. In what follows, we re-examine the evidences for and against the attribution of the M-centre to copper-red centre, and present new experimental data obtained by photocapacitance measurements on low resistivity n-type MOCVD grown ZnSe.

5.3 Evidence for the copper centre

Photocapacitance results by Grimmeiss et al[56] showed that the concentration of the M-centre in samples not intentionally doped with copper and with the SA emission only is less than 10^{15} cm^{-3}; whereas the concentration of the M-centre is larger than 10^{16} cm^{-3} in ZnSe intentionally doped with copper. They claimed that the concentrations of the M-centres found in the Cu-doped material are in good agreement with the concentrations of electrically active Cu as determined from the reduction of the free-carrier concentration (this assumes that all the compensation is by copper), although the data they presented does not show this (see Table1 of ref(56)). They concluded that the appearance of the M-centre is associated with the copper doping.

Grimmeiss et al[56] have also measured the infrared quenching spectrum of Cu-red luminescence in ZnSe: Cu, although they said the quenching observed was less than 1% (in this case it would be hard to measure the quenching spectrum accurately). The measured spectrum of optical quenching for the 6400 Å copper emission is similar to the spectrum of hole photoionization cross-section of the M-centre in the range of 0.7 eV to 1.25 eV (see Fig.5.4). This seems to further the evidence that the M-centre is a copper-red centre.

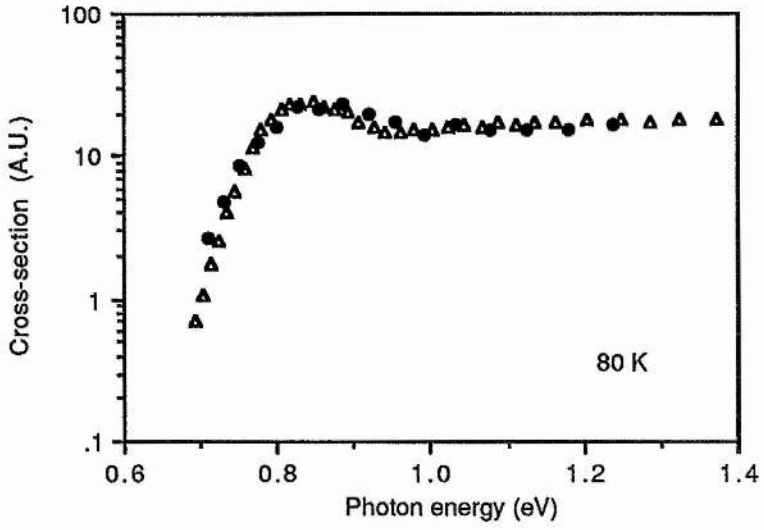

Fig.5.4 The optical quenching spectrum of the Cu-red luminescence (•) and the hole photoionization cross-section of the M-centre (Δ) in ZnSe after Grimmeiss et al[56].

In addition to the M-centre, Grimmeiss et al[56] observed another centre, which we have called the L1 centre, in the undoped material at a lower threshold energy than the M-centre. They attributed this to the self-activated centre because the hole

ionization spectrum of this L1 centre is similar to the quenching spectrum of the self-activated luminescence in ZnSe[93].

5.4 Correlation of the M-centre with copper

Here we examine the evidence in more detail. We know that copper introduces different luminescence bands (Cu-red, Cu-yellow and Cu-green etc) in ZnSe[94] and there is no good evidence: (a) that Cu produces a single level, (b) about the nature of the centres produced by introducing Cu, nor even if the centre produced actually can be Cu.

The M-centre was seen by Grimmeiss et al[56] at concentrations of 10^{14} cm^{-3} to 10^{16} cm^{-3} in Zn-treated bulk crystals. Sometimes Cu-red emission is seen in these samples, but more often the SA emission. In the presence of deliberately added Cu, the Cu-red emission is seen and the M-centre concentration increases to $.7 \times 10^{16}$ cm^{-3}. But with Zn/Cu treatment, the M-centre concentration does not correlate directly with the copper concentration, sometimes even negative. Referring to Table 5.1, which reproduces in a different format the data presented in Table 1 of ref(56), we see that in the sublimation grown ZnSe crystals the concentrations of the M-centre are the same (2×10^{16} cm^{-3}) for treatment in 0.1%Cu /99.9%Zn and in 1%Cu /99%Zn, while in the iodine vapour transported crystals the M-centre concentration had a reported value of 7×10^{16} cm^{-3} for the sample treated in 1%Cu /99%Zn, and a reported value of 2×10^{16} cm^{-3} for the sample treated in 10%Cu /90%Zn. In addition, contrary to what they have claimed in their

paper, the observed M-centre concentration is much smaller than the reduction of free carrier concentration before and after the Zn/Cu treatment. If we assume all the compensation is by copper, the concentration of the electrically active copper should be equal to the decrease of free carrier concentration.

Table 5.1 Replot of the data obtained by Grimmeiss et al[56], showing the correlation of the M-centre concentration with copper doping. (Δ) SA emission and (•) Cu-red emission.

M-centre	Zn/Cu treatment (Sublimation grown ZnSe)			
conc.(cm^{-3})	No Cu	0.1% Cu	1% Cu	10% Cu
10^{17}				
		K48 Δ •	K39 •	
10^{16}		K51 Δ •		
1015	K16 Δ			
	K26 K47			
	K50 Δ			
1014	K12 K23			

M-centre	Zn/Cu treatment (Iodine transport grown ZnSe)			
conc.(cm^{-3})	No Cu	0.1% Cu	1% Cu	10% Cu
10^{17}				
			K40 •	
				K31 •
10^{16}	K46 Δ •			
1015				
	K34 K45 Δ			
1014				

These two phenomena are not what we would expect if copper were directly responsible for the M-centre. The concentration discrepancy could happen if saturation occurred during the Zn/Cu treatment. However, earlier experiments by Aven and Halsted[95] showed that the solubility of copper in ZnSe: Cl was about 10^{18} cm^{-3} at 350 °C and one has higher copper concentrations at higher annealing temperatures. Indeed Grimmeiss et al[56] found a total copper concentration of 4×10^{18} cm^{-3} in the sample treated in 10%Cu /90%Zn as measured by radio-tracer techniques.

Therefore, some other factors have been involved in the treatment, e.g., complexing of copper with other centres, or production of lattice defects by precipitation of copper. Because lattice defects and Cu impurities are always present simultaneously in ZnSe grown at high temperatures, and the concentrations of defects and copper can be decreased by molten zinc treatment and can be increased by adding copper, hence the identification of the chemical nature of the M-centre is very difficult.

We have made photocapacitance measurements on ZnSe grown by MOCVD epitaxially on GaAs substrates. Both transient capacitance and Double Light Source Steady-state (DLSS) techniques were used. The ZnSe samples were either as-grown or had been annealed in air at temperatures ranging from 300 °C to 400 °C under high-purity conditions, see section 4.2 of chapter 2 for detail. Although deep centres have been found at 0.3 to 0.6 eV below the conduction band, the only centre found in large concentration has a hole photoionization spectrum similar to that

of the M-centre. The hole photoionization spectra of two ZnSe samples measured at liquid nitrogen temperature are shown in Fig.5.5, with threshold energy at about 0.63 eV. It is seen that the photoionization spectrum of the as-grown MOCVD ZnSe is similar to the one after annealing in air.

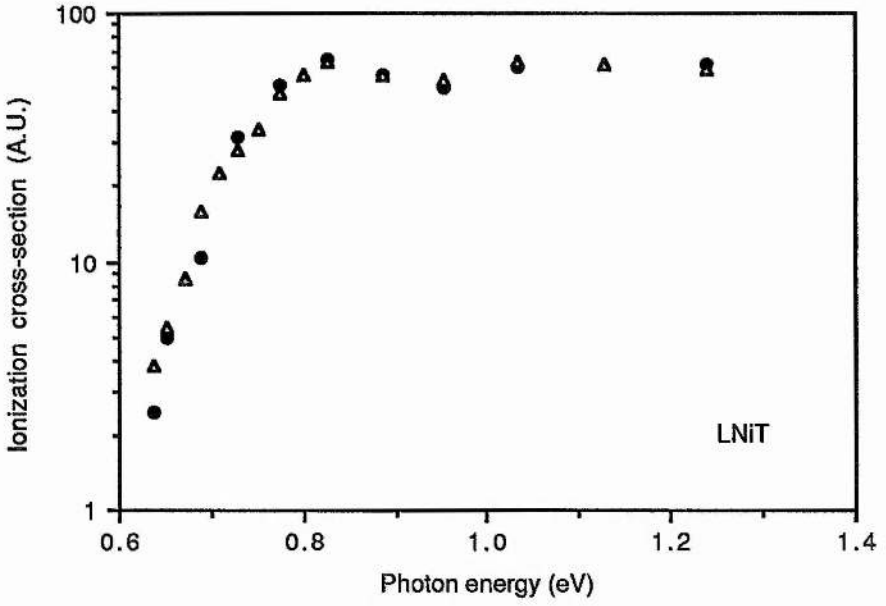

Fig.5.5 The hole photoionization spectra of a deep centre in MOCVD grown ZnSe measured by photocapacitance technique. As grown ZnSe (•) and air annealed ZnSe (Δ).

The concentration of the M-centre determined from the change in junction capacitance by methods described in section 4.3.3 of chapter 4 is 1.2×10^{17} cm^{-3} in an as-grown material with a free carrier concentration of 7.5×10^{17} cm^{-3}. As the M-centre is the main detected compensating acceptor, if we assume that the concentrations of other acceptors are small compared to the concentration of the M-centre, then this gives a compensation

ratio of our MOCVD ZnSe of about 0.16, which is a typical value for n-type MOCVD ZnSe grown at low temperature[47]. An annealed sample with a free carrier concentration of 9.2×10^{16} cm^{-3} gave an M-centre concentration of roughly 1.5×10^{17} cm^{-3}.

The copper concentration in the as-grown material detected by the SIMS (secondary ion mass spectroscopy) analysis is small. The deep level photoluminescence of our MOCVD ZnSe shows no Cu-red emission but the self-activated emission only, with the peak positions of 2.03 eV at liquid helium temperature and 2.125 eV at room temperature. The temperature dependence of the deep level emission in an as-grown MOCVD ZnSe is shown in Fig.4.2 of chapter 4. The observed shift of emission peak with temperature is typical of the SA luminescence in ZnSe. As discussed in section 4.3.3 of chapter 4, it is difficult to make an accurate measurement of the concentration of a centre in the lower half of the bandgap when the material is n-type and the estimated values tend to be lower limits. It is clear that the copper cannot have a concentration of about 10^{17} cm^{-3} in the material described above, otherwise the Cu-red emission should be strong.

From the above discussions, it is clear that the M-centre concentration does not correlate directly with copper. Although the M-centre concentration can be increased by the introduction of copper, as observed by Grimmeiss et al[56], this still leaves open the question of whether or not the M-centre contains Cu, and if so, in what way?

5.5 Luminescence quenching spectra

The second main argument for identifying the M-centre with copper is that the photoionization cross-section of the M-centre is the same as the quenching spectrum of the Cu-red emission. We now investigate this in detail. Grimmeiss et al[56] measured the Cu-red quenching spectrum which is identical to the hole ionization spectrum for the M-centre over a limited range of photon energy (0.7 - 1.25 eV). Assume that Cu-red emission is due to the transition of an electron (eg from the conduction band or shallow donor) into a centre ~ 2 eV below the conduction band containing Cu in some form. The simplest explanation of quenching is that an electron goes from the valence band to a Cu-centre, thereby stopping the luminescent transition of an electron from the conduction band or shallow donor to the centre. But this is not the only possible explanation. If the only recombination path were through the Cu-red centre, then photoionizing holes to the valence band would have no effect, as the holes would have to be recaptured by the Cu-red centres. Quenching occurs when there are different recombination paths in competition. It is possible that photoionizing holes are captured more quickly by other centres than the Cu-red centre; it is also possible that a transition from the valence band to the M-centre produces holes which could then recombine more rapidly through some other nonradiative centres with electrons (see Fig.5.6), this will decrease the electron concentration and therefore result in the quenching of the Cu-red luminescence.

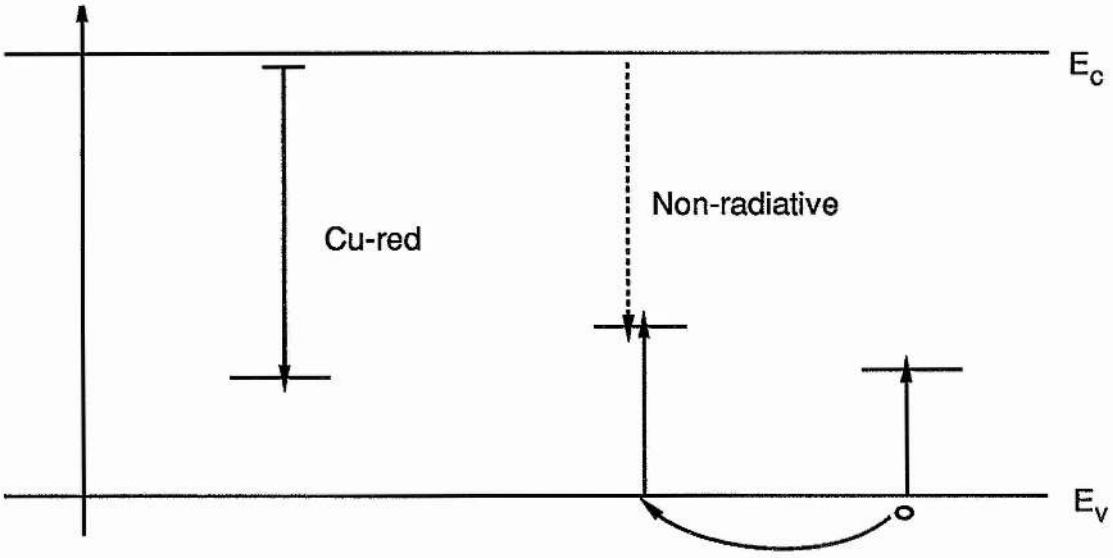

Fig.5.6 Schematical diagram showing that the quenching spectrum of the Cu-red emission might not be associated directly with the Cu-red centre (see text for detail).

Also, luminescence quenching spectra of ZnSe: Cu are not always the same. Fig.5.7 replots the quenching spectra obtained by Stringfellow and Bube[93], and Iida[94] on a photon energy scale. One sees that these spectra are different from the one obtained by Grimmeiss et al[56]. We have also measured the quenching spectrum of a bulk grown ZnSe: Cu at liquid nitrogen temperature. The photoluminescence spectrum consists the Cu-red and Cu-green emissions, which is typical of ZnSe containing Cu. The quenching was measured at 6400 Å through a narrow band interference filter and was seen up to 13%. The results are analyzed and plotted as follows. The decreases in the Cu-red emission intensity (quenching) at different probe wavelengths under steady 365 nm excitation are divided by the photon flux of each wavelength. The results are shown in Fig.5.8 together with the quenching spectrum obtained by Grimmeiss et al[56]. The

observed quenching spectrum is similar to the one obtained by Grimmeiss et al[56] except that the relative strength of the two peaks is different. These observations suggest that the two peaks in the quenching spectrum may not have the same origin, and different initial states are involved. If one accepted the argument that the M-centre and Cu-red centre are the same and that quenching is due to hole transitions from the Cu-red centre to the valence band, one would have difficulty in explaining the different spectra. However the differences can be explained if transitions to the M-centre and to other centres are competing with Cu-red transitions.

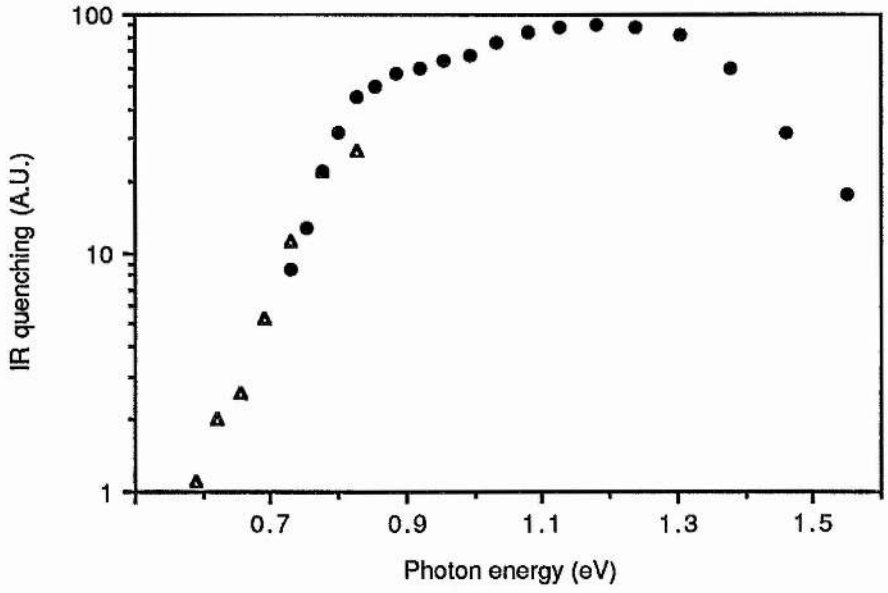

Fig.5.7 The photoluminescence quenching spectra of the Cu-red emission in ZnSe: Cu after Stringfellow and Bube[93] (Δ) and Iida[94] (•).

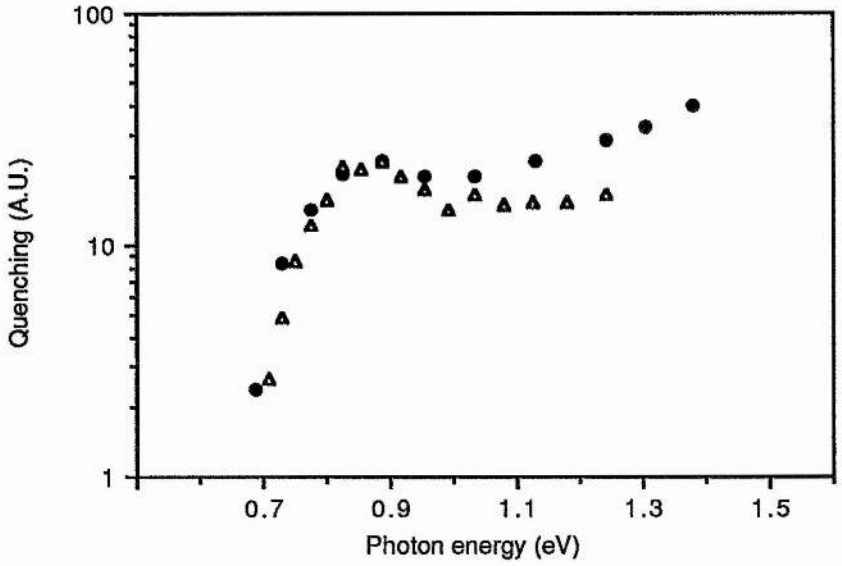

Fig.5.8 The photoluminescence quenching spectra of the Cu-red emission in ZnSe: Cu. (•) present work at 77K and (Δ) after Grimmeiss et al at 80 K[56].

Pantelides and Grimmeiss[96] suggested that a single centre could be involved in the M-centre, with the 0.85 eV peak being associated with a resonance energy level. They also suggested the relative strength of the 0.85 eV and 1.3 eV peaks in the M-centre spectrum could depend on the presence or absence of an electric field. They proposed that there are transitions to bound or quasi-bound final states (see Fig.5.9) which are induced by the strong short-range impurity potentials, and tried to explain the experimental observations that two peaks are observed in the hole ionization spectrum by photocapacitance and luminescence quenching measurements[56] while the 0.85 eV peak is absent in the photoconductivity spectrum[97]. If the final states of the transitions giving rise to the peak are very localized, rather than extended Bloch-like states, then such transitions might produce a signal in photocapacitance measurements, where a large junction

field is present and carriers can be swept out of the bound states. But it might not produce a signal in photoconductivity measurements where a large electric field is absent. Unfortunately, the photoconductivity spectrum (see Fig.5.10), which is used for the comparison with the photocapacitance spectrum by Pantelides and Grimmeiss[96], was obtained by Kosai et al[97] in a ZnSe: Na sample without added copper. This spectrum (see Fig.5.10) is actually the spectrum of the L2 centre rather than the M-centre. Therefore the arguments of the electric field dependence of the M-centre spectrum are irrelevant as they compared spectra of different centres. (i.e., the M-centre and the L2 centre).

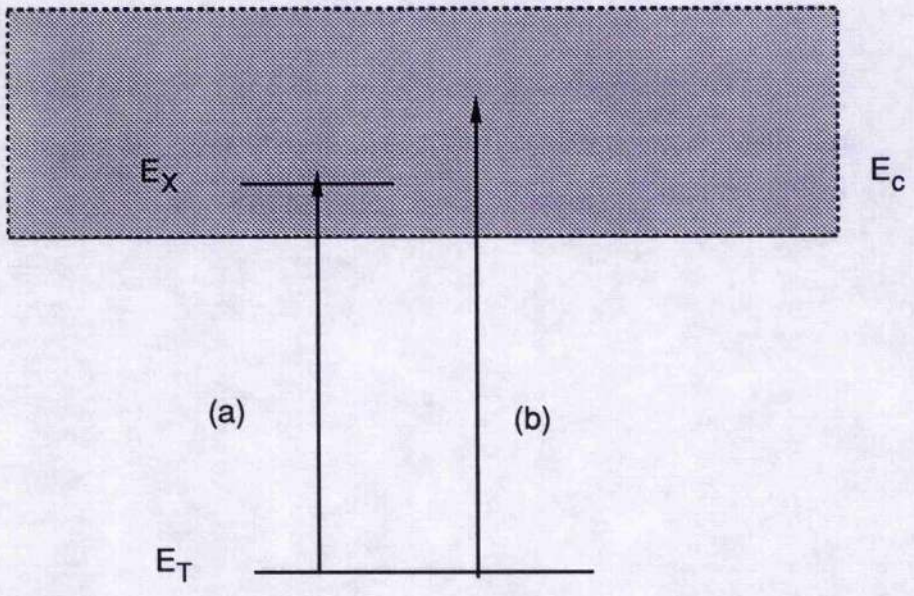

Fig.5.9 Schematical diagram of transitions to impurity-resonance state and to continuous non-resonant states from the impurity ground state.

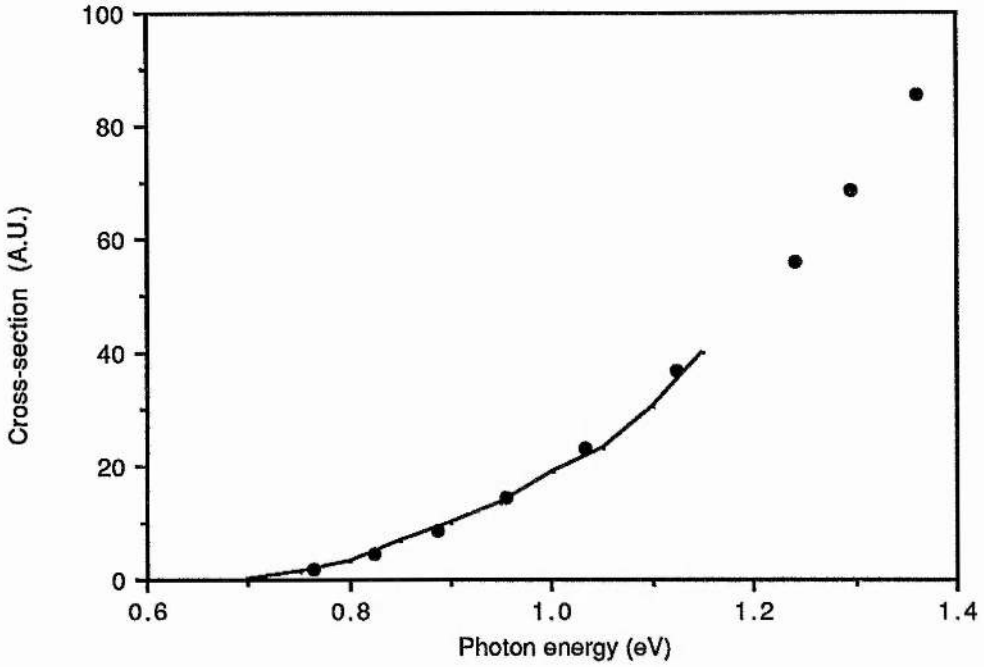

Fig.5.10 The photoionization spectra of deep centres in ZnSe as measured by photocapacitance[55] (•) and by photoconductivity[52] (solid line), showing that both the spectra are due to the L2 centre. (see Fig. 5.1).

In suitable circumstances the photocapacitance spectra will be a superposition of spectra from different centres, eg the M-centre and the L2 centre. Although the strengths of the two peaks in Cu-red quenching spectrum are not always the same, in a large number of measurements of the hole photoionization spectrum of the M-centre in St.Andrews and in Lund, most of the spectra are very similar in having the two peaks of roughly equal height. It is likely therefore that both the 0.85 eV and the 1.3 eV peaks in the photoionization spectrum come from the same centre, with usually only small distortions due to other centres. Because the photoionization spectra of free atoms are normally rich in structure due to resonances just above threshold, it is not

surprising that a resonance peak can appear above threshold in a solid.

5.6 Conclusions

ZnSe, like many other wide band gap semiconductors, can be a highly compensated material. The concentrations of native defects are governed by both the stoichiometry and the growth temperature. On the other hand, copper can very easily be introduced into ZnSe both intentionally and unintentionally during the growth and sample preparation processes. Copper can produce a number of luminescence bands in ZnSe and therefore may produce more than one energy level in the band gap. As a result of these factors the deep level characteristics of ZnSe can be complicated and it is necessary to be very careful in the interpretation of experimental data.

Although Grimmeiss et al[56] saw an increase of the M-centre concentration with deliberately added copper, the M-centre concentration is not correlated directly with the copper concentration. It seems that some other factors are involved, eg complexing of Cu with other centres, or production of lattice defects by precipitate of Cu. We see M-centre concentration ~ 10^{17} cm^{-3} in MOCVD grown ZnSe. Copper was not found at these levels in SIMS analysis. Also the deep level photoluminescence shows the distinctive self-activated emission rather than the copper-red emission.

The quenching spectra of the Cu-red emission in ZnSe obtained by Iida[94], Stringfellow and Bube[93], Grimmeiss et al[56] and

ourselves are not exactly the same, the relative strength of the two peaks in the quenching spectrum are different from one to the other. We have given two possible explanations for the luminescence quenching spectrum and indicated that the association of the quenching spectrum with Cu-red centre is not a direct one.

We conclude that the attribution of the M-centre to copper is not adequately substantiated by the evidence available. The possibility is still open that the M-centre is a lattice defect.

Chapter 6 Photocapacitance studies of deep levels in zinc sulphide

6.1 Introduction

Zinc sulphide is a semiconductor with an E-$\underline{k}$ dispersion diagram which is qualitatively similar to that of gallium arsenide[98], for example. However, its large band gap of about 3.7 eV at room temperature leads to strong self-compensation, and it has only comparatively recently been possible to make low resistivity n-type ZnS and it is still not possible to make low resistivity p-type ZnS. Also ZnS is a commercially important phosphor because the energy gap allows optical emission in the whole visible spectral region. As a result of these factors most of the studies of deep levels in ZnS have used predominantly optical techniques, such as the early measurements of thermally stimulated luminescence[99] and photoluminescence[91]. However, the luminescence spectra of deep centres are sometimes very difficult to interpret because of the contributions from several different excitation and recombination processes. The lack of information on the energy levels and the concentration of deep centres makes the absolute values of optoelectronic parameters very difficult to determine.

For more conventional semiconductors with smaller energy gaps, junction space-charge techniques such as DLTS or photocapacitance have provided powerful tools for the investigation of deep levels in these semiconductors[100].

Extension of these techniques to ZnS has been slowed by the absence of good p-n junctions, the difficulty of making good Schottky contacts and the complications of making measurements below room temperature because of carrier freeze-out, shallow donor ionization energies being typically about 100 meV[64,101]. Grimmeiss et al[59] made DLTS and photocapacitance measurements on crystals in the ZnS_xSe_{1-x} series using Schottky contacts on cleaved crystal surfaces, but could only go to $x = 0.95$ and could not make measurements on ZnS itself. Fornell et al[60] made Dual Light Source Steady-state (DLSS) photocapacitance measurements on ZnS and ZnS: Mn crystals, again using Schottky contacts on cleaved surfaces. They restricted themselves to a single pump photon energy and presented hole photoionization spectra in the range between 0.75 eV and 1.55 eV.

In this chapter we present rather more extensive photocapacitance measurements of deep levels in ZnS. We exploited the flexibility of the DLSS method. Two beams of light shine on the sample. The stronger one is the pump light at a fixed photon energy. It determines the fractional occupancy of the energy levels in the depletion region. The weaker one is the probe light and is used to perturb the occupancy. By spectrally scanning the probe light and by measuring changes of the occupancy of the deep levels through the junction capacitance, one can in suitable conditions determine photoionization spectra in relative units. Measurements of absolute cross-sections or level concentrations require transient capacitance measurements which are much slower but which need be made at only a few photon energies instead of throughout the spectrum. By choosing an appropriate

pump photon energy one can selectively fill or empty different deep levels and it is this which makes it a powerful technique. Also because we used a true resistance-capacitance bridge it was possible to use Schottky contacts made on etched surfaces, with poorer electrical characteristics than those made on cleaved surfaces. Clearly this is important if photocapacitance techniques are to be used on, say, epitaxial layers of ZnS.

6.2 Materials and apparatus

Two single crystals of ZnS were used. One, ZnS1, was melt-grown by Eagle Picher at 1800 °C and the second, ZnS2, was grown in our laboratory by iodine transport at 820 °C. To extract impurities such as copper and to make the crystals conducting, slices of the material were heated in high-purity molten zinc containing a small amount of aluminium. After polishing and eching in bromine/methanol, followed by 5 minutes in a solution of NaOH (50% saturation) at 50 °C, ohmic contacts were made on one face by alloying indium and a Schottky contact on the opposite face by evaporating a 1mm diameter gold or aluminium contact. The sample was then mounted on a copper cold finger in a cryostat by a pressure contact.

The photocapacitance measuring apparatus is in a dark-room and is remotely controlled by a microcomputer. The block diagram of this system is shown in Fig.6.1. Monochromatic pump and probe beams were obtained from two large-aperture grating monochromators with tungsten-halogen lamps driven from stabilized power supplies. For some experiments filters were

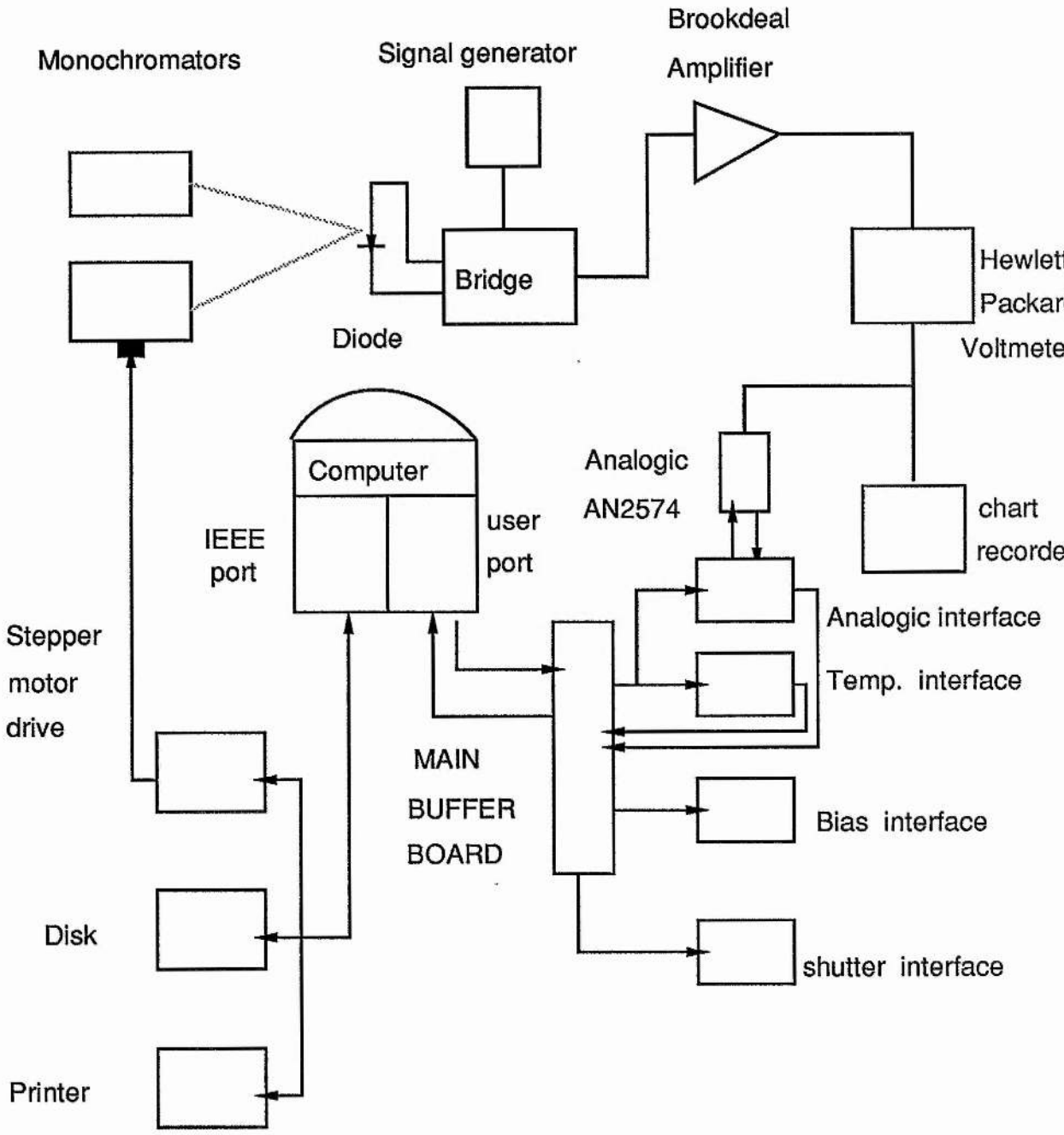

Fig.6.1 Schematic diagram of the microcomputer-controlled photocapacitance measuring system.

employed instead of one of the monochromators in order to increase the photon flux. Capacitance measurements were made with a specially constructed transformer ratio arm bridge, the balance being made against a series combination of capacitance and resistance. For the range of experimental conditions used, the off-balance signal is directly proportional to the change in the sample capacitance. The AC voltage at the diode was 30 mV peak-to-peak at 400 kHz. Photon fluxes were measured by a thermopile with a flat spectral response over the relevant range.

All the capacitance measurements were done at room temperature because carriers freeze out rapidly at lower temperature, as shown in Fig.6.2. The cryostat served as a thermal reservoir to maintain a constant temperature. The reason why the measurements can be made at such high temperature will be given in the next section. The electron concentration of ZnS2 was found to be about $3 \times 10^{16}\ cm^{-3}$ at room temperature by capacitance-voltage measurements.

The photoluminescence measurements were made on the ZnS sample with a 365 nm line from a high intensity mercury lamp as the excitation source, the sample being in a cryostat so that the temperature could be varied between liquid nitrogen and room temperature. The resolution of the monochromator used to resolve the photoluminescence is 8.2 Å/mm. The spectra have been corrected for system response by calibration against a black body radiation.

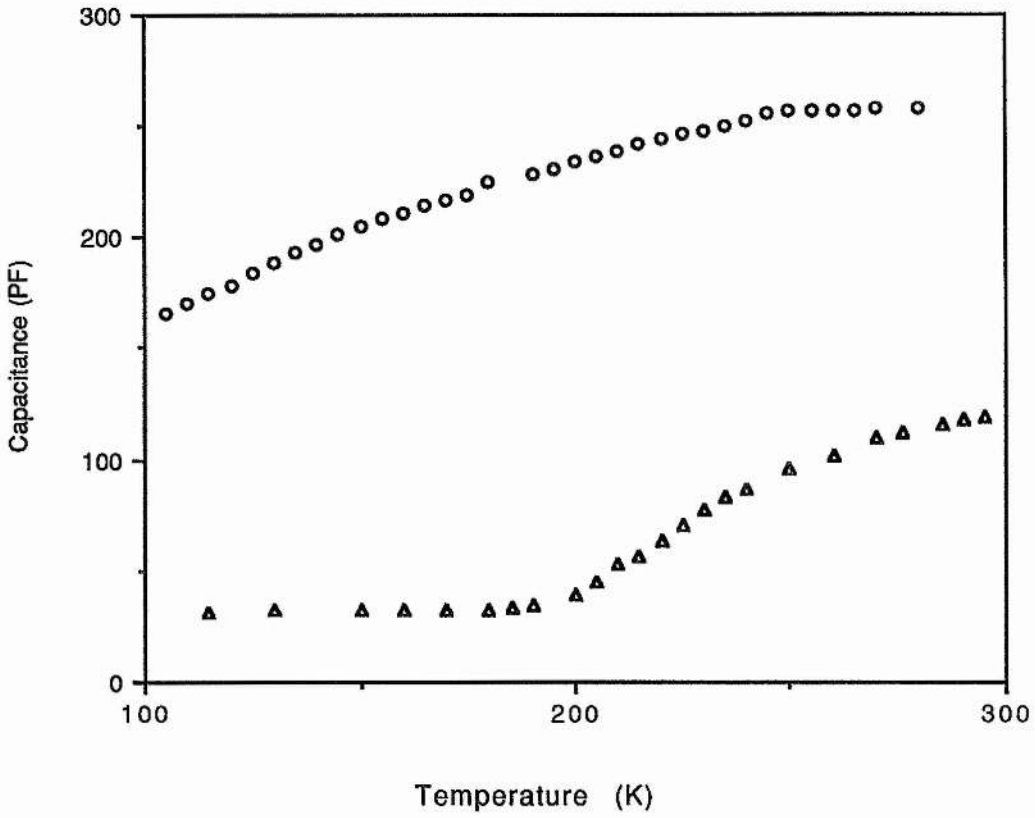

Fig.6.2 Temperature dependence of the depletion layer capacitance of Schottky diodes made on melt-grown ZnS1 (Δ) and iodine-transported ZnS2 (o), showing the effect of carrier freeze-out.

6.3 The principles of photocapacitance measurements

A Schottky diode possesses a depletion region which is adjacent to the metal contact and is devoid of free carriers except for a few Debye lengths at the edge of the depletion region. Consider the depletion region of a Schottky diode on an n-type semiconductor with a shallow donor concentration N_D and

a deep level concentration N_T. Then the capacitance of this Schottky barrier can be written as

$$C = \left(\frac{A^2 q \varepsilon \varepsilon_o}{2(V_d + V_r)} (N_D + sN_T) \right)^{1/2} , \qquad (6.1)$$

where A is the area of the Schottky contact, V_d is the built in potential, V_r is the applied reverse bias and s is the charge factor of the impurity with respect to the lattice. For example s = -1 when the impurity is a singly charged acceptor.

If the concentration of electrons on the deep centres n_T is changed by Δn_T uniformly throughout the depletion region (eg by photoionization) then the fractional change of capacitance $\Delta C/C$ is proportional to Δn_T if it is small. In the case that $N_T << N_D$ then

$$\Delta C/C = -\Delta n_T/2N_D . \qquad (6.2)$$

Hence by making the above approximations it leads to the simple result that the change of junction capacitance is directly proportional to the change in the electron occupancy of a deep centre. This is the basis of photocapacitance measurements. The minus sign in equation(6.2) shows that a decrease in the trapped electron concentration gives rise to an increase in the junction capacitance. Therefore the magnitude and sign of the capacitance change gives information about the magnitude and sign of Δn_T, so one can tell if an optical transition is to the conduction band (Δn_T negative) or from the valence band (Δn_T positive).

6.3.1 The rate equation

Optical and thermal transition rates between a deep level and the conduction band and between a deep level and the valence band are denoted as e_n^o, e_n^t and e_p^o, e_p^t respectively. And the capture constants from the conduction band into a deep level and from the valence band into a deep level are denoted as c_n and c_p. The change in the electron occupancy of a deep level can be expressed by the following rate equation

$$\frac{dn_T}{dt} = (c_n n+e_p)(N_T-n_T) - (c_p p+e_n)n_T \,, \qquad (6.3)$$

where $e_{n,p}=e_{n,p}^o+e_{n,p}^t$, n and p are the free electron and hole concentrations in the conduction band and the valence band within the depletion region.

For an energy level initially filled with electrons, integration of equation (6.3) gives

$$n_T(t)= \frac{c_n n+e_p}{c_n n+c_p p+e_n+e_p}N_T$$

$$+ \frac{c_p p+e_n}{c_n n+c_p p+e_n+e_p}(\exp(-(c_n n+c_p p+e_n+e_p)t))N_T \qquad (6.4)$$

and for an energy level initially empty, then

$$n_T(t) = \frac{c_n n+e_p}{c_n n+c_p p+e_n+e_p}(1-\exp(-(c_n n+c_p p+e_n+e_p)t))N_T \qquad (6.5)$$

It is readily seen from equation(6.4) and equation(6.5) that the electron occupancy of the deep level varies exponentially with time in both cases and the time constant of the decay is given by

$$\tau = \frac{1}{c_n n+c_p p+e_n+e_p} \,, \qquad (6.6)$$

which is independent of both the initial conditions and the concentration of the deep centre. The steady state electron occupancy of the deep level is given by

$$\frac{n_T}{N_T} = \frac{c_n n + e_p}{c_n n + c_p p + e_n + e_p} \quad . \tag{6.7}$$

6.3.2 Transient photocapacitance

For simplicity we make the abrupt approximation, i.e., free carrier depletion is assumed to be complete up to some width W, with no depletion beyond W, so that n = p = 0 in the depletion region. This is a good approximation as the free carriers are swept out under the high electric field within the depletion region. Therefore the time constant of a transient process is given by

$$\tau = \frac{1}{e_n^o + e_p^o + e_n^t + e_p^t} \quad . \tag{6.8}$$

If the experiment is performed below the freeze-out temperature so that the thermal emission can be neglected, then the time constant is determined by the optical emission rates only,

$$\tau = \frac{1}{e_n^o + e_p^o} \quad . \tag{6.9}$$

In the case that the deep level is in the upper half or lower half of the band gap, such that $e_n^o >> e_p^o$ in n-type material or $e_n^o << e_p^o$ in p-type material is satisfied, then a time constant is obtained which is given by

$$\tau = \frac{1}{e_n^o} \quad \text{or} \quad \tau = \frac{1}{e_p^o} \; . \qquad (6.10)$$

In principle, therefore, if experiments can be arranged so that the signal obtained is directly proportional to the change in junction capacitance, the time dependence of this signal would give absolute values of emission rates. However, in practice some problems occur. One problem is that the observed transient signal is frequently not of simple exponential form. There are many reasons for this non-exponential behaviour, for example the refilling of electrons from the edge of the depletion region[102], the field dependence of optical cross-section, and the condition $N_T << N_d$ not being satisfied. A second problem is that if there are several deep levels in the band gap, the results are difficult to interpret because centres with widely different transition rates empty simultaneously. A third problem is that the incident light is spectrally narrow and therefore very weak, the time constant of a transient process can be very long, so it is a very time consuming measurement.

6.3.3 Dual Light Source Steady-state photocapacitance

In the DLSS measurements, two beams of light were used. A pump light is used to fix the initial occupancy of the deep centre and a probe light is used to perturb the occupancy of the deep centre to produce an optical cross-section spectrum for electrons or holes. In order to have a better insight into the principle of

DLSS capacitance measurements, a general case is considered here for the derivation of the formula. Figure 6.3(a) shows an energy band diagram with shallow and deep centres, and Fig 6.3(b) shows all the possible transitions which can occur during a DLSS measurement.

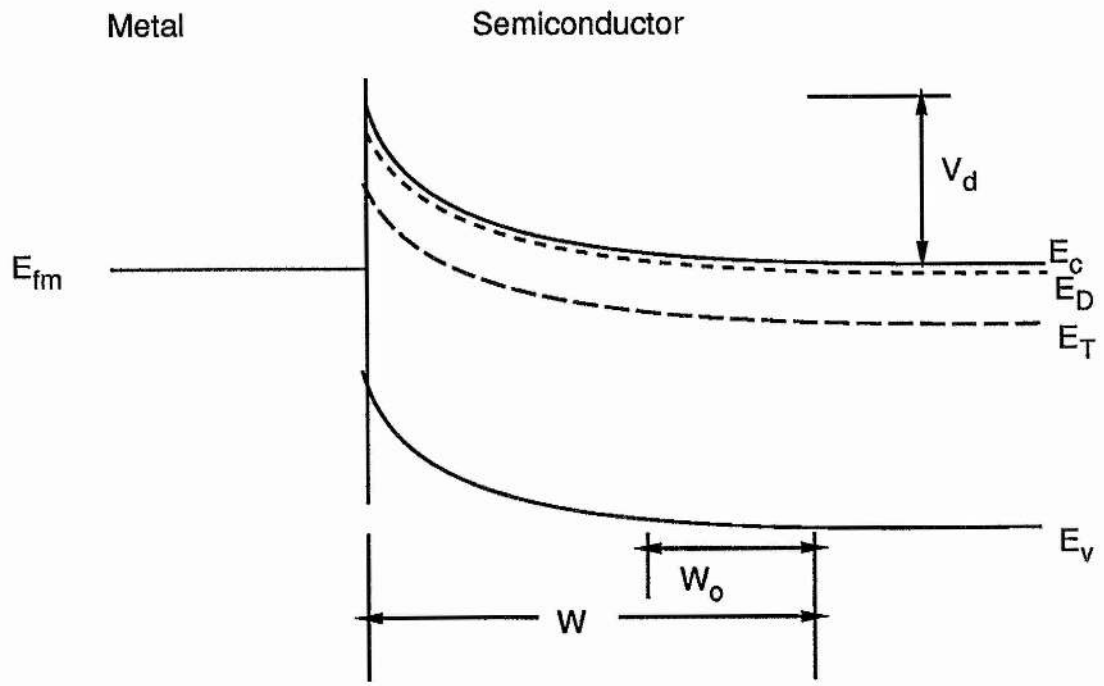

Fig.6.3(a) Energy diagram of a Schottky barrier with shallow donors N_D at energy E_D and deep centres N_T at energy E_T, W is the width of the depletion region and W_o is the length of free-carrier tails.

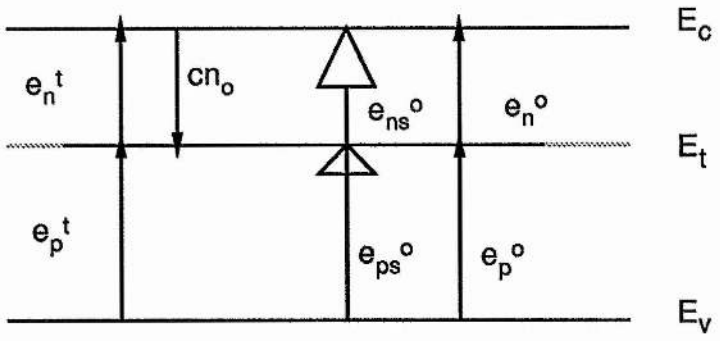

Fig.6.3(b) Schematic diagram of transitions within the depletion region of a Schottky diode due to simultaneous illumination with two beams of light. o-optical; t-thermal; c-capture constant; e-emission rate; n-electron; p-hole; s-pump light.

When the steady-state is established using the pump beam only, the electron occupancy of the deep level is given by

$$\frac{n_T}{N_T} = \frac{e_{ps}^o + e_p^t + c_n n}{e_{ns}^o + e_n^t + e_{ps}^o + e_p^t + c_n n} , \qquad (6.11)$$

where e_{ns}^o and e_{ps}^o are the electron and hole emission rates produced by the pump light. When the probe light is added, the steady-state electron occupancy will be given by

$$\frac{n_T'}{N_T} = \frac{e_p^o + e_{ps}^o + e_p^t + c_n n}{e_p^o + e_n^o + e_{ns}^o + e_n^t + e_{ps}^o + e_p^t + c_n n} . \qquad (6.12)$$

When the pump light is much stronger than the probe light, i.e., $e_{ns}^o + e_{ps}^o >> e_p^o + e_n^o$, then subtracting equation (6.11) from equation (6.12) gives the change of the electron occupancy (Δn_T) produced by the probe light alone to be

$$\frac{\Delta n_T}{N_T} = \frac{(e_{ns}^{o}+e_n^{t})e_p^{o} - (e_{ps}^{o}+e_p^{t}+c_n n)e_n^{o}}{(e_{ns}^{o}+e_n^{t}+e_{ps}^{o}+e_p^{t}+c_n n)^2} = \frac{Ae_p^{o} - Be_n^{o}}{(A+B)^2}, \qquad (6.13)$$

where $A = e_{ns}^{o}+e_n^{t}$ and $B = e_{ps}^{o}+e_p^{t}+c_n n$. The quantities A and B are constant at a fixed temperature and with the same pump light. This is the reason why the DLSS measurements can be performed at higher temperature than the transient measurements. As an example, if a deep level is in the upper half of the band gap there is a range of energies for which e_p^{o} is zero or negligible and

$$\frac{\Delta n_T}{N_T} = - \frac{Be_n^{o}}{(A+B)^2}. \qquad (6.14)$$

In this case the capacitance change is proportional to the optical emission rate to the conduction band produced by the probe light. Since this rate is $\phi\sigma$, where ϕ is the probe photon flux and σ is the photoionization cross-section, measurements of ΔC for different probe energies give the spectrum of photoionization.

Similarly, for other deep levels, one can manipulate the magnitudes of A and B by the choice of the pump photon energy and thereby make one or other of the terms in the numerator of equation (6.13) dominate. If there are several deep levels in the energy gap one can preferentially fill or empty a particular level by choosing an appropriate pump photon energy and the probe light can be used to study this particular centre.

In a typical experiment, pump light of a suitable photon energy is shone on the diode. The microcomputer then samples the capacitance at regular time intervals (which are settable) until the difference between successive readings is sufficiently small for a steady state to be deemed to have been reached. The probe

light shutter is then opened and again capacitance readings are taken until steady state has been reached. Next the probe wavelength is changed to the next value by a step-motor controlled by the microcomputer and the procedure is repeated. The change of the steady-state capacitance between probe light off and on is divided by the photon flux at each wavelength and this gives a photoionization spectrum in arbitrary units.

An advantage of DLSS, where the pump source can be spectrally broad and therefore strong, over single-beam transient techniques, where the source has to be narrower and therefore usually weak, is that the total optical emission rate is greater. Hence the time constant is shorter and it takes less time to measure the photoionization spectrum. (A balance has to be struck since equation (6.13) shows that as the pump strength increases Δn_T decreases and hence ΔC is smaller). A disadvantage is that only relative values of the cross-section are obtained. When conditions are favourable, eg with a level in the upper half of the band gap for n-type material or with a level in the lower half of the band gap for p-type material and with negligible thermal emission, only one term in equation(6.9) dominates. It is then possible to obtain an absolute value of the cross-section by a capacitance transient method with a single monochromatic beam. As this is a slow process, the absolute value is only measured at one or a few photon energies and this is used to calibrate the photoionization spectrum.

6.4 Results

Initially, single-beam photocapacitance measurements were made on diodes from both sources of ZnS. The object was to get information about levels in the upper half of the band gap and to get some indication of other levels as a guide for the DLSS measurements. The capacitance bridge was balanced in the dark, then the light was switched on and the off-balance signal was recorded at different photon energies. The capacitance change was positive, showing that there were transitions to the conduction band. The spectra are shown in Fig.6.4.

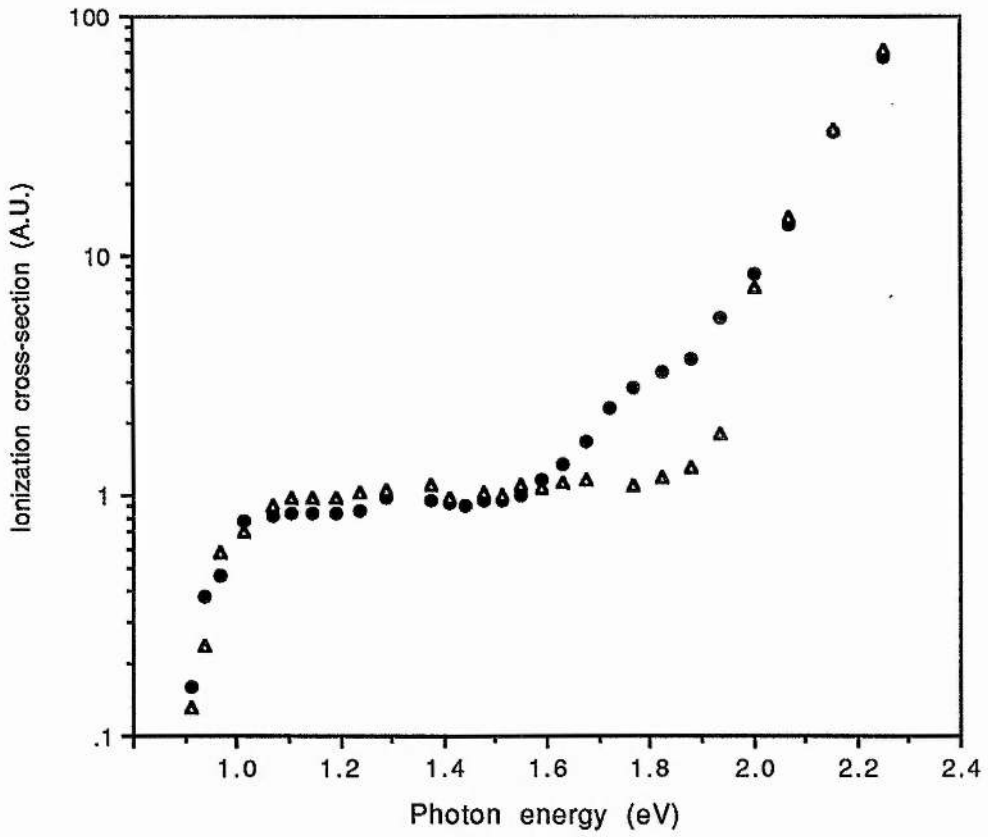

Fig.6.4 Single-beam photocapacitance spectra for melt-grown ZnS 1 (Δ) and iodine-transported ZnS 2 (•). The spectra are normalized at 2.16 eV. The sign of capacitance change shows that the transitions are to the conduction band.

From Fig.6.4 one see that for both samples there is a sharp threshold demonstrating the existence of a level at around 0.9 eV below the conduction band. Both samples show a level at about 2.0 eV and ZnS2 has an extra level at about 1.6 eV, both energies being with respect to the conduction band.

To investigate the 2.0 eV level in ZnS1, a pump light of 2.15 eV was chosen. In order to fill the level preferentially with electrons, choice is restricted. The pump photon energy must be sufficiently far above 1.7 eV (the energy separation from the valence band) for transitions from the valence band to the level to be strong, yet not too far above 2.0 eV otherwise transitions to the conduction band would appreciably decrease the occupation of the level by electrons. Figure 6.5 shows the spectrum of the electron photoionization cross-section. If phonon coupling is weak in the optical transition, a plot of $(\sigma h\nu)^{2/3}$ against $h\nu$ should be linear in the threshold region or, if the transition to the band edge is allowed a plot with an exponent different from 2/3 but still small should be linear[103]. This is found not to be the case here, so phonon coupling is medium or strong. It is then difficult to find the ionization energy accurately, but the observed threshold at approximately 2.0 eV should correspond with the zero-phonon transition energy.

Figure 6.5 also shows the electron photo ionization spectrum for a diode made from ZnS2. At higher photon energies there is excellent agreement between the spectra for the two materials, showing that the 2.0 eV level is common to both.

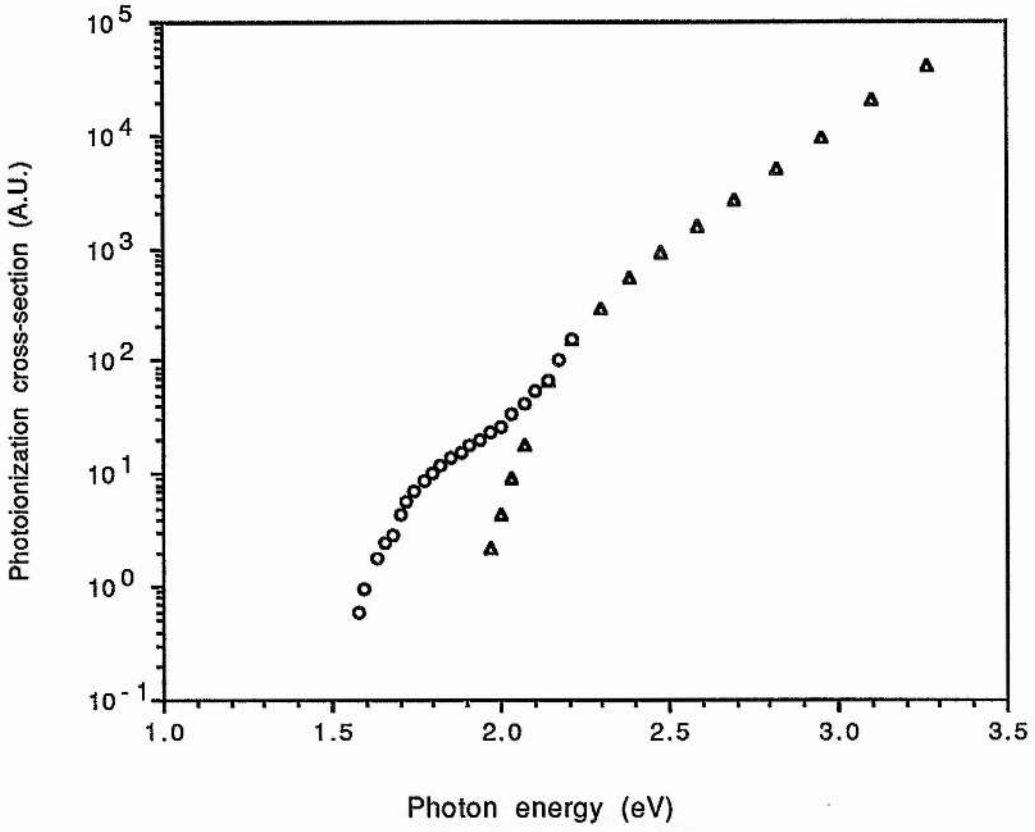

Fig.6.5 The photoionization cross-section spectra for transitions to the conduction band for the melt-grown ZnS1 (Δ) and iodine-transported ZnS2 (o). A pump photon energy of 2.15 eV with spectra width of 0.05 eV was used. The spectra for the two materials are normalized in the higher energy range.

The extra level in ZnS2 at lower energy is evident from the spectrum shown in Fig.6.5. A plot of $(\sigma h\nu)^{2/3}$ against $h\nu$ for the spectrum of ZnS2 is given in Fig.6.6. There is a linear region, with a departure from linearity at higher energy because of the 2.0 eV level. Extrapolation of the linear part gives an ionization energy of 1.58 ± 0.02 eV. In principle it should be possible to empty this level by the use of a suitable pump photon energy, leaving just the 2.0 eV level in the spectrum.

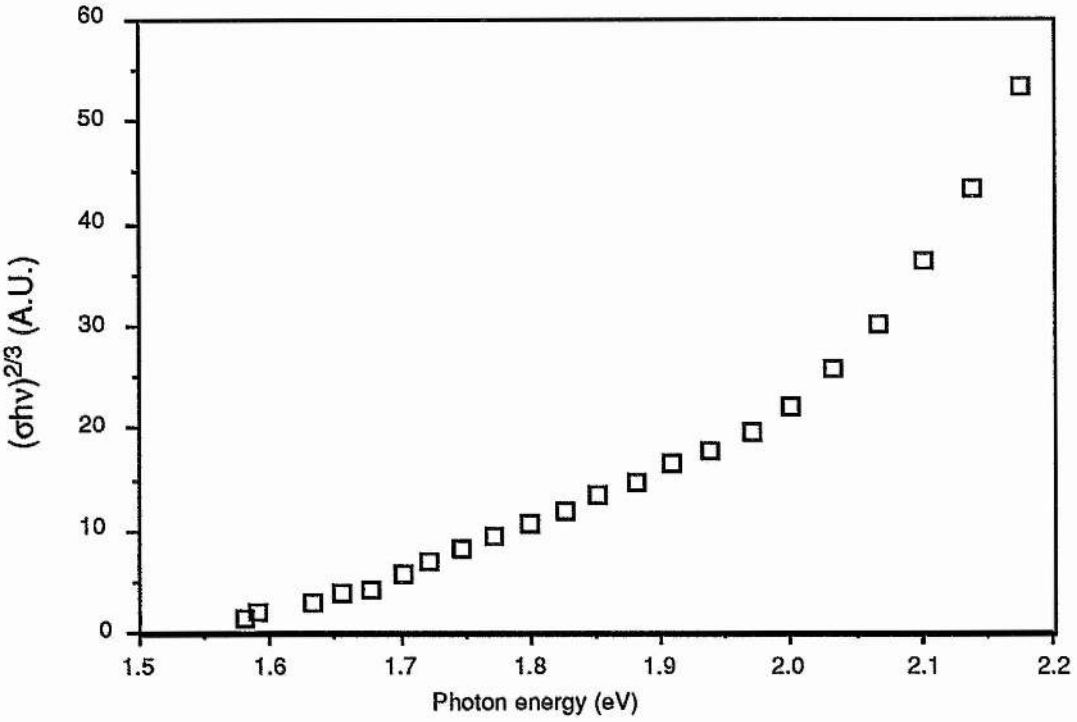

Fig.6.6 A plot of $(\sigma h\nu)^{2/3}$ as a function of photon energy for ZnS 2 shown in Fig.6.5, showing the linear relation near the threshold for the lower-energy transition.

With 1.75 eV pump photon energy and no voltage bias the 1.58 eV level was still seen. This is because in these conditions the abrupt approximation for the depletion layer width is inadequate and some of the levels near the edge of the depletion region can be populated by electrons thermally excited into that region. The effect can be reduced by applying a reverse bias since then a greater fraction of the depletion region is almost completely depleted. Application of 10 V reverse bias did indeed substantially reduce the contribution of the 1.58 eV level with 1.75 eV pump light, but did not remove it completely, which is shown in Fig.6.7.

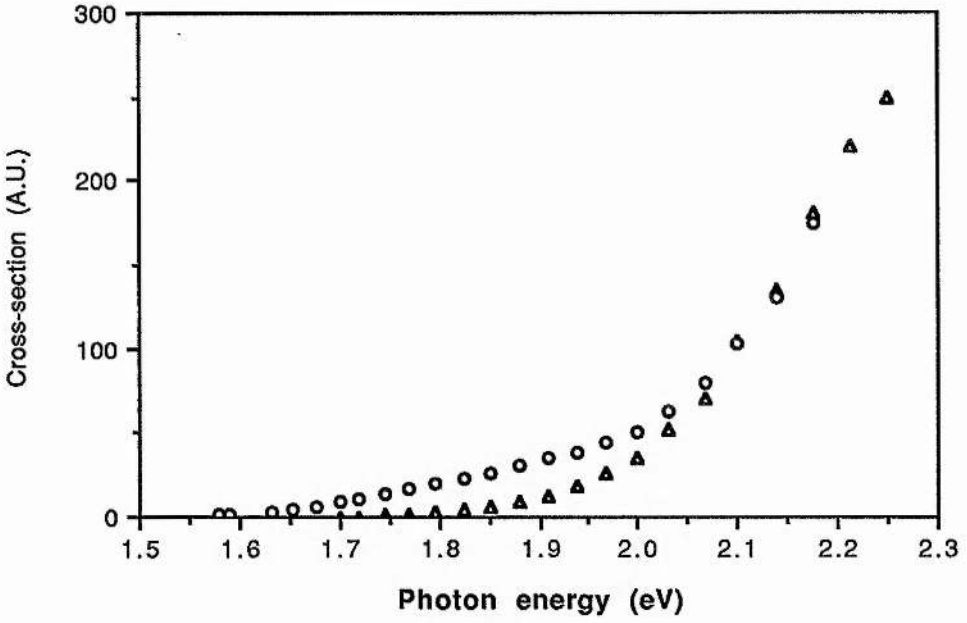

Fig.6.7 The photoionization cross-section spectra for transitions to the conduction band for ZnS 2 with pump photon energy of 1.75 eV. (o) without reverse bias and (Δ) with 10 V reverse bias. The two spectra are normalized at higher-energy region.

A deeper level was revealed by using pump photon energy of 2.95 eV, which partially emptied the level (i.e., the pump light can ionize electrons from the level to the conduction while it can also excite electrons from the valence band to refill the level). With probe light photon energy greater than 0.8 eV the junction capacitance decreased, showing that the probe light was repopulating the level by transitions of electrons from the valence band. Diodes from both ZnS1 and ZnS2 showed the same spectrum, which is plotted in Fig.6.8. A plot of $(\sigma h\nu)^2$ against $h\nu$ gave a straight line near the threshold, with an ionization energy for the level of 0.81 ± 0.01 eV determined by extrapolation. The reason for the use of this plot is that equation (6.15) in the discussion section suggests that this is the form near threshold for a sharply-peaked spectrum.

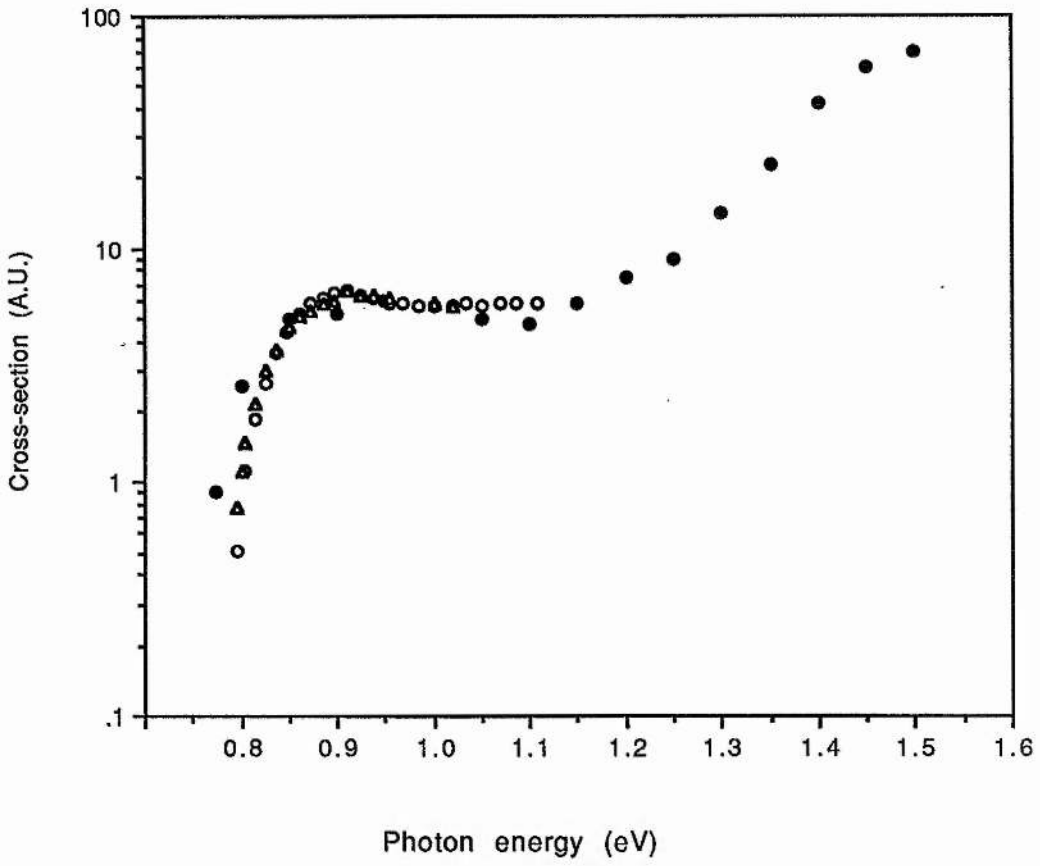

Fig.6.8 Spectra of photoionization cross-section for transitions from the valence band to a deep level. (Δ) ZnS 1 and (o) ZnS2 of present work with 2.95 eV pump photon energy, and (•) from ref(60) with near-band-gap pump photon energy. The spectra have been normalized for comparison.

Under 365 nm excitation the iodine-transported sample ZnS2 showed a blue luminescence with an emission peak at about 2.55 eV (being corrected for system response) which shifted to lower energy when the temperature decreased from room temperature to liquid nitrogen temperature. Figure 6.9 shows the photoluminescence spectra at liquid nitrogen temperature and room temperature with and without the correction for the system response. Its position, width and temperature shift identifies it

as the self-activated luminescence[104]. The melt-grown sample ZnS1 had only a very weak blue luminescence.

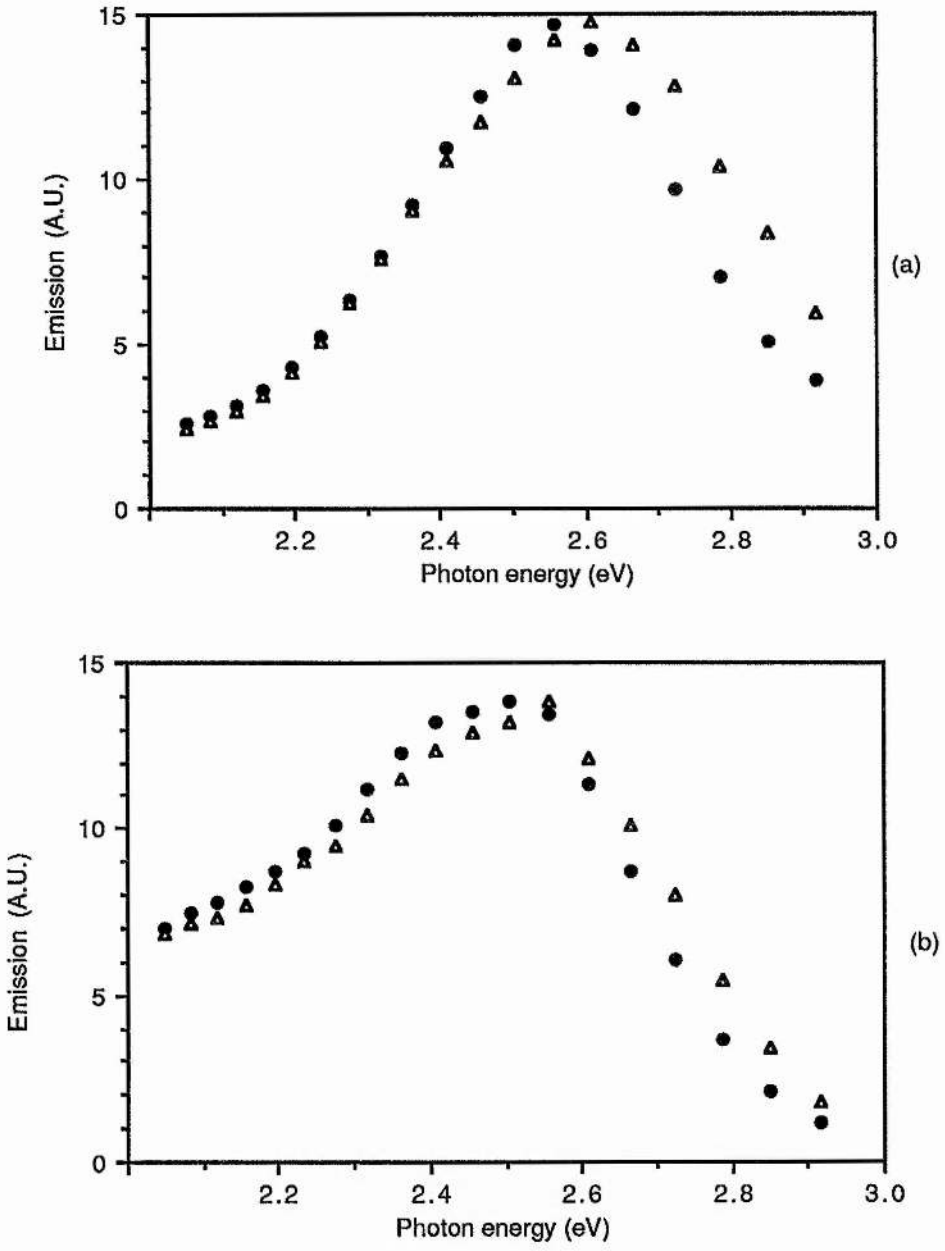

Fig.6.9 Photoluminescence spectra of ZnS 2 at liquid nitrogen temperature (•) and room temperature (Δ) under Ultra-violet light excitation. (a) without and (b) with correction for system response.

6.5 Discussion

It is interesting that the levels 0.9 eV and 2.0 eV below the conduction band and 0.8 eV above the valence band appear in diodes from both the iodine transported and the melt-grown ZnS. (It should be noted however that both materials had been through a treatment in molten zinc/aluminium to reduce the resistivity). The similarity suggests that the levels may be due to lattice defects, although a persistent impurity like copper cannot be entirely ruled out. Other than this, the present experiments give no clue as the identity of the centres producing the levels.

The only photocapacitance data of which we know which are directly comparable with our own are in the work of Grimmeiss et al[59] and Fornell et al[60]. These authors used iodine-transported ZnS treated in molten zinc or zinc/aluminium. Their single crystals were cleaved in air before Schottky contacts were made. Fornell et al[60] used ZnS and ZnS:Mn while Grimmeiss et al[59] used ZnS_xSe_{1-x} with x up to 0.95. Their published data mainly refer to transitions from the valence band. Fig.6.8 shows a cross-section spectrum for these transitions in ZnS obtained by Fornell et al[60]. It covers a wider spectral range than ours but in the range of overlap there is good agreement in the shape of the spectrum. (It should be mentioned here that our spectrum was measured before they published the data). There is evidence that the features with peaks at about 0.9 eV and 1.5 eV are associated with different centres rather than being associated with, say, the ground and the excited state of a single centre. For example, Fornell et al[60] found that incorporation of manganese suppresses

the 0.9 eV peak. Grimmeiss et al[59] observed the two peaks for $0.59 \leq x \leq 0.95$ and found that at $x = 0.59$ the upper peak depended strongly on the pump photon energy while the lower peak was, within experimental error, unchanged. It was suggested that the centre involved was the self-activated (A) centre because the photoionization spectrum is similar to that for quenching of the self-activated luminescence[105] and of the A-centre spin-resonance[106]. However, if the 0.9 eV and 1.5 eV peaks do arise from different centres, the exact form of association between the spectra and the A-centre is unclear.

The situation here seems to be different from that for the M-centre discussed in chapter 5 where the sharp and broad peaks appear to be correlated.

Most photoionization spectra show a broad peak and the narrowness of the 0.9 eV peak is unexpected. Peaks can occur due to excited states either below the continuum energy (requiring photothermal or two-step optical ionization) or within the continuum as a resonance. An explanation in terms of an excited state seems unlikely here because there is no evidence of a transition to a related continuum. Szawelska[107] showed that a peak just above threshold, with a half-width only a small fraction of the photoionization energy, is predicted by a simple model. She considered a transition between a centre of a definite parity and a band with the opposite parity at the Brillouin zone centre, with an impurity wavefunction with radial variation $r^{-1}\exp(-\alpha r)$. The cross-section σ is then given by

$$\sigma(h\nu) \propto \frac{E^{1/2}}{h\nu(E_\alpha + E)^2}, \qquad (6.15)$$

Where E is the energy above threshold and E_α is $h^2\alpha^2/(8\pi^2 m^*)$ if the wavefunction above is an effective-mass envelope function or is $h^2\alpha^2/(8\pi^2 m)$ in the opposite extreme when it is the actual function rather than an envelope. We find that the shape of the 0.9 eV peak is approximately reproduced by taking the latter situation with α about $(4Å)^{-1}$, which is reasonable for a tightly bound deep centre. The spectrum calculated by this model together with the measured hole ionization spectrum are shown in Fig.6.10.

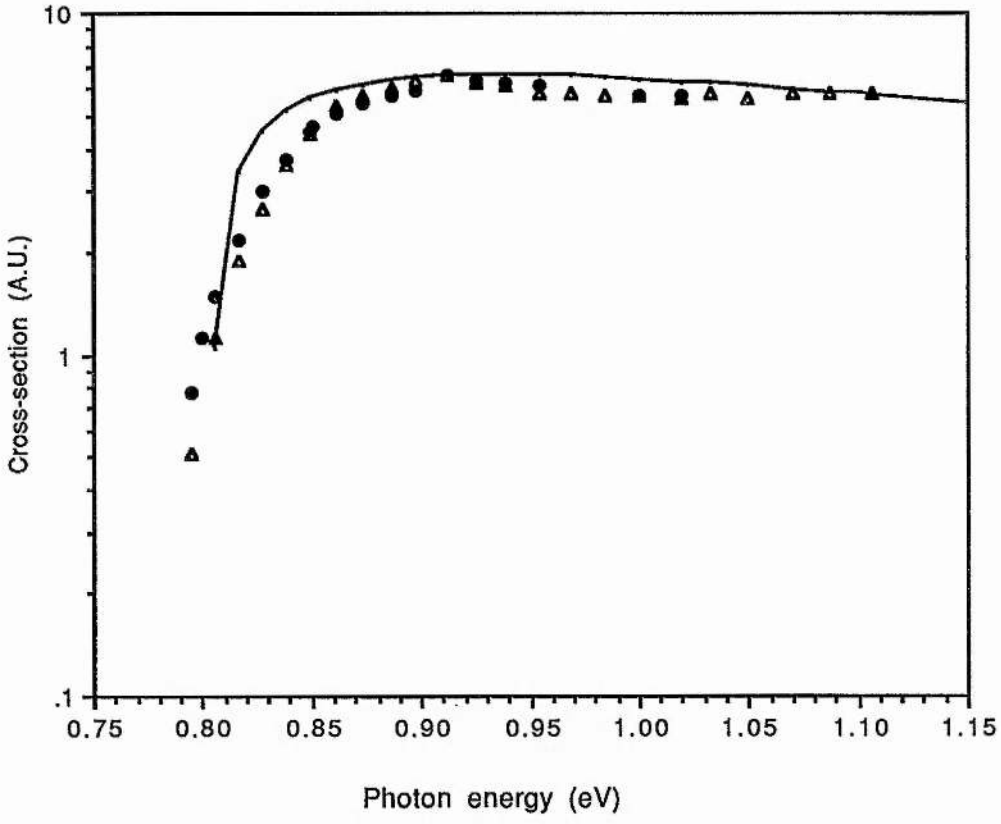

Fig.6.10 Comparison of photoionization spectrum (solid line) calculated by equation (6.15) with the experimental data (dots and triangles), α in equation (6.15) being taken as $(4Å)^{-1}$.

6.6 Conclusions

Deep impurity levels have been found by photocapacitance measurements at 0.9 eV and 2.0 eV below the conduction band and at 0.8 eV above the valence band in both melt-grown and iodine transported ZnS. These levels may be due to lattice defects as they appear in both sources of material without any deliberate doping, though both materials had been through molten zinc/aluminium treatments. An additional level at about 1.6 eV below the conduction band was seen in the iodine-transported material. The measurements were performed using evaporated Schottky contacts on chemically etched surfaces. As attention is focused more and more on the properties of ZnS as a semiconductor, for example in quantum wells[108], rather than simply as a phosphor, this extension of common semiconductor characterization techniques to ZnS is a useful step forward.

Chapter 7 Conclusion

7.1 This thesis

We have made extensive characterization work on ZnSe and ZnS through electrical, optical and deep level studies. An overview of the work contained in this thesis can be obtained by reading the concluding sections of chapter 2 to chapter 6. Instead of simply repeating these, we wish to bring all these conclusions together and find out the wider implications behind them.

ZnSe, with a 'blue' direct gap of 2.7 eV at room temperature, has long been considered as a promising material for blue light-emitting diodes and blue semiconductor lasers. This could be misleading without bearing in mind that to realize these optical devices, the following two basic conditions have to be accomplished. One is the efficient blue emission at room temperature and the other is the conductivity control in both the n-type and p-type material. Despite the long history of luminescence study in ZnSe, the mechanism for producing the room temperature blue luminescence has not previously been positively identified. We have provided evidence that the room temperature blue luminescence arises from a transition between a free hole and an electron bound to a donor as pointed out by Shirakawa and Kukimoto[40], but not all donors contribute to the transition when the donor concentration (which is not synonymous with electron concentration) is high enough for an appreciable spread of donor energies to occur. We suggest that

only those donors, which by statistical fluctuation are much more separated from other donors than is average, contribute to the emission because their wavefunctions in **k**-space are more spread out and have larger recombination rates with free holes. This conclusion indicates that the intensity of the blue band increases with donor concentration, as has been observed in chlorine and iodine doped ZnSe[30,31]. Because most of the shallow donors in ZnSe are ionized at room temperature, when the electron concentrations are higher than a certain level (say 10^{18} cm^{-3}), some other effects such as Auger quenching of luminescence will become dominant.

Features of low temperature photoluminescence spectra, including the bound exciton linewidths, the ratio of the dominant near-band-edge (NBE) to deep level intensities (R value), and the intensity of the dominant NBE emission, are frequently used in the literature[88,109] to judge the relative quality of ZnSe films. Linewidths, measured at the half maximum of emission bands, serve as a criterion of the film quality since the exciton lines broaden as the density of impurities and the sample inhomogeneity increase[110]. (Electron mobility at low temperature can also be used as an indication of film quality because the mobility depends on the concentration of the ionized impurity scattering centres). It is not the low temperature, but the room temperature R value and the room temperature intensity of the blue emission that are important. As the intensity of the blue emission increases with donor concentration while the exciton linewidths increase and electron mobility decreases with donor concentration, it is incorrect to imply that the low

impurity concentration and high mobility ZnSe is most suitable for light emitting diodes. For the improvement of the crystal growth in ZnSe, it is essential to grow firstly high quality material (good surface morphology, low impurity concentration, etc), and then to dope with donor or acceptor species to the level showing highest intensity of the blue emission at room temperature.

The difficulty in the conductivity control of both n-type and p-type ZnSe is mainly due to the high compensation, which is a common feature in wide band gap semiconductors. Suppose we have low resistivity n-type material, i.e., a substantial free electron concentration. If acceptors are introduced then electrons will go from the conduction band onto the acceptors. If the formation energy of the acceptors is less than the depth of the acceptors below the conduction band then compensated high-resistivity material is thermodynamically stable. The compensation can be reduced by low temperature non-equilibrium growth such as MBE and MOCVD, and indeed high n-type conductivity can easily be grown[30,31]. On the other hand, it has been shown in chapter 4, for the iodine doped high electron concentration MOCVD ZnSe samples, annealing in the temperature range 300 to 450 °C can lead to large increase in resistivity. The effect is larger for annealing in air or selenium vapour and smaller for annealing in vacuum or zinc vapour, and is thought to be due to the introduction of an acceptor which is likely to be a lattice defect. The results indicate that the compensation happens even at low temperature and could also explain why the

MOCVD ZnSe grown at temperatures higher than 375 °C exhibits high resistivity[89,111].

Room temperature blue electroluminescence from both MIS structures and p-n junction ZnSe have been demonstrated in a number of laboratories, but none of them could be made reproducibly at present. Due to the unavailability of p-type ZnSe in our laboratory, we have made MIS structures on high carrier concentration n-type MOCVD ZnSe. With the higher blue emission intensity, we have been able to measure the spectrum of blue electroluminescence at room temperature with relatively high resolution. It shows the same nature as the one observed in photoluminescence, i.e., with the emission peak at 2.69 eV. The measured peak position of the blue emission from ZnSe p-n junction is lower than 2.69 eV[32,33] which is probably due to the self-absorption.

We have discussed the origin of the M-centre in ZnSe. The M-centre is a predominant deep level in many crystals of ZnSe. Various attributions to different defects or impurities have been made in the past, in particular there is some evidence that it is the copper red luminescence centre[56]. We have re-examined the evidence for the Cu centre and shown that it is not conclusive. Moreover, the M-centre with concentration ~ 10^{17} cm^{-3} has also been seen in our MOCVD ZnSe. Copper was not found at these levels in SIMS analysis. Also the deep level photoluminescence shows no Cu-red emission. It is suggested that the possibility is still open that the M-centre is a lattice defect. It is worth saying that in ZnSe there is always a problem to distinguish between the foreign impurities and lattice defects, eg. in the electrical

conductivity, in the bound exciton emission (I_1^{deep}), and in the deep level spectroscopy.

We have also studied deep levels in ZnS by using the double light source steady-state method. The measurements were performed using evaporated Schottky contacts on chemically cleaned surfaces. Four levels have been seen with their characteristic photoionization spectra. Although the identity of these deep levels have not been found since the material used is not deliberately doped, this is, to our knowledge, the first extensive study of deep levels in ZnS. The technique used provides a good basis for future study of deep levels in ZnS.

One indication of the deep level study in ZnSe and ZnS is that the holes produced optically are not immediately captured by the deep centres, but can be transported in the valence band to the edge of the depletion region under an electric field. The same should be true for the holes generated by the band-to-band impact ionization or by a two-step impact ionization. This could be used for minority injection in MIS diodes as being proposed by Thompson and Allen[79].

7.2 Future work

In order to realize the ZnSe p-n junction LEDs and lasers, it is essential to grow p-type ZnSe controllably and reproducibly. p-type ZnSe can be grown by the non-equilibrium low temperature techniques such as MBE and MOCVD which avoid thermodynamic effect. The problem now is still the compensation. If possible, it

is necessary to identify which compensation factor (i.e., lattice defects or foreign impurities which could be amphoteric) is the dominant one. With improving the source purity and finding the best growth parameters such as the substrate temperature and flux ratio of II/ VI, it is hoped that p-type ZnSe could be grown in a controllable manner like the n-type ZnSe.

There have been some reports on the optical properties of ZnSe-$ZnSe_XS_{1-X}$ quantum wells. Photoluminescence measurements show that the band offsets are mainly in the valence band[112,113]. This large valence band offset is useful in these materials because electron concentrations can be easily manipulated by doping during growth, optical pumping etc, but holes are difficult to inject efficiently by electrical means and tend to have short lifetime before being trapped by lattice defects or impurities. The possibility of structures with quantum confinement of holes without confinement of electrons would have interesting consequences for both physics and devices. This remains to be seen.

There has been increasing interest in optical nonlinearities in semiconductors because of their underlying physics and potential applications to optical and electric-optic devices. Optical switching devices (which are based on the properties of optical bistability) working in the blue and near ultra-violet wavelengths are needed for optical data processing. Optical bistability has been observed in ZnSe or ZnS interference filters[34], and nonlinear excitonic effects have also been observed in MBE grown ZnSe thin films[35]. For optical bistability applications and for

optimization of logic devices, it is necessary to fully understand the optical nonlinearities and related properties in ZnSe and ZnS.

The shallow donors typical of III_{Zn} and VII_{Se} substituents in ZnSe span a total energy range of only 3.2 meV[37], which is not much greater than the donor bound exciton (D^o,X) linewidth of ~ 2 meV typical of many MOCVD layers. Thus there is no possibility of chemical identification of the donors from the (D^o,X) emission. The two-electron satellites of the (D^o,X) lines, which involve energy shifts of 1s $\rightarrow$ 2s, 2p below these principal lines, turn out to be relatively poorly resolved for the MOCVD layers[64] and MBE layers[114] using non-selective photoexcitation. It was pointed out by Dean[64] that reliable information on donor species can be obtained only with selective excitation by a tuneable laser into the (D^o,X) lines and their excited states. The identification of donor species in not deliberately doped MBE and MOCVD ZnSe will provide valuable information for better growth of p-type ZnSe.

In the identification of the origin of the blue emission in ZnSe at room temperature, we have suggested that only those donors below a certain cut-off energy contribute to the recombination with free holes. We have also suggested one possible form of the donor density of states in the donor band. We know that donor banding happens when the concentration is high, which is usually deduced from electrical measurements, but the exact shape of the donor band is difficult to obtain. In low temperature photoluminescence, we observed the contribution from the tail of the donor band, and we assume that the tail is of an exponential form. One possibly way to test this is to use a tuneable blue laser

to excite the material, and measure the resulting shape of the luminescence for different excitation wavelengths (near the band edge). It is known that if the donor thermalization is faster than the recombination, then no change in the emission shape will be seen, and so the density of states in the tail of the donor band could be obtained.

The identity of the M-centre in ZnSe is still a matter for debate. If high p-type conductivity (hole concentration ~ 10^{16} cm^{-3}) ZnSe material is available, it is worth doing the DLTS or photocapacitance measurements to identify the origin of the M-centre because the structure and concentration of lattice defects will be quite different in n-type and p-type materials. Identification of dominant deep levels such as the M-centre is important for the control and improvement of the optical and electrical properties of ZnSe and ZnS.

References

(1) J. Bardeen and W.H. Brattain, Phys.Rev., **74** (1948) 230.

(2) W. Shockley, Bell Syst.Tech.J., **28** (1949) 435.

(3) J.L. Moll, M. Tanenbaum, J.M. Goldey, and N. Holonyak, Jr., Proc.IRE, **44** (1956) 1174.

(4) R.D. Deslattes, A. Henins, R.M. Schoonover, C.L. Carroll, and H.A. Bowman, Phys.Rev.Lett., **36** (1976) 898.

(5) J.B. Gunn, Solid State Commin., **1** (1963) 88.

(6) J.B. Gunn, IEEE Trans.Electron Devices, **ED-23** (1976) 705.

(7) R. Dingle, H.L. Stormer, A.C. Gossard, and W. Wiegmann, Appl.Phys.Lett., **33** (1978) 665.

(8) H.M. Macksey, T.G. Blocher, and F.H. Doerbeck, Electron.Lett., **13** (1977) 312.

(9) R.J. Keyes and T.M. Quist, Proc.IRE, **50** (1962) 1822.

(10) R.N. Hall, G.E. Fenner, J.D. Kingsley, T.J. Soltys, and R.O. Carlson, Phys.Rev.Lett., **9** (1962) 366.

(11) M.I. Nathan, W.P.Dumke, G. Burns, F.H. Dill, Jr., and G.J.Lasher, Appl.Phys.Lett., **1** (1962) 62.

(12) N. Holonyak, Jr., and S.F. Bevacqua, Appl.Phys.Lett., **1** (1962) 82.

(13) A.H. Herzog, D.L. Keune, and M.G. Craford, J.Appl.Phys., **43** (1972) 600.

(14) I. Hayashi, M.B. Panish, P.W. Foy, and S. Sumski, Appl.Phys. Lett., **17** (1970) 109.

(15) R.D. Dupuis and P.D. Dapkus, Appl.Phys.Lett., **32** (1978) 406.

(16) H.C. Casey, Jr., and M.B. Panish, "Heterostructure lasers", Academic Press, New York (1978).

(17) L.C. Chiu, and A. Yariv, J.Luminesc., **30** (1985) 551.

(18) W.T. Tsang, Appl.Phys.Lett., **39** (1981) 786.

(19) S.D. Hersee, B.De Cremoux and J.P. Duchemin, Appl.Phys.Lett., **44** (1984) 476.

(20) W.T. Tsang, Appl.Phys.Lett., **44** (1984) 288.

(21) E.A. Rezek, R. Chin, N. Holonyak, Jr., S.W. Kirchoefer and R.M. Kolbas, J.Elect.Mater., **9** (1980) 1.

(22) H. Temkin, K. Alavi, W.R. Wagner, T.P. Pearsall and A.Y. Cho, Appl.Phys.Lett., **42** (1983) 845.

(23) W.D. Laidig, P.J. Caldwell, Y.F. Lin and C.K. Peng, Appl.Phys. Lett., **44** (1984) 653.

(24) T. Miya, Y. Terunuma, T. Hosaka, and T. Miyaslita, Electronics Lett., **15** (1979) 108.

(25) T.A. Fulton, D.B. Fitchen, and G.E. Fenner, Appl.Phys.Lett., **4** (1964) 9.

(26) R.J. Nelson, N. Holonyak, Jr., W.R. Hitchens, D. Lazarus, and M. Altarelli, Solid State Commun., **18** (1976) 321.

(27) G. Destriau, J De Chimie Physique, **33** (1936) 587.

(28) T. Inoguchi, M. Takeda, Y. Kakihara, Y. Nakata and M. Yoshida, SID Intern.Symp.Dig., (1974) 86.

(29) J.W. Allen, J.Luminesc., **31&32** (1984) 665.

(30) A. Yoshikawa, H.Nomura, S. Yamaga, and H. Kasai, J.Appl.Phys. **65** (1989) 1223.

(31) K. Ohkawa,T. Mitsuyu, and O. Yamazaki, J.Appl.Phys., **62**, (1987) 3216.

(32) T. Yasuda, I. Mitsuishi, and H. Kukimoto, Appl.Phys.Lett., **52** (1988) 57.

(33) M.A. Haase, H. Cheng, J.M. Depuydt, and J.E.Potts, J.Appl.Phys., **67** (1990) 488.

(34) J.Y. Bigot, A. Daunois, R. Leonelli, M. Sence, J.G.H. Mathew,

S.D. Smith, and A.C. Walker, Appl.Phys.Lett., **49** (1986) 844.

(35) N. Peyghambarian, S.H. Park, S.W. Koch, A. Jeffery, J.E. Potts and H. Cheng, Appl.Phys.Lett., **52** (1988) 182.

(36) J.L. Merz, H. Kukimoto, K. Nassau, and J.W.Shiver, Phys.Rev., B **6** (1972) 545.

(37) P.J. Dean and D.C. Herbert, Phys.Rev., B **23** (1981) 4888.

(38) M. Isshiki, T. Kyotani, K. Masumoto, W. Uchida, and S.Suto, Phys.Rev.B, **36** (1987) 2568.

(39) M.D. Ryall and J.W. Allen, J. Phys. Chem. Solids, **34** (1973) 2137.

(40) Y. Shirakawa and H. Kukimoto, J.Appl.phys., **51** (1980) 2014.

(41) S. Fujita, H. Mimoto, and T. Nogushi, J.Appl.Phys., **50** (1979) 1079.

(42) J.Z. Zheng and J.W. Allen, J.Appl.Phys., **67** (1990) 2060.

(43) M. Yamaguchi, A. Yamamoto, and M. Kondo, J.Appl.Phys., **48** (1977)196.

(44) X.W. Fan and J. Woods, IEEE Trans. Ed. **28** (1981) 428, also J.Phys.C: Solid State Phys., **14** (1981) 1863.

(45) Y. L.Hua, M.C. Petty, G.G. Roberts, M.M. Ahmad, H.M. Yates, N.J. Maung, and J.O. Willians, Electronics Letters,**23** (1987) 231.

(46) H.H. Woodbury and M. Aven, Phys.Rev., B **9** (1974) 5195.

(47) K. Morimoto, J.Appl.Phys., **64** (1988) 4951.

(48) P.G. Konstantinos,D.C. Lu, and K.F. Jensen, Appl.Phys.Lett., **54** (1989) 353.

(49) G.F. Neumark, J.Appl.Phys., **51** (1980) 3383.

(50) J.Z. Zheng and J.W. Allen, J.Cryst.Growth, **101** (1990) 850.

(51) Y. Shirakawa and H. Kukimoto, J.Appl.Phys., **51** (1980) 5859.

(52) K. Kosai, J.Appl.Phys., **53** (1982) 1018.

(53) P. Besomi and B.W. Wessels, J.Appl.Phys., **53** (1982) 3076.

(54) S. Braun, H.G. Grimmeiss, and J.W. Allen, Phys.Stat.Sol.(a) **14** (1972) 527.

(55) H.G. Grimmeiss, C. Ovrén, and J.W. Allen, J.Appl.Phys., **47** (1976) 1103.

(56) H.G.Grimmeiss,C. Ovrén, W. Ludwig, and R. Mach, J.Appl.Phys., **48** (1977) 5122.

(57) H.G. Grimmeiss, C. Ovrén and R. Mach, J.Appl.Phys., **50** (1979) 6328.

(58) J.Z.Zheng and J.W. Allen, International Conference on Optical Characterization of Semiconductor (Sofia, 1990), to be published.

(59) H.G. Grimmeiss, E.Meijer, R.Mach and G.O. Müller, J.Appl.Phys., **56** (1984) 2768.

(60) J-O Fornell, H.G. Grimmeiss, R.Mach and G.O.Müller, Semicond. Sci.Technol., **3** (1988) 511.

(61) J.Z. Zheng and J.W. Allen, to be published in Semicond.Sci. Technol., **5** (1990).

(62) J.C. Bouley, P. Blanconnier, A. Herman, P. Ged, P. Henoc, and J.P. Noblanc, J. Appl. Phys., **46** (1976) 3549.

(63) G.E. Hite, D.T. Marple, M. Aven and B.Segall, Phys.Rev.,**156** (1967) 850.

(64) P.J. Dean, Phys.Status Solidi, A **81** (1984) 625.

(65) N.F. Mott and E.A. Davis, Electronic Processes in Non-crystalline Materials (Clarendon, Oxford, 1971).

(66) S. Colak, R.N. Bhargava, B.J. Fitzpatrick and A. Sicignano, J.Luminesc., **31/32**, (1984) 430.

(67) J.W. Allen, Private communication.

(68) J. Nishizawa, R. Suzuki, and Y. Okuno, J.Appl.Phys., **59** (1986) 2256.

(69) A. Yashikawa, S. Muto, S. Yamaga, and H. Kasai, J.Crystal Growth, **86** (1988) 279.

(70) A.W. Livingstone, K. Turvey, and J.W. Allen, Solid-State Electronics,**16** (1973) 351.

(71) A.M. Cowley, J.Appl.Phys., **37** (1966) 3024.

(72) K. Turvey and J.W. Allen, J.Phys.C: Solid St.Phys., **6** (1973) 2887.

(73) H.J. Lozykowski, J. Sekulski, and B. Kostanska-Sekulska, J.Luminesc., **20** (1979) 83.

(74) A.G. Fischer and H.J. Moss, J.Appl.Phys., **34** (1963) 2112.

(75) H.C. Card and E.H. Rhoderick, Solid-State Electron., **16** (1973) 365.

(76) H.C. Card and B.L. Smith, J.Appl.Phys., **42** (1971) 5863.

(77) J.W. Allen, Physica Polonica A **77** (1990) 5.

(78) A.G. Fischer, 7th International Conference on Physics of Semiconductors:Radiative Recombination in Semiconductors (Dunod: Paris) (1964) 259.

(79) T.D.Thompson and J.W.Allen, J.Cryst.Growth.,**101**(1990) 981.

(80) G. Mandel, F.F. Morehead and P.R. Wagner, Phys.Rev. A**136** (1964) 826.

(81) R.N. Bhargava, J.Cryst.Growth, **59** (1982) 15.

(82) F.T.J. Smith, Solid State Communn., **7** (1969) 1757.

(83) S. Kishida, K. Matsuura, H. Mori, T. Yanagawa, I. Tsurumi and C. Hamaguchi, Phys.Stat.Sol., A **106** (1988) 283.

(84) S. Iida, J. Phys. Soc. Japan, **25** (1968) 177.

(85) G. Jones and J. Woods, J.Luminesc., **9** (1974) 389.

(86) H. Roppischer, J. Jacobs, and B.V. Novikov, Phys.Stat.Sol., A **27** (1975) 123.

(87) P.J. Dean, Czech: J.Phys., B **30** (1980) 272.

(88) J.M.Depuydt,H.Cheng, J.E.Potts, T.L.Smith, and S.K. Mohapatra, J.Appl.Phys., **62** (1987) 4756.

(89) S. Fujita, Y. Matsuda, and A. Sasaki, J.Cryst.Growth,**68** (1984) 231.

(90) M. Lannoo, J.Phys.C: Solid State Phys., **17** (1984) 3137.

(91) K. Era, S. Shionoya, and Y. Washizawa, J.Phys.Chem.Solids, **29** (1968)1827.

(92) M. Godlewski, W.E. Lamb, and B.C. Cavenett, Solid State Commun., **39** (1981) 595.

(93) G.B. Stringfellow and R.H. Bube, Phys.Rev., **171** (1968) 903.

(94) S. Iida, J.Phys.Soc.Japan, **26** (1969) 1140.

(95) M. Aven and R.E. Halsted, Report of General Electric Research Laboratory, no 64-RL-3743G (1964).

(96) S.T. Pantelides and H.G. Grimmeiss, Solid State Commun., **35** (1980) 635.

(97) K. Kosai, B.J. Fitzpatrick, H.G. Grimmeiss, R.N. Bhargava, and G.F. Neumark, Appl.Phys.Lett., **35** (1979) 194 .

(98) J.P. Walter and M.L. Cohen, Phys.Rev., **183** (1969) 763.

(99) W. Hoogenstraaten, Philips Res.Rep., **13** (1958) 515.

(100) C.T. Sah, Solid-State Electron., **19** (1976) 975.

(101) H. Kukimoto, S. Shionoya, T. Kada and R. Hioki, J.Phys.Chem. Solids, **29** (1968) 935.

(102) J.M. Noras and H.R. Szawelska, J.Phys.C: Solid State Phys., **15** (1982) 2001.

(103) J.W. Allen , Private communication.

(104) S. Shionoya, T. Koda, K. Era, and H. Fujiwara, J.Phys.Soc. Japan, **19** (1964) 1157.

(105) T. Koda and S. Shionoya, Phys.Rev., A **136** (1964) 541.

(106) G.D. Watkins, Solid-State Commun., **12** (1973) 589.

(107) H.R. Szawelska PH.D Thesis (1980) St.Andrews University (unpublished).

(108) T. Yokogawa, M. Ogura and T. Kajiwara, Appl.Phys.Letts., **49** (1986) 1702.

(109) K.P. Giapis, D.C Lu, and K.F. Jensen, Appl.Phys.Lett., **54** (1989) 353.

(110) G.B. Stringfellow and R. Linnebach, J.Appl.Phys., **51** (1980) 2212.

(111) K. Morimoto, J.Appl.Phys., **66** (1989) 4206.

(112) K. Shahzad, D.J. Olego, C.G. Van de walle, Phys.Rev., B **38** (1988)1417.

(113) K. Shahzad, D.J. Olego, C.G. Van de walle and D.A. Cammack, J.Luminesc., **46** (1990) 109.

(114) H.A. Mar and R.M. Park, J.Appl.Phys., **60** (1986) 1229.